

**PRESSURE TRANSIENT ANALYSIS FOR
MULTILAYERED GAS RESERVOIRS UNDER VARIOUS
RESERVOIR CONDITIONS**

ZULFIQUAR ALI REZA



DEPARTMENT OF PETROLEUM & MINERAL RESOURCES ENGINEERING

BUET, DHAKA

BANGLADESH



#91279#

**PRESSURE TRANSIENT ANALYSIS FOR
MULTILAYERED GAS RESERVOIRS UNDER VARIOUS
RESERVOIR CONDITIONS**

A Thesis

Submitted to the Department of Petroleum & Mineral Resources
Engineering

in partial fulfillment of the requirements for the degree of Master of
Science in Engineering (Petroleum).

By

ZULFIQUAR ALI REZA

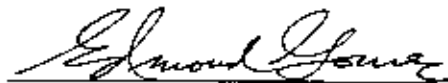
**DEPARTMENT OF PETROLEUM & MINERAL RESOURCES ENGINEERING
BANGLADESH UNIVERSITY OF ENGINEERING & TECHNOLOGY,
DHAKA
BANGLADESH**

JUNE, 1997.

RECOMMENDATION OF THE BOARD OF EXAMINERS

The undersigned certify that they have read and recommend to the Department of Petroleum and Mineral Resources Engineering, for acceptance, a thesis entitled PRESSURE TRANSIENT ANALYSIS FOR MULTILAYERED GAS RESERVOIRS UNDER VARIOUS RESERVOIR CONDITIONS submitted by ZULFIQUAR ALI REZA in partial fulfillment of the requirements for the degree of MASTER OF SCIENCE IN ENGINEERING in PETROLEUM ENGINEERING.

Chairman (Supervisor) :



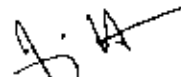
Dr. Edmond Gomes
Assistant Professor
Dept. of Petroleum & Mineral Resources Eng.
BUET

Member (Ex-Officio)



Dr. Mohammad Tamim
Head
Dept. of Petroleum & Mineral Resources Eng
BUET

Member :



Dr. Ijaz Hossain
Associate Professor
Dept. of Chemical Eng.
BUET

Member (External) :



Mr Kazi Shahidur Rahman
General Manager
Reservoir Study Cell
Petro Bangla, Dhaka

Date : June 5, 1997.

ABSTRACT

Most reservoirs are heterogeneous in nature. Reservoir heterogeneity can be in the vertical direction (layered reservoirs) as well as in the radial direction (composite reservoirs). Fluid flow is complicated for the gas reservoirs because of the inertial and turbulence effects and the pressure dependence of gas properties. This study develops a semi-analytical model for pressure transient analysis of heterogeneous gas reservoirs. Reservoir heterogeneity has been considered by drawing upon the layered and composite nature of the reservoirs. The diffusivity equation has been solved as a generalized eigenvalue problem utilizing the pseudopressure and pseudotime schemes. The model takes into account the high velocity effects, wellbore storage and skin, and different possible inner and outer boundary conditions. Finite formation damage can also be modeled.

The model has been validated by comparing the results with those of some analytical models and simulation results published in the literature. Different schemes for calculating high velocity effects have been studied and evaluated. For the same amount of skin, both thin and finite damaged zone responses have been compared. Both these responses have been found to be quite different for certain cases. All possible outer boundary conditions, partial penetration and bottom water conditions may be studied. Its application is enormous in the field of pressure transient analysis of gas reservoirs. This versatile model, to my knowledge, includes more features for gas reservoirs than any other previously published pressure transient models.

ACKNOWLEDGEMENTS

I would like to thank Dr. Edmond Gomes for his supervision and guidance throughout this work. His relentless encouragement had certainly added great value to the work.

I would like to express my gratitude to Dr. M. Tamim, Head of the Department of Petroleum and Mineral Resources Engineering, for his encouragement and cooperation to complete this work.

I feel extremely grateful to Dr. Ijaz Hossain, former Head of the Department of Petroleum and Mineral Resources Engineering, for his support and interest in this work.

I would also like to thank the University of Alberta-BUET (Bangladesh University of Engineering and Technology)-CIDA (Canadian International Development Agency) Linkage Program Officials for setting up this department and equipping the department with fantastic computing facilities without which the work could not have progressed.

TABLE OF CONTENTS

Chapter	Page
ABSTRACT.....	i
ACKNOWLEDGEMENTS.....	ii
TABLE OF CONTENTS.....	iii
LIST OF FIGURES.....	v
1.0 INTRODUCTION.....	1
2.0 LITERATURE REVIEW.....	3
3.0 STATEMENT OF THE PROBLEM.....	8
4.0 MODEL DEVELOPMENT.....	9
4.1 Model Formulation.....	9
4.2 Model Development for Laminar Solution.....	14
4.3 Incorporation of the High Velocity Effect.....	24
4.4 Convolution Scheme for Layer Flow Rate and Incorporation of Wellbore Storage.....	27
4.5 Solution Methodology.....	32
4.5.1 Solution Methodology for Laminar Solution.....	33
4.5.2 Computation of Real Variables.....	33

4.5.3	Solution Methodology for High Velocity Solution.....	36
4.5.4	Solution Methodology to Incorporate the Convolution Scheme with Wellbore Storage.....	38
4.5.5	Derivative determination.....	39
5.0	MODEL VALIDATION	40
6.0	RESULTS AND DISCUSSION.....	45
6.1	Effect of Wellbore Storage and Skin.....	45
6.2	Effect of Velocity or Turbulence Coefficient.....	46
6.3	Effect of Velocity or Flow Rate.....	54
6.4	Effect of Initial Pressure.....	58
6.5	Effect of Permeability.....	60
6.6	Effect of Finite Formation Damage.....	66
6.7	Effect of Layering.....	74
6.8	Effect of Closed Outer Boundary.....	81
6.9	Effect of Composite Nature of the Reservoir.....	81
7.0	CONCLUSIONS.....	89
8.0	RECOMMENDATIONS.....	91
	NOMENCLATURE.....	92
	REFERENCES.....	98
	APPENDIX A: Computer Program.....	103

LIST OF FIGURES

Figure		Page
Figure 2.1	Layered reservoir with interlayer crossflow.....	4
Figure 2.2	Radial, layered composite reservoir.....	4
Figure 4.1	Schematic of an n-layer composite reservoir in radial Geometry with different rock and/or fluid types in each layer	10
Figure 4.2	Flow diagram showing the sequences and interconnections Between various schemes of the developed model.....	34
Figure 5.1	Comparison of this study with Al-Hussainy <i>et al.</i> solution for a homogeneous gas reservoir.....	41
Figure 5.2	Comparison of this study with Wattenbarger and Ramey solution with high velocity effect.....	41
Figure 5.3	Comparison of this study with Lee <i>et al.</i> solution with high velocity effect.....	43
Figure 5.4	Comparison of this study with Oren <i>et al.</i> solution with wellbore storage and skin.....	43
Figure 6.1	Effects of wellbore storage and skin on pseudo-dimensionless pressure responses for an infinite-acting homogeneous reservoir....	47
Figure 6.2	Effect of velocity coefficient on pseudopressure and derivative responses (skin = 0).....	47

Figure 6.3	Effect of velocity coefficient on pseudopressure and derivative responses (skin = 2).....	49
Figure 6.4	Effect of velocity coefficient on pseudopressure and derivative responses (skin = 5).....	49
Figure 6.5	Effect of velocity coefficient on pseudopressure responses (skin = 0).....	50
Figure 6.6	Effect of velocity coefficient on pseudopressure derivative responses (skin = 0).....	50
Figure 6.7	Effect of velocity coefficient on pseudopressure responses (skin = 5).....	51
Figure 6.8	Effect of velocity coefficient on pseudopressure derivative responses (skin = 5).....	51
Figure 6.9	Effect of skin on pseudopressure and derivative responses with Geertsma correlation.....	53
Figure 6.10	Effect of flow rate on pseudopressure and derivative responses (skin = 0, Geertsma correlation).....	53
Figure 6.11	Effect of flow rate on pseudopressure and derivative responses (skin = 5, Geertsma correlation).....	55
Figure 6.12	Effect of flow rate on pseudopressure responses (skin = 0, Geertsma correlation).....	55
Figure 6.13	Effect of flow rate on pseudopressure responses (skin = 5, Geertsma correlation).....	56

Figure 6.14	Effect of flow rate on pseudopressure derivative responses (skin = 0, Geertsma correlation)	56
Figure 6.15	Effect of flow rate on pseudopressure derivative responses (skin = 5, Geertsma correlation).....	57
Figure 6.16	Effect of flow rate on pseudopressure and derivative responses (skin = 5, Firoozabadi and Katz correlation).....	57
Figure 6.17	Effect of initial pressure on pseudopressure and derivative responses (skin = 0, constant Q_D basis).....	59
Figure 6.18	Effect of initial pressure on pseudopressure and derivative responses (skin = 5, constant Q_D basis).....	59
Figure 6.19	Effect of permeability on pseudopressure and derivative responses (Geertsma correlation, constant Q_{sc} basis).	61
Figure 6.20	Effect of permeability on pseudopressure and derivative responses (Firoozabadi and Katz correlation, constant Q_{sc} basis).....	61
Figure 6.21	Effect of permeability on pseudopressure and derivative responses (skin = 5, constant Q_D basis).....	63
Figure 6.22	Effect of permeability on pseudopressure and derivative responses (skin = 0, constant Q_D basis).....	63
Figure 6.23	Effect of permeability on pseudopressure responses (skin = 5, constant Q_D basis).....	64
Figure 6.24	Effect of permeability on pseudopressure responses (skin = 0, constant Q_D basis).....	64

Figure 6.25	Effect of permeability on pseudopressure derivative responses (skin = 5, constant Q_D basis).....	65
Figure 6.26	Effect of permeability on pseudopressure derivative responses (skin = 0, constant Q_D basis).....	65
Figure 6.27	Effect of permeability on pseudopressure and derivative responses (skin = 5, Firoozabadi and Katz correlation, constant Q_D basis).....	67
Figure 6.28	Effect of permeability on pseudopressure and derivative responses (skin = 0, Firoozabadi and Katz correlation, constant Q_D basis)....	67
Figure 6.29	Effect of finite formation damage on pseudopressure and derivative responses (skin = 2, Firoozabadi and Katz correlation)...	69
Figure 6.30	Effect of finite formation damage on pseudopressure and derivative responses (skin = 2, Geertsma correlation).....	69
Figure 6.31	Effect of finite formation damage on pseudopressure responses (skin = 2, Firoozabadi and Katz correlation).....	71
Figure 6.32	Effect of finite formation damage on pseudopressure responses (skin = 2, Geertsma correlation).....	71
Figure 6.33	Effect of finite formation damage on pseudopressure derivative responses (skin = 2, Firoozabadi and Katz correlation).....	72
Figure 6.34	Effect of finite formation damage on pseudopressure derivative responses (skin = 2, Geertsma correlation).....	72
Figure 6.35	Effect of finite formation damage on pseudopressure and derivative responses (skin = 5, Geertsma correlation).....	73

Figure 6.36	Comparison of this study with Osman and Mohammed for a 2-layer infinite-acting commingled reservoir system.....	73
Figure 6.37	Effect of layering on pseudopressure and derivative responses of a commingled reservoir.....	76
Figure 6.38	Effect of layering on pseudopressure responses of a commingled reservoir.....	76
Figure 6.39	Effect of layering on pseudopressure derivative responses of a commingled reservoir.....	77
Figure 6.40	Effect of layer ordering on pseudopressure and derivative responses of a commingled reservoir.....	77
Figure 6.41	Effect of layering on pseudopressure and derivative responses of a reservoir with interlayer crossflow ($q_{sc} = 7.5 \text{ m}^3/\text{s}$).....	79
Figure 6.42	Effect of layering on pseudopressure responses of a reservoir with interlayer crossflow ($q_{sc} = 7.5 \text{ m}^3/\text{s}$).....	79
Figure 6.43	Effect of layering on pseudopressure derivative responses of a reservoir with interlayer crossflow ($q_{sc} = 7.5 \text{ m}^3/\text{s}$).....	80
Figure 6.44	Effect of layering on pseudopressure responses of a reservoir with interlayer crossflow ($q_{sc} = 0.1 \text{ m}^3/\text{s}$).....	80
Figure 6.45	Effect of outer boundary radii on pseudopressure and derivative responses for a closed boundary reservoir.....	82
Figure 6.46	Effect of outer zones permeability on pseudopressure and derivative responses of an infinite-acting composite reservoir.....	82

Figure 6.47	Schematic of a 2-layer 3- zone composite reservoir in radial Geometry with different rock and/or fluid types in each layer.....	84
Figure 6.48	Effect of outer zones permeability on pseudopressure and derivative responses of a closed boundary reservoir.....	85
Figure 6.49	Effect of ordering of zone permeability on pseudopressure and derivative responses of an infinite-acting composite reservoir.. ..	85
Figure 6.50	Effect of ordering of zone permeability on pseudopressure and derivative responses of a closed boundary composite reservoir.....	87

1.0 INTRODUCTION



With the ever-increasing energy demand in the world, the scientific community is looking all the more for newer alternatives for energy generation to curb the present crisis. Even a few decades back, in the developed nations, the notion of using natural gas as an energy source seemed to have ridiculed many. The scenario has now changed completely; the reason being not only the increasing demand for energy but also the increased awareness of the people and the governments for an environment friendly fuel. These factors have enhanced the use of natural gas, and not surprisingly have escalated its price as well. The scenario in Bangladesh is quite different as natural gas is the most important natural resource of the country. Sound reservoir engineering judgment and techniques in identifying the reservoir characteristics and controlling the production play a significant role to meet the present demand and maximize the recovery of the gas in place. Pressure transient analysis is an important tool for such reservoir characterization.

Pressure transient analysis deals with generating and measuring pressure variations with time in wells. These pressure profiles are subsequently used for the estimation of rock, fluid and reservoir properties. Information like reservoir pressure, permeability, porosity, reserves, reservoir heterogeneities, wellbore volume, damage, and improvement and other relevant data may be obtained from pressure transient analyses. All this information can be used to assist in analyzing, improving and forecasting reservoir performance. Pressure transient testing techniques, such as buildup, drawdown, injectivity, falloff, and

interference, are important part of pressure transient analyses for reservoir characterization.

The focus of this study is the pressure transient analysis of heterogeneous gas reservoirs. A semi-analytical model has been developed in the present study to investigate the reservoir heterogeneity and also some other significant single phase fluid flow phenomena like inertial or turbulence effect and variation of fluid properties. This model has the potential to study numerous reservoir conditions – partial penetration of the wells, the effect of water coning, edge- and bottom water drives, pseudoskins, etc. This model can also be used for automatic type-curve matching.

A number of areas have been investigated with this model. The effect of different parameters (wellbore storage coefficient, skin, velocity coefficient, flow rate, initial pressure, permeability and outer boundary conditions) on the pressure transient responses of homogeneous reservoirs are investigated. Pressure transient responses for finite formation damage have been examined. Layering effects have been studied for both the commingled and non-commingled reservoirs. Effect of layer ordering is also studied for multilayered reservoirs. Some composite reservoir pressure transient responses have been analyzed.

2.0 LITERATURE REVIEW

Pressure transient analysis of gas reservoirs is complex as compared to that for oil reservoirs; the reason being the variations of viscosity, super-compressibility factor or gas deviation factor, and fluid compressibility with pressure and temperature. These variations make the governing partial differential equation nonlinear for gas. Further complications arise due to different flow regimes. For the flow of real gases through porous media, the inertial and turbulence effects are very important when flow rates become high.

Evidently the pressure transient analysis of a homogeneous gas reservoir is a difficult task in hand; reservoir heterogeneity makes the task even more intricate. Since reservoir deposition occurs over a geologic period of time, most of the reservoirs are heterogeneous in nature. Reservoir heterogeneity may occur in the vertical direction with the presence of layers and in the lateral direction having different zones of fluids and/or lithofacies in the reservoir. Figures 2.1 and 2.2 show a layered reservoir and a composite layered reservoir respectively. A composite layered reservoir situation occurs when all or some of the layers have two or more regions of different rock and/or fluid properties. The horizontal lines show the layering while the arrows indicate the presence of crossflow. The layers may be communicating or non-communicating. When the layers are communicating, formation crossflow is present. When the non-communicating layers have communication only through the wellbore, the reservoir is called 'commingled reservoir'. Apart from the natural causes (change in the depositional environments,

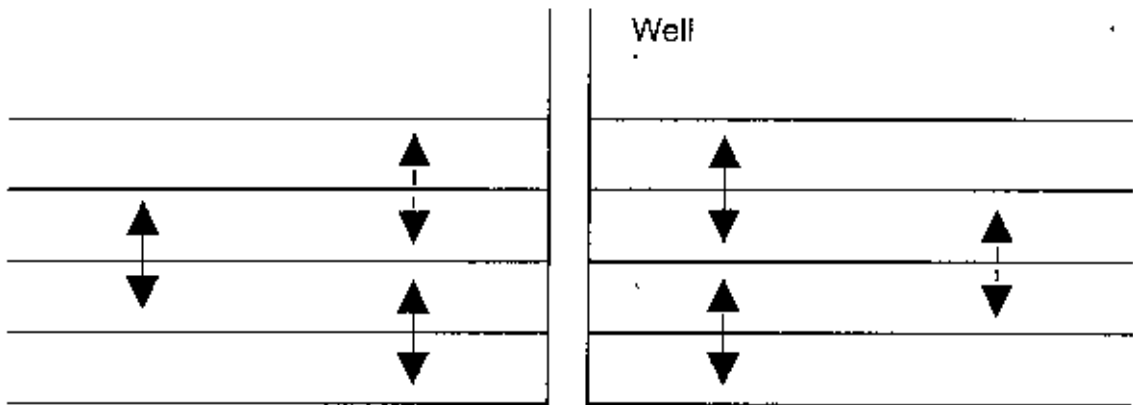


Figure 2.1 : Layered reservoir with interlayer crossflow

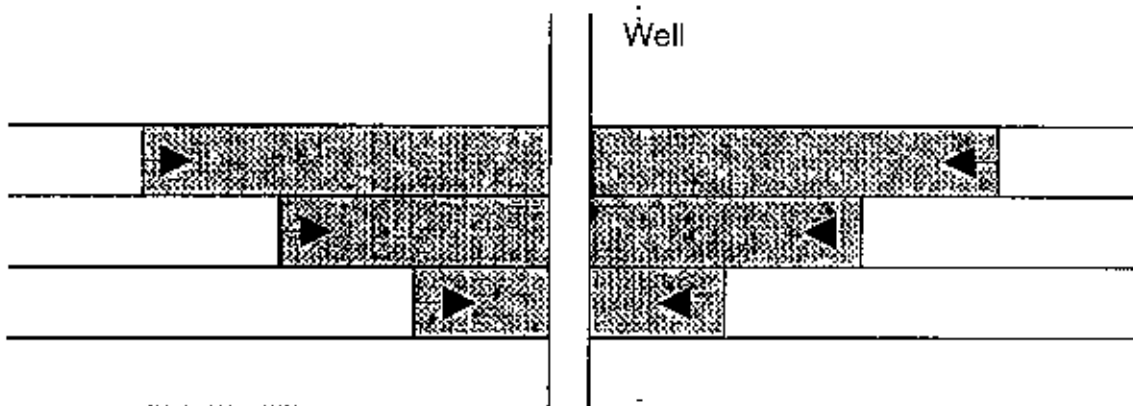


Figure 2.2 : Radial, layered composite reservoir

tectonic activities, faulting, folding, etc.), composite layered reservoir may result from different field operations. For an oil reservoir, secondary and tertiary oil recovery methods create composite zones. A gas reservoir may be of composite nature because of tectonic activities, formation damage, acidizing, etc.

Study of pressure transient analysis of heterogeneous gas reservoir systems is scarce in literature, although numerous studies have been reported for oil reservoirs. Formation crossflow is a key aspect of the oil reservoir models. Formation crossflow (Gao, 1984) has been modeled mainly by two methods : pseudo-steady state crossflow and transient crossflow. The pseudo-steady state crossflow assumes the resistance to crossflow is confined to the inter-layer boundary and the flow is horizontal within each layer. This essentially reduces the two-dimensional problem to an one-dimensional one. The transient crossflow method utilizes a two-dimensional diffusivity equation for each layer.

For real gas flow through porous media, a large number of studies have been reported dealing with different aspects of modeling like development of pseudo-variables, high velocity effect (i.e. inertial effect or turbulence effect), etc. Variations in the viscosity and the super-compressibility factor were first incorporated via Kirchoff (1894) transformation which, in the parlance of petroleum engineering, is known as real gas pseudopressure. This approach was first conceived by Al-Hussainy *et al* (1966). The concept of pseudo-time came in to allow the variation of compressibility of real gases. Agarwal *et al*. (1970) first introduced this concept. The high effects are modeled by a quadratic equation which was first suggested by Forchheimer (1901). Various studies

have been focused on the high velocity effects of real gas flow through porous media, inertial and turbulence effect. Smith (1961) obtained an empirical correlation to allow the high velocity phenomena. Swift and Kiel (1962) corroborated Smith's notions. Geertsma (1974) and Firoozabadi and Katz (1979) presented the correlations for the coefficient of the velocity squared term in the Forchheimer equation for dry gas reservoirs. Lee *et al.* (1987) attempted to quantify the "turbulence intensity" by introducing a new dimensionless number called the "Forchheimer number". Oren *et al.* (1988) quantified the effects of wellbore storage along with those of skin and turbulence intensity.

For multilayered reservoirs, the pressure transient analysis with a constant surface flow rate introduces variation in the contribution of each layer. This variation reflects the layer properties. Hence, any analysis based on a constant surface flow rate will not be proper. In such cases, a superposition scheme on the changing fractional flow rate is required. The use of a convolution scheme based on Duhamel's (1833) integral formula is a rational approach for the superposition. Chu and Raghavan (1981) have applied the method while studying the effect of commingled layers on interference tests. Whitson and Sognesand (1990) studied methods for incorporating high velocity effect in the convolution scheme.

Osman and Mohammed (1993) attempted to incorporate most of these features (high velocity effect, wellbore storage and formation damage) for a multilayered gas reservoir. Their model could handle only commingled infinite boundary gas reservoirs. They did

not consider crossflow between layers or the possibility of the composite nature of the reservoirs. Detail discussion of this paper is given in Section 6.7.

3.0 STATEMENT OF THE PROBLEM

The limited literature on the pressure transient analysis of heterogeneous gas reservoirs corroborates the need to take up studies on this topic to have a better understanding of the subject. From the perspective of Bangladesh, which has a number of multilayered and heterogeneous gas reservoirs, this work is certainly a cognate one.

Primarily the objectives of this work are

- to develop a semi-analytical model for a multilayered composite reservoir to generate pressure transient responses
- to identify the parameters affecting the pressure transient responses
- to investigate finite formation damage responses
- to analyze the multilayer reservoir responses by layering heterogeneity
- to explore composite reservoir responses

In this study, it will be attempted to integrate all the aforementioned phenomena for real gas flow and incorporate the effect of reservoir heterogeneity in terms of the layered and composite nature of the formation. This study should be able to develop a versatile semi-analytical model to examine these effects. This model should be able to investigate the effects of different parameters like finite formation damage or skin effect, composite nature of reservoir, layering effects in a multilayer reservoir, partial penetration of wells, bottom- and edge- water drives, etc.

4.0 MODEL DEVELOPMENT

4.1 Model Formulation

This study is an extension of the work done by Gomes (1994) which was based on the pressure transient analysis of composite layered oil reservoirs. The present study is a similar kind of work for gas reservoirs. From the discussion in the preceding chapters, it is quite apparent that the property variation of the gas, high velocity effects and the variation in the layer contribution over time are the key aspects of this present work. Undertaking the pseudo-pressure and pseudo-time approach, the property variation of gas is handled and the laminar solution is obtained in a similar manner, the oil solution is obtained by Gomes (1994).

To account for the high velocity effect, this study assumes superposition of the high velocity effect on the laminar pressure responses. This method is not uncommon. Various other investigators undertook similar approach (Raghavan, 1993, Lee *et al.*,1987). A radial composite layered reservoir, with a symmetrically located well penetrating the reservoir, as shown in Figure 4.1, is considered in this work. The well is assumed to be producing at a constant surface flow rate.

The crossflow has been considered by the pseudosteady-state formation crossflow model (Gao, 1984). Anbarci *et al.* (1989) approach has been taken as the initial step to solve the problem. The discontinuity boundaries in each layer have been vertically extended across all the layers. This results in zoning each layer of an n-layer reservoir into m

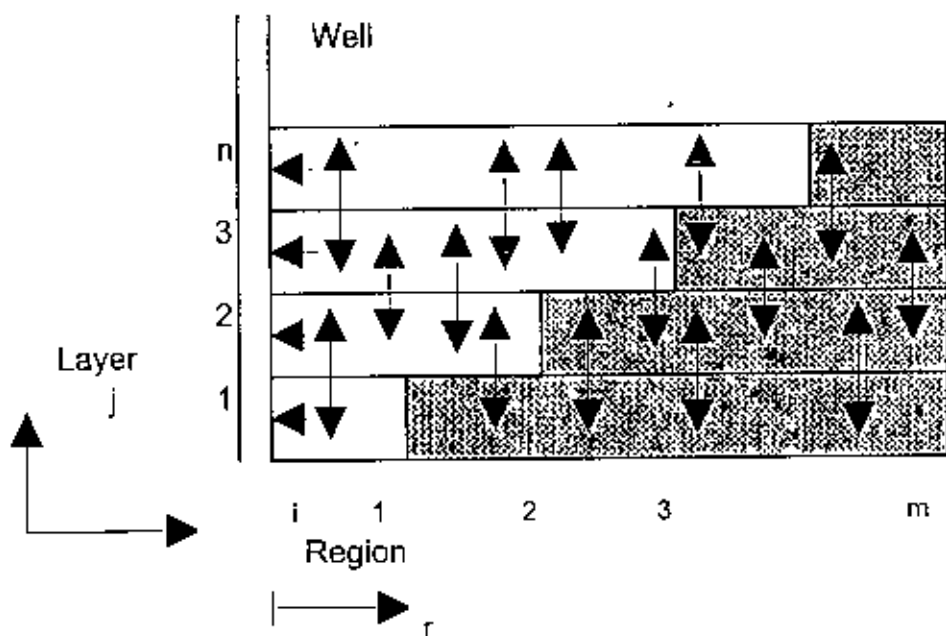


Figure 4.1 : Schematic of an n -layer composite reservoir in a radial geometry with two different rock and/or fluid types in each layer

regions depending on the number and location of the discontinuity boundaries. So the reservoir is divided into $n \times m$ blocks with each of them identified by (i,j) , where i represents region and j layer. Different zones may have different rock and/or fluid properties. If the locations of the discontinuity boundaries are distinct, there will be $m=n+1$ regions in each of the layers. Layers are assumed to have constant thickness throughout the reservoir.

Pseudosteady-state crossflow model, proposed by Gao (1984), is used to model the crossflow between the layers in the reservoir. The crossflow resistance is assumed to be confined to the interlayer boundary. The uppermost and the bottommost boundaries are considered to be closed.

The pseudopressure, first introduced by Al-Hussainy *et al.* (1966), and pseudotime, introduced by Agarwal *et al.* (1970) concepts have been adapted. Other assumptions for the development of the mathematical model are as follows :

1. Gravity effects and capillary forces are considered to be negligible.
2. The laminar solution has been obtained by considering Darcy's law.
3. Pressure and flow continuity across the zone interfaces.

The derivation of the flow equation is as follows .

The continuity equation is

$$\nabla(\rho\bar{v}) = -\frac{\partial p\phi}{\partial t} \quad \dots [4.1]$$

Swift and Kiel (1962) formulation of the Forchheimer equation is ,

$$\bar{v} = \frac{\delta_r k}{\mu} \frac{\partial p}{\partial r}, \quad \dots [4.2]$$

where

$$\delta_r = \frac{1}{1 + \frac{\beta \rho k}{\mu} |\bar{v}|}, \quad \dots [4.3]$$

and the gas law ,

$$\rho = \frac{pM}{zRT}. \quad \dots [4.4]$$

Combining these equations leads to the pressure differential form , the diffusivity equation,

$$\frac{1}{r} \frac{\partial}{\partial r} (r \rho \bar{v}) = \frac{\partial}{\partial t} (\phi \rho), \quad \dots [4.5]$$

$$\frac{1}{r} \frac{\partial}{\partial r} \left(r \frac{pM}{zRT} \frac{\delta_r k}{\mu} \frac{\partial p}{\partial r} \right) = \frac{\partial}{\partial t} \left(\phi \frac{pM}{zRT} \right), \quad \dots [4.6]$$

$$\frac{1}{r} \frac{\partial}{\partial r} \left(r \frac{p}{z\mu} \delta_r k \frac{\partial p}{\partial r} \right) = \frac{\partial}{\partial t} \left(\phi \frac{p}{z} \right). \quad \dots [4.7]$$

Now introducing the pseudopressure, Al-Hussainy *et al.* (1966),

$$m(p) = 2 \int_0^p \frac{p'}{z\mu} dp' \quad \dots [4.8]$$

and differentiating Equation [4.8], it is obtained,

$$\frac{\partial m(p)}{\partial p} = \frac{2p}{z\mu}, \quad \dots [4.9]$$

Now chain rule is applied to obtain,

$$\frac{\partial m}{\partial t} = \frac{\partial m}{\partial p} \cdot \frac{\partial p}{\partial t} \quad \dots [4.10]$$

$$\Rightarrow \frac{\partial p}{\partial t} = \frac{z\mu}{2p} \frac{\partial m}{\partial t} \quad \dots [4.11]$$

Similarly,

$$\frac{\partial n}{\partial t} = \frac{\partial n}{\partial p} \cdot \frac{\partial p}{\partial t} \quad \dots [4.12]$$

$$\frac{\partial p}{\partial t} = \frac{z\mu}{2p} \frac{\partial n}{\partial t} \quad \dots [4.13]$$

Introducing equation [4.11] and Equation [4.13] into Equation [4.7],

$$\frac{1}{r} \cdot \frac{\partial}{\partial t} \left(r\delta_r k \frac{\partial m}{\partial r} \right) = 2 \frac{\partial}{\partial t} \left(\phi \frac{p}{z} \right) = 2\phi \frac{\partial}{\partial p} \left(\frac{p}{z} \right) \frac{\partial p}{\partial t} \quad \dots [4.14]$$

The definition of the fluid compressibility is,

$$c = \frac{1}{\rho} \frac{\partial \rho}{\partial p} = \frac{zRT}{pM} \frac{\partial}{\partial p} \left(\frac{pM}{zRT} \right) = \frac{z}{p} \frac{\partial}{\partial p} \left(\frac{p}{z} \right) \quad \dots [4.15]$$

Combining Equation [4.14] and Equation [4.15], it is obtained,

$$\frac{1}{r} \cdot \frac{\partial}{\partial t} \left(r\delta_r k \frac{\partial m}{\partial r} \right) = 2\phi \frac{cp}{z} \frac{\partial p}{\partial t} = c\phi \frac{2p}{\mu z} \frac{\partial p}{\partial t} = c\phi\mu \frac{\partial m}{\partial t} \quad \dots [4.16]$$

Introducing the pseudotime, Agarwal *et al.* (1970),

$$t_p = \int_0^t \frac{1}{c\mu} dt' \quad \dots [4.17]$$

where $X_{A,i,j}$ and $X_{B,i,j}$ are defined as follows :

$$X_{A,i,j} = \frac{2}{\left(\frac{h}{k_v}\right)_{i,j} + \left(\frac{h}{k_v}\right)_{i,j+1}}, \quad \dots [4.24]$$

$$X_{B,i,j} = \frac{2}{\left(\frac{h}{k_v}\right)_{i,j} + \left(\frac{h}{k_v}\right)_{i,j-1}}, \quad \dots [4.25]$$

$$X_{A,i,n} = 0 \quad \text{for } i = 1, \dots, m, \quad \dots [4.26]$$

$$X_{B,i,1} = 0 \quad \text{for } i = 1, \dots, m. \quad \dots [4.27]$$

The laminar flow Equation [4.23] is first solved with the appropriate conditions which are in the pressure formulation as follows :

Initial Condition (IC) is given by,

$$P_{i,j}(r,0) = P_m. \quad \dots [4.28]$$

Inner Boundary Conditions (IBC) for constant flow rate are given by,

$$P_{wf} = P_{1,j}(r_w, t) - s_j \left(r \frac{\partial P_{1,j}}{\partial r} \right) \quad \text{for } j=1, \dots, n, \quad \dots [4.29]$$

$$q = -C \frac{\partial P_{wf}}{\partial t} + 2\pi r_w \sum_{j=1}^n \left(\frac{kh}{\mu} \right)_{1,j} \left(\frac{\partial P_{1,j}}{\partial r} \right)_{r=r_w}. \quad \dots [4.30]$$

The Outer Boundary Conditions (OBC) can be these three following conditions ,

Infinite OBC

$$P_{m,j} = P_m \quad r \rightarrow \infty \quad j=1, \dots, n, \quad \dots [4.31]$$

Constant Pressure OBC

$$p_{m,j} = p_m \quad r = r_{e_j} \quad j=1, \dots, n, \quad \dots [4.32]$$

Closed OBC

$$\frac{\partial p_{m,j}}{\partial r} = 0 \quad r = r_{e_j} \quad j=1, \dots, n. \quad \dots [4.33]$$

Interface Conditions

At the interfaces, pressure and pressure derivative are same for all zones. So,

$$p_{i,j} = p_{i+1,j} \quad r = r_{a_i} \quad i=1, \dots, m \quad j=1, \dots, n, \quad \dots [4.34]$$

$$\frac{\partial p_{i,j}}{\partial r} = \frac{\left(\frac{kh}{\mu}\right)_{i+1,j}}{\left(\frac{kh}{\mu}\right)_{i,j}} \frac{\partial p_{i+1,j}}{\partial r} \quad r = r_{a_i} \quad i=1, \dots, m-1 \quad j=1, \dots, n. \quad \dots [4.35]$$

Defining the following dimensionless variables ,

$$r_D = \frac{r}{r_w}, \quad \dots [4.36]$$

$$m_{i,j} = \frac{2\pi(\overline{kh})}{Q} \frac{T_u}{TP_{sc}} (m_{in} - m_{i,j}), \quad \dots [4.37]$$

$$m_{D,i} = \frac{2\pi(\overline{kh})}{Q} \frac{T_w}{TP_{sc}} (m_{in} - m_{w,i}), \quad \dots [4.38]$$

$$t_{pD} = \frac{t_p}{r_w^2} \left(\frac{\overline{kh}}{\phi h}\right), \quad \dots [4.39]$$

the following is obtained,

$$\frac{\partial \bar{\sigma}}{\partial \bar{\sigma}_D} = r_w, \quad \dots [4.40]$$

$$\frac{\partial m_{i,j}}{\partial m_{D,i}} = -\frac{Q}{2\pi} \frac{TP_w}{T_{sc}} \left(\frac{1}{kh} \right), \quad \dots [4.41]$$

$$\frac{\partial m_{i,j}}{\partial \bar{\sigma}} = -\frac{Q}{2\pi} \frac{TP_w}{T_{sc}} \left(\frac{1}{kh} \right) \frac{1}{r_w} \frac{\partial m_{D,i}}{\partial \bar{\sigma}_D}, \quad \dots [4.42]$$

$$\frac{\partial^2 m_{i,j}}{\partial \bar{\sigma}^2} = -\frac{Q}{2\pi} \frac{TP_{sc}}{T_{sc}} \left(\frac{1}{kh} \right) \frac{1}{r_w} \frac{\partial^2 m_{D,i}}{\partial \bar{\sigma}_D^2}, \quad \dots [4.43]$$

$$\frac{\partial m_{i,j}}{\partial \bar{\alpha}_p} = -\frac{Q}{2\pi} \frac{TP_w}{T_{sc}} \left(\frac{1}{\phi h} \right) \frac{1}{r_w^2} \frac{\partial m_{D,i}}{\partial \bar{\alpha}_{pD}}, \quad \dots [4.44]$$

Introducing these dimensionless equations, the diffusivity equation [4.23] becomes ,

$$\begin{aligned} & -(kh)_{i,j} \left[\frac{Q}{2\pi r_w^2} \frac{1}{(kh)} \frac{\partial^2 m_{D,i}}{\partial \bar{\sigma}_D^2} + \frac{Q}{2\pi r_w} \frac{1}{kh} \frac{1}{r} \frac{\partial m_{D,i}}{\partial \bar{\sigma}_D} \right] \\ & = (\phi h)_{i,j} \frac{Q}{2\pi r_w^2} \frac{TP_{sc}}{T_{sc}} \frac{1}{(\phi h)} \frac{\partial m_{D,i}}{\partial \bar{\alpha}_{pD}} - X_{A,i,j} \frac{Q}{2\pi (kh)} \frac{TP_{sc}}{T_{sc}} (m_{D,i} - m_{D,i+1}) \\ & \quad - X_{R,i,j} \frac{Q}{2\pi (kh)} \frac{TP_{sc}}{T_{sc}} (m_{D,i} - m_{D,i-1}) \\ \Rightarrow & \kappa_{i,j} \left[\frac{\partial^2 m_{D,i}}{\partial \bar{\sigma}_D^2} + \frac{1}{r_D} \frac{\partial m_{D,i}}{\partial \bar{\sigma}_D} \right] = \omega_{i,j} \frac{\partial m_{D,i}}{\partial \bar{\alpha}_{pD}} + \lambda_{A,i,j} (m_{D,i} - m_{D,i+1}) + \lambda_{R,i,j} (m_{D,i} - m_{D,i-1}), \end{aligned} \quad \dots [4.45]$$

$$\text{where,} \quad \kappa_{i,j} = \frac{(kh)_{i,j}}{(kh)}, \quad \dots [4.46]$$

$$\omega_{i,j} = \frac{(\phi h)_{i,j}}{(\phi h)} , \quad \dots [4.47]$$

$$\lambda_{A,i,j} = \frac{X_{A,i,j} r_w^2}{kh} , \quad \dots [4.48]$$

$$\lambda_{B,i,j} = \frac{X_{B,i,j} r_w^2}{kh} . \quad \dots [4.49]$$

The initial and boundary conditions in the dimensionless pseudo units will be as follows:

Initial condition , Equation [4.28],

$$m_{D,i,j}(r_D,0) = 0 \quad i=1, \dots, m \quad j=1, \dots, n . \quad \dots [4.50]$$

IBC, Equation [4.29],

$$m_{D_w} = m_{D_{i,j}} - s_j \frac{\partial m_{D_{i,j}}}{\partial r_D} \quad j=1, \dots, n \quad \dots [4.51]$$

Equation [4.30],

$$\begin{aligned} q = & -C \frac{\partial m_{D_w}}{\partial r_D} \left(-\frac{Q}{2\pi(kh)} \frac{T_{p_{sc}}}{T_{sc}} \right) \left(\frac{\mu z}{2p} \right)_{wf} \left(\frac{1}{r_w^2} \frac{kh}{\phi h} \right) \left(\frac{1}{c\mu} \right) \\ & + 2\pi r_w \sum_{i=1}^n \left(\frac{kh}{\mu} \right)_{i,j} \left(\frac{\partial m_{D_{i,j}}}{\partial r_D} \right) \left(\frac{Q}{2\pi(kh)} \frac{T_{p_{sc}}}{T_{sc}} \right) \left(\frac{\mu z}{2p} \right)_{i,j} \left(\frac{1}{r_w} \right) , \\ \therefore 1 = & C_D \frac{\partial m_{D_w}}{\partial r_D} - \sum_{j=1}^n \kappa_{1,j} \frac{\partial m_{D_w}}{\partial r_D} , \quad \dots [4.52] \end{aligned}$$

since
$$q = Q \frac{zT_{p_{sc}}}{T_{sc}P_{wf}} = Q \frac{zT_{p_{sc}}}{T_{sc}P_{wf}} , \quad \dots [4.53]$$

where
$$C_D = \frac{C}{2\pi r_w^2 (\phi h) c} \quad \dots [4.54]$$

The OBCs are given by ,

Infinite OBC

$$m_{D_{r,j}} = 0 \quad r_D \rightarrow \infty \quad j=1, \dots n. \quad \dots [4.55]$$

Constant Pressure OBC

$$m_{D_{r,j}} = 0 \quad r_D = r_{eD_i} \quad j=1, \dots n. \quad \dots [4.56]$$

Closed Boundary OBC

$$\frac{\partial m_{D_{r,j}}}{\partial r_D} = 0 \quad r_D = r_{eD_i} \quad j=1, \dots n. \quad \dots [4.57]$$

Interface conditions, Equations [4.34] and [4.35] , become

$$m_{D_{i,j}} = m_{D_{i+1,j}} \quad r_D = r_{eD_i} \quad i=1, \dots m-1 \quad j=1, \dots n, \quad \dots [4.58]$$

$$\frac{\partial m_{D_{i,j}}}{\partial r_D} = M_{i,i} \frac{\partial m_{D_{i+1,j}}}{\partial r_D} \quad r_D = r_{eD_i} \quad i=1, \dots m-1 \quad j=1, \dots n, \quad \dots [4.59]$$

where,
$$M_{i,i} = \frac{(kh)_{i+1,j}}{(kh)_{i,j}} \quad \dots [4.60]$$

The solution scheme of the diffusivity equation [4.45] along with the boundary conditions have been sought in the Laplace space which is a convenient approach. The Laplace transformations of Equations [4.45] , [4.51] , [4.52] and [4.55] through [4.59] are as follows (Laplace variable l):

$$\kappa_{i,j} \left[\frac{\partial^2 \bar{m}_{D,i,j}}{\partial r_D^2} + \frac{1}{r_D} \frac{\partial \bar{m}_{D,i,j}}{\partial r_D} \right] = \omega_{i,j} \bar{m}_{D,i,j} l + \lambda_{A,i,j} (\bar{m}_{D,i,j} - \bar{m}_{D,i,j+1}) + \lambda_{B,i,j} (\bar{m}_{D,i,j} - \bar{m}_{D,i,j-1}), \quad \dots [4.61]$$

IBC's

$$\bar{m}_{D,n} = \bar{m}_{D,n} - s_j \frac{\partial \bar{m}_{D,i,j}}{\partial r_D} \quad j=1, \dots, n, \quad \dots [4.62]$$

$$\frac{1}{l} = C_D \bar{m}_{D,n} l - \sum_{j=1}^n \kappa_{i,j} \frac{\partial \bar{m}_{D,i,j}}{\partial r_D}. \quad \dots [4.63]$$

OBC's

Infinite OBC

$$\bar{m}_{D,n} = 0 \quad r_D \rightarrow \infty \quad j=1, \dots, n \quad \dots [4.64]$$

Constant Pressure OBC

$$\bar{m}_{D,n} = 0 \quad r_D = r_{eD}, \quad j=1 \dots n, \quad \dots [4.65]$$

Closed Boundary OBC

$$\frac{\partial \bar{m}_{D,i,j}}{\partial r_D} = 0 \quad r_D = r_{eD}, \quad j=1, \dots, n. \quad \dots [4.66]$$

Interface Conditions

$$\bar{m}_{D,i} = \bar{m}_{D,i+1} \quad r_D = r_{eD}, \quad i=1, \dots, m-1 \quad j=1, \dots, n, \quad \dots [4.67]$$

$$\frac{\partial \bar{m}_{D,i}}{\partial r_D} = M_{i,j} \frac{\partial \bar{m}_{D,i+1}}{\partial r_D} \quad r_D = r_{eD}, \quad i=1, \dots, m-1 \quad j=1, \dots, n. \dots [4.68]$$

This diffusivity equation, Equation [4.61], has the form of modified Bessel's equation , thus has a solution of the following form :

$$\bar{m}_{D,i,j} = A_{i,j} K_0(\sigma r_D) + B_{i,j} I_0(\sigma r_D) . \quad \dots [4.69]$$

Introducing this solution, the left hand side of the Equation [4.61] becomes

$$\kappa_{i,j} \left[\frac{\partial^2 \bar{m}_{D,i,j}}{\partial r_D^2} + \frac{1}{r_D} \frac{\partial \bar{m}_{D,i,j}}{\partial r_D} \right] = \kappa_{i,j} \sigma^2 \bar{m}_{D,i,j} . \quad \dots [4.70]$$

Thus the diffusivity equation , Equation [4.61], now becomes

$$\lambda_{A,i,j} \bar{m}_{D,i,j+1} + \left(\sigma^2 \kappa_{i,j} - \omega_{i,j} I - \lambda_{A,i,j} - \lambda_{B,i,j} \right) \bar{m}_{D,i,j} + \lambda_{B,i,j} \bar{m}_{D,i,j-1} = 0 . \quad \dots [4.71]$$

This equation having the form of the generalized eigenvalue system, has a non-trivial solution if and only if its coefficient matrix is singular (Ehlig-Economides and Joseph, 1987). The coefficient matrix is an $n \times m$ by $n \times m$ tridiagonal matrix. As pointed out by Gomes and Ambastha (1992), this matrix can be divided into m smaller real-symmetric, positive definite tridiagonal matrices, where the σ^2 acts as the eigenvalues that are always positive. The determinant of each of these matrices is an n th order polynomial in σ^2 from which n eigenvalues can be obtained. Hence the general solution for each zone can be written as :

$$\bar{m}_{D,i,j} = \sum_{k=1}^n \left[A_{i,j}^k K_0(\sigma_i^k r_D) + B_{i,j}^k I_0(\sigma_i^k r_D) \right] . \quad \dots [4.72]$$

Constants $A_{i,j}^k$ and $B_{i,j}^k$ can be split into the following equations (Gomes and Ambastha, 1992),

$$A_{i,j}^k = E_{i,j}^k A_i^k \quad \dots [4.73]$$

and

$$B_{i,j}^k = E_{i,j}^k B_i^k \quad \dots [4.74]$$

where $E_{i,j}^k$ is the eigenvector for region i , and this eigenvector can be calculated from Equation [4.71]. The above constants are determined from the boundary conditions. The general solution for region i and layer j becomes :

$$\bar{m}_{D,i,j} = \sum_{k=1}^n \left[A_i^k E_{i,j}^k K_0(\sigma_i^k r_D) + B_i^k E_{i,j}^k I_0(\sigma_i^k r_D) \right] \quad \dots [4.75]$$

The $2n \times m$ constants can be determined from the boundary equations.

The solution is first computed without considering the wellbore storage which is later accounted for. The inner boundary condition, without wellbore storage, becomes:

$$\bar{m}_{D,w} = \sum_{k=1}^n \left[\left(A_i^k E_{i,j}^k K_0(\sigma_i^k) + B_i^k E_{i,j}^k I_0(\sigma_i^k) \right) - s_i \sigma_i^k \left(A_i^k E_{i,j}^k K_1(\sigma_i^k) + B_i^k E_{i,j}^k I_1(\sigma_i^k) \right) \right] \quad j = 1, \dots, n \quad \dots [4.76]$$

$$\frac{1}{j} = \sum_{k=1}^n \kappa_{1,j} \sum_{k=1}^n \sigma_i^k \left[A_i^k E_{i,j}^k K_1(\sigma_i^k) - B_i^k E_{i,j}^k I_1(\sigma_i^k) \right] \quad j=1, \dots, n \quad \dots [4.77]$$

Infinite OBC now becomes,

$$\sum_{k=1}^n \left[A_m^k E_{m,j}^k K_0(\sigma_m^k r_D) + B_m^k E_{m,j}^k I_0(\sigma_m^k r_D) \right] = 0 \quad r_D \rightarrow \infty \quad j=1, \dots, n \quad \dots [4.78]$$

For the pressure to be bounded for infinite OBC . Equation [4.78] , mathematically leads to the following equation :

$$\sum_{k=1}^n B_m^k = 0 \quad j=1, \dots, n. \quad \dots [4.79]$$

Constant pressure OBC becomes,

$$\sum_{k=1}^n \left[A_m^k E_{m,j}^k K_0(\sigma_m^k r_{D_w}) + B_m^k E_{m,j}^k I_0(\sigma_m^k r_{D_w}) \right] = 0 \quad j=1, \dots, n. \quad \dots [4.80]$$

Closed OBC is,

$$\sum_{k=1}^n \left[A_m^k E_{m,j}^k K_1(\sigma_m^k r_{D_w}) + B_m^k E_{m,j}^k I_1(\sigma_m^k r_{D_w}) \right] = 0 \quad j=1, \dots, n. \quad \dots [4.81]$$

The interface conditions yield :

$$\begin{aligned} \sum_{k=1}^n \left[A_i^k E_{i,j}^k K_0(\sigma_i^k r_{D_w}) + B_i^k E_{i,j}^k I_0(\sigma_i^k r_{D_w}) \right] &= \sum_{k=1}^n \left[A_{i+1}^k E_{i+1,j}^k K_0(\sigma_{i+1}^k r_{D_w}) \right] \\ &+ \sum_{k=1}^n \left[B_{i+1}^k E_{i+1,j}^k I_0(\sigma_{i+1}^k r_{D_w}) \right] \quad i=1, \dots, m-1 \quad j=1, \dots, n, \quad \dots [4.82] \end{aligned}$$

$$\begin{aligned} \sum_{k=1}^n \left[A_i^k E_{i,j}^k K_1(\sigma_i^k r_{D_w}) - B_i^k E_{i,j}^k I_1(\sigma_i^k r_{D_w}) \right] &= \sum_{k=1}^n \left[A_{i+1}^k E_{i+1,j}^k K_1(\sigma_{i+1}^k r_{D_w}) \right] \\ &- \sum_{k=1}^n \left[B_{i+1}^k E_{i+1,j}^k I_1(\sigma_{i+1}^k r_{D_w}) \right] \quad i=1, \dots, m-1 \quad j=1, \dots, n. \quad \dots [4.83] \end{aligned}$$

The above boundary conditions give a total of $2n \times m$ simultaneous equations. solution of which gives the $2n \times m$ unknown constants (A_m^k, B_m^k) .

The preceding solution model gives the laminar flow solution in dimensionless pseudopressure for any dimensionless pseudotime. This scheme is a very efficient one inasmuch as for a reservoir with 5 layers 6 zones, this model requires the solution of only

60 (= 2×5×6) simultaneous equations. Assigning a constant boundary at the bottommost layer, this model can handle bottom-water drive also. This model can treat any irregular shaped boundary by dividing the reservoir into a number of mathematical layers.

4.3 Incorporation of the High Velocity Effect :

Various investigators (Forchheimer, 1901, Smith, 1961, Swift and Kiel, 1962, Wattenbarger and Ramey, 1968, Geertsma, 1974, Firoozabadi and Katz, 1979, Ding 1986, Lee *et al.*, 1987, Oren *et al.*, 1988, Whitson and Sognesand, 1990, Civan and Evans, 1991, Osman and Mohammed, 1993, Raghavan, 1993) have studied extensively the high velocity effect. Raghavan (1993) has formulated high velocity pseudo-dimensionless pressure drop as follows :

$$\Delta p(p)_{DN} = \bar{D} q_{sc} \int_{r_w}^{r_n} \frac{dr}{kr^2}, \quad \dots [4.84]$$

where the extra subscript 'N' implies non-Darcy or high velocity responses, r_n is the radius of the small region in which the high velocity flow exists and

$$\bar{D} = \alpha_D \frac{Mk\beta\gamma_r P_{sc}}{2RT_{sc}\pi h} \quad \dots [4.85]$$

In this approach, it is assumed that stabilized steady flow exists in the region $r_w < r < r_n$, that is the mass of fluid stored in this region is constant over time. The author also commented that the integral in Equation [4.89] may be approximated with

$$\int_{r_w}^{r_n} \frac{dr}{\mu r^2} = \frac{1}{\tilde{\mu}} \left(\frac{1}{r_w} - \frac{1}{r_n} \right). \quad \dots [4.86]$$

A number of options for computing $\tilde{\mu}$ studied by Ding (1986) are as follows :

$$\begin{aligned} \tilde{\mu} &= \mu_w, \\ \tilde{\mu} &= \mu_1 = \frac{\mu_w + \mu_1}{2}, \\ \tilde{\mu} &= \mu_2 = \sqrt{\frac{\mu_w^2 + \mu_1^2}{2}}. \end{aligned} \quad \dots [4.87]$$

Lee *et al* (1987) suggested that the above approach violates the material balance principle. Their extensive research modified the high velocity pressure responses with a correlating factor C_1 . Their proposed solution is of the form :

$$\Delta m(p)_{DN} = C_1 D(\mu_i) q_{scD}. \quad \dots [4.88]$$

The correlating parameter, C_1 , depends on the product of dimensionless flow rate, q_{scD} , and turbulence intensity, N_T , for each flow regime, specifically as follows,

Laminar : $0 < q_{scD} N_T < 0.1, D=0$

$$C_1 = 1, \quad \dots [4.89]$$

Transition : $0.1 \leq q_{scD} N_T \leq 1.0,$

$$C_1 = \left(1 - \frac{r_w}{r_i} \right) F_{\mu}, \quad \dots [4.90]$$

Turbulent : $1.0 < q_{scD} N_T$

$$C_1 = \left(1 - \frac{r_w}{r_i} \right) F_{\mu} (q_{scD} N_T)^{-0.028}, \quad \dots [4.91]$$

where
$$q_{scD} = \alpha_Q \frac{P_{sc} T q_{sc}}{\pi k_r h T_{sc} m(p_i)} , \quad \dots [4.92]$$

$$N_T = \alpha_N \frac{k_r^2 \beta \gamma_r m(p_i)}{T \mu_i F_\nu} , \quad \dots [4.93]$$

$$F_\nu = \frac{\mu_i}{\mu} . \quad \dots [4.94]$$

They defined the product of dimensionless flow rate and turbulence intensity as the Forchheimer number, N_{Fo} .

$$N_{Fo} = q_{scD} \times N_T . \quad \dots [4.95]$$

The definition of turbulence factor, $D(\mu)$ is as follows,

$$D(\mu) = \alpha_D \frac{\gamma_r}{h} \int_r^r \frac{\beta k_r}{\mu r^2} dr . \quad \dots [4.96]$$

In this study, both of these methods have been investigated along with their modifications. Lee *et al.* (1987) approach is found to be more dependable. In their approach, the rigorous integration of Equation [4.96] is not undertaken, instead the integration is simplified by $D(\mu_i)$; the result is found to be almost similar to that obtained by their finite difference simulator . So their procedure is adapted. The equations are modified to incorporate the reservoir heterogeneity.

In the computation of high velocity solution with either of the above methods, the velocity coefficient, β , has to be applied. Geertsma (1974), Firoozabadi and Katz (1979) and few other investigators (Civan and Evans, 1991, Frederick and Graves, 1994) have

studied this factor. From some experimental studies, Geertsma (1974) found that this coefficient is a function of the reservoir permeability and porosity for a dry gas reservoir. Firoozabadi and Katz (1979) have given a number of options to measure β ; among which one, used in the present study, is quite frequently used. Other investigators have only slightly modified these correlations depending on their experimental findings and the presence of multiphase. One point to note is that, Geertsma (1974) correlation is suitable mainly for unconsolidated sands which may have porosity variation, while Firoozabadi and Katz (1979) correlation is suitable only for compacted sandstones.

Geertsma's (1974) relation is :

$$\beta = \frac{\alpha_{\beta 1}}{\phi^{5.5} \sqrt{k}} \quad \dots [4.97]$$

Firoozabadi and Katz (1979) relation is:

$$\beta = \frac{\alpha_{\beta 2}}{k^{1.2}} \quad \dots [4.98]$$

4.4 Convolution Scheme for Layer Flow Rate and Incorporation of Wellbore Storage :

For a multilayered reservoir, the laminar solution and high velocity solution have been determined for a constant surface flow rate. But for the surface flow rate to be constant, individual flow rate from the layers will change with the time and pressure because of wellbore storage effect and layer property variation. To take into account this variation in the layer fractional flow rates a superposition scheme is required. The use of a

convolution scheme based on Duhamel's (1833) integral formula is a rational approach. Some of the investigators (Raghavan, 1993, Whitson and Sognesand, 1990) have used this scheme. This scheme also satisfies the inner boundary condition with wellbore storage.

Literally, convolution scheme is a mathematical tool to find the value of some dependent variable while some other dependent variable is changing simultaneously with the independent variables. This tool can be used when some means are available to compute the values of the desired dependent variable with the changes in the independent variables when the other dependent variable is kept constant.

Denoting $m_{Dw}(r_D, t_D)$ as the pseudo-dimensionless pressure distribution as a result of the well producing at a constant rate, the variable flow rate may be incorporated using the general convolution property (Churchill, 1972). The pseudo-dimensionless pressure distribution with this flow rate variation will be given by (subscript p has been omitted in the following equation for t_D)

$$m_D(r_D, t_D) = \frac{\partial}{\partial t_D} \int_0^{t_D} q_D(t_D - \tau) m_{Dw}(r_D, \tau) d\tau \quad \dots [4.99]$$

Equation [4.99] may be written in view of the initial condition as

$$\begin{aligned} m_D(r_D, t_D) &= \int_0^{t_D} q_D(t_D - \tau) m'_{Dw}(r_D, \tau) d\tau, \\ \Rightarrow m_D(r_D, t_D) &= \int_0^{t_D} q_D(\tau) m'_{Dw}(r_D, t_D - \tau) d\tau, \end{aligned} \quad \dots [4.100]$$

where

$$m'_{D_w} = \frac{dm_{D_w}}{dt_D} \quad \dots [4.101]$$

Integrating by parts, Equation [4.100] may be written as for flowing well pseudo-dimensionless pressure

$$m_{D_w}(t_D) = q_D(0+)m_{D_w}(t_D) + \int_0^{t_D} q'_D(t_D - \tau)m_{D_w}(\tau)d\tau \quad \dots [4.102]$$

Partitioning (Churchill, 1972) the total time interval under consideration into subintervals, such that $0=t_0 < t_1 < \dots < t_j < t_{j+1} < \dots < t_{n+1} = t$, the Equation [4.102] becomes

$$m_{D_w}(t_D) = \sum_{j=0}^n \int_{t_j}^{t_{j+1}} q_D(\tau)m'_{D_w}(t_D - \tau)d\tau \quad \dots [4.103]$$

Now, there should be some means to compute $q_D(\tau)$. Assuming $q_D(\tau)$ to be approximated by a linear combination of the rates at t_{rj} and t_{rj+1} , a time \tilde{t}_{Dj} (Churchill, 1972) may be chosen, such that

$$\tilde{t}_{Dj} = \theta_j t_{Dj} + (1 - \theta_j)t_{Dj+1} \quad \dots [4.104]$$

where $0 \leq \theta_j \leq 1$.

Ignoring the truncation errors, Equation [4.103] may again be approximated by

$$m_{D_w}(t_D) = \sum_{j=0}^n q_D(\tilde{t}_{Dj}) \left[m_{D_w}(t_D - t_{Dj}) - m_{D_w}(t_D - t_{Dj+1}) \right] \quad \dots [4.105]$$

which is equivalent to

$$m_{D_w}(t_D) = q_D(\tilde{t}_{D0})m_{D_w}(t_D) + \sum_{j=0}^{n-1} [q_D(\tilde{t}_{Dj+1}) - q_D(\tilde{t}_{Dj})]m_{D_w}(t_D - t_{Dj+1}) \quad \dots [4.106]$$

For the case of multilayered reservoir, this general convolution scheme should be little modified to accommodate the fractional flow rate of each layer, the high velocity effect and the wellbore storage. Taking the suggestions by Whitson and Sognesand (1990) and using $\theta_j=0$ in Equation [4.104], the convolution scheme is formulated as following

$$m_{D_w}(t_D) = \frac{1}{\kappa_{1,j}} \left[f_j(t_{D1})m_{D_wLj}(t_D) + \sum_{k=1}^n [f_j(t_{Dk+1}) - f_j(t_{Dk})]m_{D_wHj}(t_D - t_{Dk}) \right] + \frac{f_j(t_D)m_{D_wNj}(t_D)}{\kappa_{1,j}} \quad j=1,2, \dots, 1, \quad \dots [4.107]$$

where j denotes the layer and the subscripts 'L' and 'N' in pseudo-dimensionless pressure denote laminar solution and high velocity solution respectively. Rearranging Equation [4.107], it becomes

$$m_{D_w}(t_D) - \frac{m_{D_wLj}(t_D - t_{Dn}) + m_{D_wNj}(t_D)}{\kappa_{1,j}} f_j(t_D) = \frac{f_j(t_{D1})}{\kappa_{1,j}} m_{D_wLj}(t_D) - \frac{f_j(t_{Dn})}{\kappa_{1,j}} m_{D_wLj}(t_D - t_{Dn}) + \frac{1}{\kappa_{1,j}} \left[\sum_{k=1}^{n-1} [f_j(t_{Dk+1}) - f_j(t_{Dk})]m_{D_wHj}(t_D - t_{Dk}) \right] \quad \dots [4.108]$$

Now Equation [4.108] should be solved satisfying the other inner boundary constraint which includes also the wellbore storage :

$$1 = C_D \frac{\partial m_{D_w}}{\partial t_D} + \sum_{j=1}^n f_j(t_D) \quad \dots [4.109]$$

Using the following approximation in the above equation,

$$\frac{dm_{D_n}}{dt_D} = \frac{m_{D_n}(t_D) - m_{D_n}(t_{Dn})}{t_D - t_{Dn}}, \quad \dots [4.110]$$

Equation [4.109] becomes

$$\frac{C_D}{t_D - t_{Dn}} m_{D_n}(t_D) + \sum_{j=1}^l f_j(t_D) = 1 + \frac{C_D}{t_D - t_{Dn}} m_{D_n}(t_{Dn}). \quad \dots [4.111]$$

So the system of Equations [4.108] and [4.111] may be written in the form

$$Ax = b \quad \dots [4.112]$$

where the coefficient matrix may be written as

$$A = \begin{bmatrix} d_1 & 0 & \dots & 0 & 1 \\ 0 & d_2 & \dots & 0 & 1 \\ 0 & 0 & \dots & & 1 \\ \cdot & \cdot & \cdot & \cdot & \cdot \\ \cdot & \cdot & \cdot & \cdot & \cdot \\ \cdot & \cdot & \cdot & d_l & 1 \\ 1 & 1 & \dots & 1 & f \end{bmatrix}, \quad \dots [4.113]$$

$$x = \begin{bmatrix} f_1(t_D) \\ f_2(t_D) \\ \cdot \\ \cdot \\ f_l(t_D) \\ m_{D_n}(t_D) \end{bmatrix}, \quad b = \begin{bmatrix} c_1 \\ c_2 \\ \cdot \\ \cdot \\ c_l \\ g \end{bmatrix}, \quad \dots [4.114]$$

where
$$d_j = -\frac{m_{D_n, lj}(t_D - t_{Dn}) + m_{D_n, nj}(t_D)}{\kappa_{lj}}, \quad \dots [4.115]$$

$$c_j = \frac{1}{K_{1,j}} \left[f_j(t_{D1}) m_{D_n, L_j}(t_D) + f_j(t_{Dn}) m_{D_n, L_j}(t_D - t_{Dn}) \right] + \frac{\sum_{k=1}^{n-1} [f_j(t_{Dk+1}) - f_j(t_{Dk})] m_{D_n, L_j}(t_D - t_{Dk})}{K_{1,j}}, \quad \dots [4.116]$$

$$f = \frac{C_D}{t_D - t_{Dn}}, \quad \dots [4.117]$$

$$g = 1 + f \cdot m_{D_n}(t_{Dn}). \quad [4.118]$$

To solve this set of simultaneous equations [4.112], as the initial fractional flow rates and pressure drops are zero, the following is used

$$f_j(t_{D0}) = 0, \quad m_{D_n}(t_{D0}) = 0, \quad t_{100} = 0. \quad \dots [4.119]$$

The numerical procedure yields accurate answers if 22 points per log cycle are used (Onur *et al.*, 1986). For any cycle the points are

$$t_{i+K} = t_i (1 + 0.2K), \quad \dots [4.120]$$

$$t_{i+10+K} = t_i (3 + 0.5K), \quad \dots [4.121]$$

for $K = 1, 2, \dots, 10$,

$$t_{i+20+K} = t_i (8 + K), \quad \dots [4.122]$$

for $K = 1, 2$.

4.5 Solution Methodology

The pressure responses for a composite multilayered reservoir are obtained from the preceding discussion. To arrive at the final response, the following sequences of steps are

followed. Figure 4.2 illustrates a flow diagram showing all the sequences and interconnections between the steps of arriving at the final solution.

4.5.1 Solution Methodology for Laminar Solution

Steps involved to solve the laminar flow Equation [4.72] are :

- From Equation [4.71] eigenvalues and eigenvectors are calculated using appropriate subroutine from the IMSL Math Library (User's Manual, 1994).
- From the boundary conditions, $2n \times m$ simultaneous equations are set up and solved using Gauss' elimination routine from the IMSL Math Library (User's Manual, 1994) for the constants A_i^k and B_i^k .
- Dimensionless pressure in Laplace space is calculated using Equation [4.72] and then numerically inverted into real space using Stehfast (1970) algorithm.

The computation process involves iterated calculation of Bessel's functions. Very small and large arguments of Bessel's functions might cause overflow problem. To avoid this, a dimensionless radius, r_D , is used based on the minimum front radius, R_1 , instead of nondimensionalizing them based on the wellbore radius. Also the exponentiated form of Bessel's function is used for the overflow problem.

4.5.2 Computation of real variables :

In the next step the real variables are obtained by the following procedures :

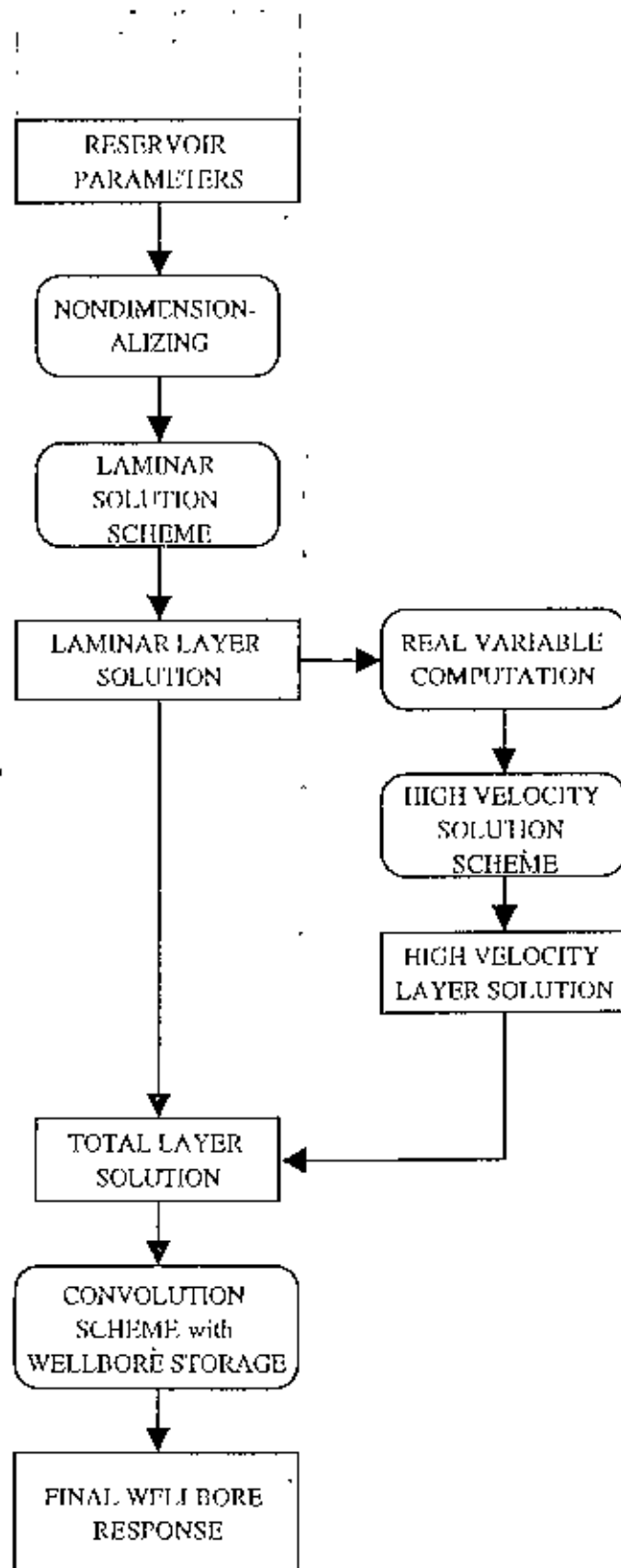


Figure 4.2 : Flow Diagram showing the sequences and the interconnections between the various schemes of the model.

First, the pseudopressures and pseudotimes are obtained by algebraic manipulation of Equation [4.38] and Equation [4.39] ,

$$m_{D_w} = \frac{2\pi(\overline{kh})}{Q} \frac{T_{sc}}{Tp_{sc}} (m_w - m_{wf}) , \quad \dots [4.38]$$

$$t_{pD} = \frac{t_p}{r_w^2} \left(\frac{\overline{kh}}{\phi \mu} \right) , \quad \dots [4.39]$$

with
$$m_{wf} = m_w - \frac{Q}{2\pi(\overline{kh})} \frac{Tp_{sc}}{T_w} m_{D_w} , \quad \dots [4.123]$$

$$t_p = t_{pD} r_w^2 \left(\frac{\overline{\phi h}}{\overline{kh}} \right) \quad \dots [4.124]$$

Now from the definition of pseudopressure, Equation [4.8], the pseudopressure is obtained for any corresponding pressure. For which, some correlations for compressibility factor and viscosity of real gases are used. For compressibility factor, the options are the two correlations : Dranchuk and Abou-Kassem (1975) correlation, and Hall and Yarborough (1973) correlation. For viscosity, the options used are the two correlations : Lee, Gonzales and Eakin (1966) correlation, and Carr, Kobayashi and Burrows (1954) correlation. Then an interpolation scheme is used to have the value of pressure for any corresponding pseudopressure. ,

Now by algebraic manipulation of the definition of pseudotime, Equation [4.17], the real time is obtained,

$$t_p = \int_0^t \frac{1}{c\mu} dt' \quad \dots [4.17]$$

The above equation is transformed into

$$t = \int_0^{t_p} c(p_w)\mu(p_w) dt'_p \quad \dots [4.125]$$

For this scheme a correlation is used for isothermal compressibility of the gas with pressure and the corresponding pressure values are used for any incremental pseudotime values obtained from the laminar solutions. Mattar, Brar and Aziz (1975) correlation is used for the compressibility computation. So all the real variables are obtained. For any dimensionless pseudotime, the corresponding laminar pressure drop and real time are determined.

As the real time is known, conventional dimensionless real time can be computed using the following definition of dimensional time,

$$t_D = \frac{\overline{kht}}{\phi h i(\mu c) r_w^2} \quad \dots [4.126]$$

The radius of investigation is also computed using the definition

$$\frac{r_i}{r_w} = 1.5\sqrt{t_D} \quad \dots [4.127]$$

4.5.3 Solution Methodology for High Velocity Solution

After calculation of real variables, the high velocity effect is incorporated undergoing the following steps :

- For any dimensionless pseudotime, the corresponding laminar solution is taken as the initial guess in the iteration process to evaluate high velocity responses.
- For this initial guess, the real variables (pressure, time) are measured and the radius of investigation is determined.
- Equivalent permeability and porosity along the radial direction are evaluated to incorporate reservoir heterogeneity in the computation of the velocity coefficient β . For calculating β , the options are either of Geertsma (1974) or Firoozabadi and Katz (1979) relation.
- With the computed β , the turbulence intensity, N_T , is measured from Equation [4.93].
- For the constant flow rate the dimensionless flow rate, q_{scD} is determined, and from the product of this and the turbulence intensity, the Forchheimer number, N_{Fo} , is obtained.
- For this value of Forchheimer number the flow regime is determined according to the Equations [4.89], [4.90] and [4.91]. Determining the flow regime, the correlating parameter, C_f is Viscosity ratio, F_{μ} , is calculated from Equation [4.94] using the present wellbore pressure and corresponding fluid properties.
- Having measured the above quantities, $D(\mu)$ is measured from Equation [4.96]. The integration is performed for each zone separately as the variables of integration remain constant in any zone or region.

$$D(\mu_i) = \alpha_D \frac{\gamma_s}{h\mu_i} \left[\left(\frac{\beta_1 k'_1}{r_1 - r_w} \right) + \left(\frac{\beta_2 k'_2}{r_2 - r_1} \right) + \dots + \left(\frac{\beta_m k'_m}{r_i - r_{m-1}} \right) \right]$$

$m =$ zone up to which radius of investigation reaches ... [4.128]

- Now the pseudopressure drop due to inertial and turbulence effect is measured from Equation [4.88] and the total pseudopressure drop is computed from the Equation [4.129].

$$\Delta m(p)_{DV} = C_1 D(\mu_i) q_{sc} \quad \dots [4.88]$$

and

$$\Delta m(p)_{DTotal} = \Delta m(p)_{DI} + \Delta m(p)_{DV} \quad \dots [4.129]$$

This total pseudopressure drop is now taken as the next approximation and the whole exercise is repeated until the pseudopressure drop converges

4.5.4 Solution Methodology to Incorporate the Convolution Scheme with Wellbore Storage :

The steps involved in the laminar solution (Section 4.5.1), real variable determination (Section 4.5.2) and high velocity responses (Section 4.5.3) are undertaken for each layer for a multilayered reservoir. For each layer, the elements of the matrices defined in Equation [4.113] and [4.114] are determined and stored sequentially. The simultaneous equations in Equation [4.112] are set up and solved using Gauss' elimination routine from the IMSL Math Library (User's Manual, 1994) for the final wellbore dimensionless

pseudopressure and also the fractional flow rate from each layer. This scheme has been adapted in such a manner so that it takes into account the wellbore storage effect.

4.5.5 Derivative Determination :

Having obtained the final wellbore pseudo-dimensionless pressure using the preceding schemes, the derivative of the pseudo-dimensionless pressure is determined. A simple scheme is used for the computation. The algorithm uses one point before and one point after the point of interest, takes the difference of these two values, and divides the difference by the interval. This value is updated by taking a narrower interval within a tolerance value. For every log cycle the interval is modified by an amplification factor

5.0 MODEL VALIDATION

The present study develops a semi-analytical model for composite multilayered gas reservoirs. Not much work has been done on gas well testing of heterogeneous reservoirs. The validation of this semi-analytical model is done by generating some homogeneous reservoir responses and comparing them with familiar pressure transient responses for the corresponding homogeneous cases. Homogeneous reservoir situation, which is a subset of the general reservoir model, is simulated by assigning same permeability, porosity and thickness values for each of the regions and layers.

Al-Hussainy *et al.* (1966) correlated the solutions for flow of ideal gases in homogeneous reservoirs with liquid flow solutions by computing the viscosity term in the dimensionless time at the initial pressure. High velocity effect is not considered in their work. Figure 5.1 shows a comparison of laminar responses (i.e. without any high velocity effect) of the present study with Al-Hussainy *et al.* (1966) solutions. The triangles and the dots show Al-Hussainy *et al.* (1966) responses and the solid lines show responses from this study. The figure suggests that the laminar solutions are not functions of the flow rate inasmuch as the change in the flow rate does not change the dimensionless laminar pressure responses. In fact, the laminar responses are exactly equal to the liquid solutions. This figure also shows the effect of the closed boundary reservoir on the laminar solution. Value of the dimensionless outer boundary radius used here is 4800. Bounded reservoir responses are the same as that of the infinite reservoir until the

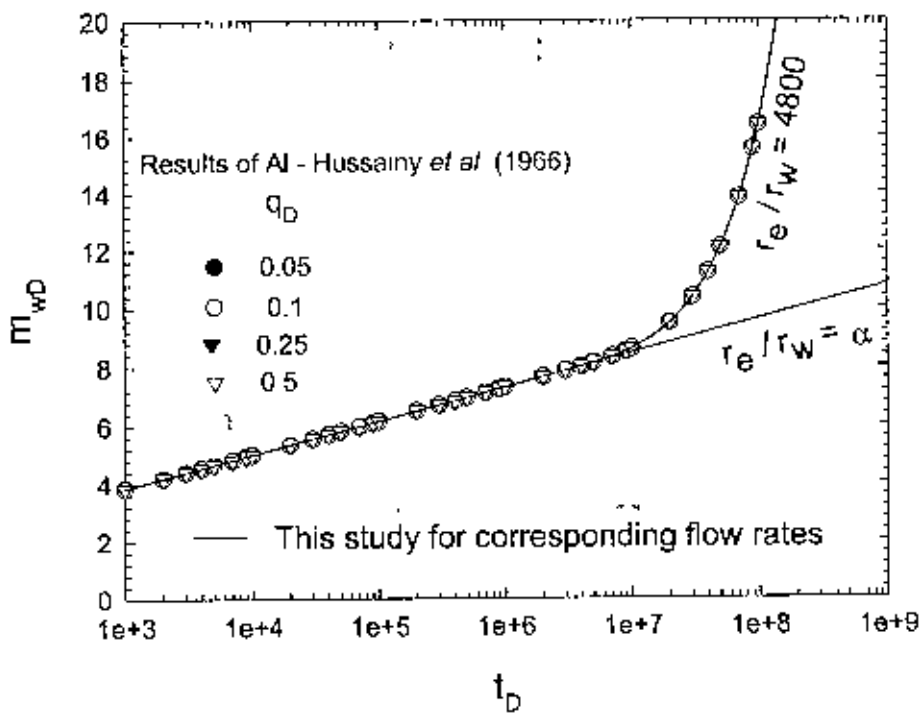


Figure 5.1 : Comparison of this study with Al-Hussainy *et al.* (1966) solution for a homogeneous reservoir.

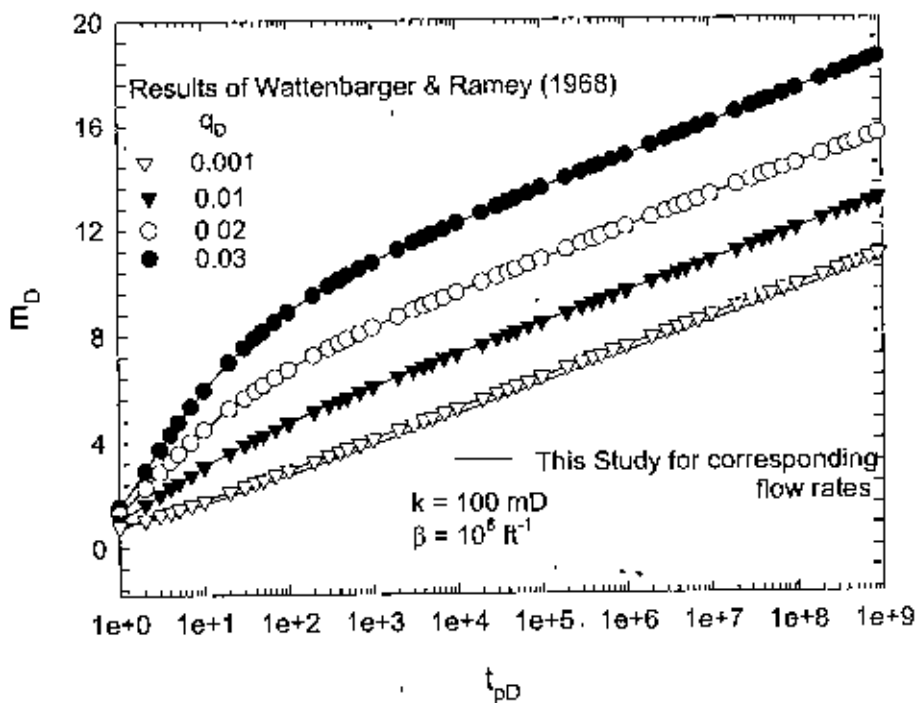


Figure 5.2 : Comparison of this study with Wattenbarger and Ramey (1968) solution with high velocity effect.

pressure responses reach the outer boundary when it deviates from the infinite-acting solution. Wattenbarger and Ramey (1968) used a numerical model to generate solutions for real gas flow problems in homogeneous reservoir conditions. Their model included formation damage, wellbore storage and high velocity effect. Figure 5.2 shows the influence of inertial effects on the responses of infinite acting homogeneous gas reservoirs. The triangles and the dots show Wattenbarger and Ramey (1968) results and the solid lines show responses from this study. Figure 5.2 shows that the results from this study exactly match with those of Wattenbarger and Ramey (1968) for different flow rates. This figure also reveals that with the increasing flow rate the pressure drop increases, whereas for the laminar responses, dimensionless pseudopressure drop is not a function of flow rate as shown in the figure. The solution has been generated for a constant β factor (10^8 ft^{-1}) and homogeneous reservoir permeability of 100 mD.

Simulating a large of real gas flow situations, Lee *et al* (1987) suggested a new approach to modify the turbulence factor, $D(\mu)$, in the existing literature of high velocity effect, by a correlating parameter, C_1 . They validated their new approach by the responses generated with a finite difference simulator. Figure 5.3 compares the responses of this model with the solutions generated by Lee *et al*: (1987). The triangles and the dots show their generated results and the solid lines show responses from this study. This figure also shows the effect of turbulence intensity, N_T , on the wellbore pressure responses. The responses have been generated for a constant dimensionless flow rate of 0.01. It is worth

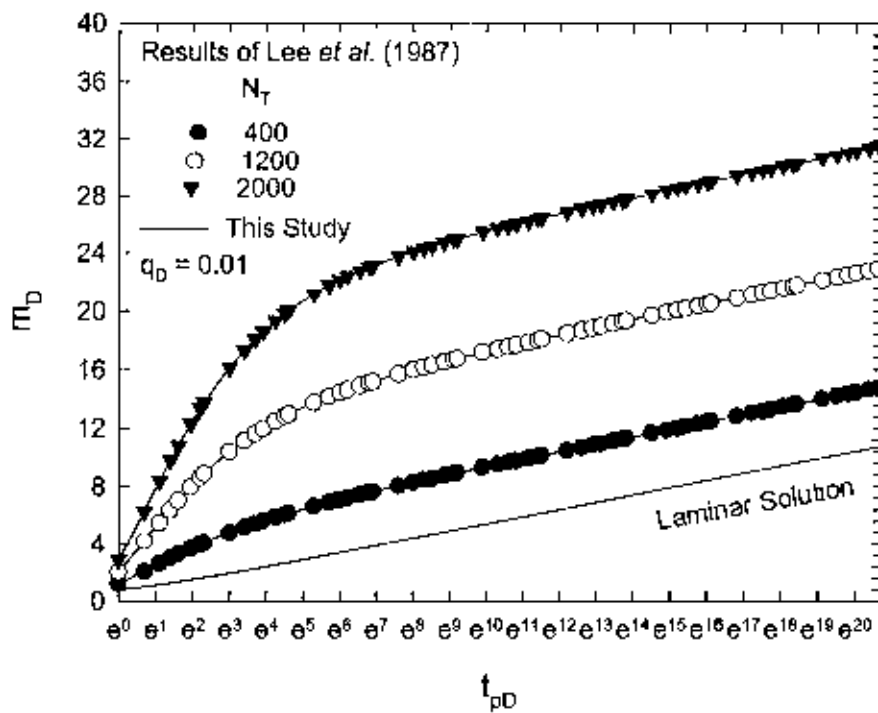


Figure 5.3 : Comparison of this study with Lee *et al.* (1987) solution with high velocity effect.

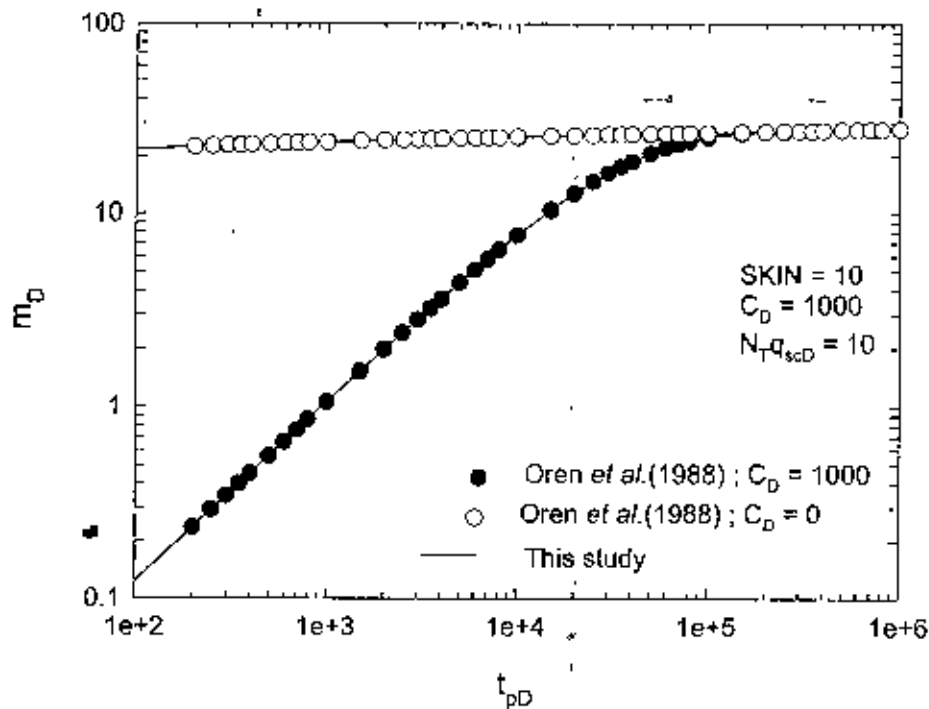


Figure 5.4 : Comparison of this study with Oren *et al.* (1988) solution with wellbore storage and skin.

mentioning here that in this study responses have been generated for different sets of initial pressure level and permeability, but the responses are found to be same for a particular turbulence intensity level. The reason for this is that the responses depend on the turbulent intensity, which depends on β , velocity coefficient. The velocity coefficient, in turn, is a function of permeability and porosity (Geertsma, 1974, Firoozabadi and Katz, 1979). Thus, if the turbulence intensity is changed by arbitrarily changing β irrespective of the reservoir properties, the responses would not reflect the actual reservoir characteristics. Hence, it is not sensible to arbitrarily fix a constant β (or the turbulence intensity level) and change the permeability and porosity.

Lee *et al.* (1987) could not handle wellbore storage in their model. Their model was extended by Oren *et al.* (1988) to include effect of wellbore storage. Oren *et al.* (1988) used an exponential decay factor multiplied to the solution obtained by Lee *et al.* (1987). Figure 5.4 includes the combined effect of wellbore storage and skin. The responses of the present work are compared with those obtained by Oren *et al.* (1988). The dots show their results while the solid lines show responses from this study.

Osman and Mohammed (1993) have studied multilayered commingled reservoir and have generated a number of figures for certain layer heterogeneities. Some discrepancies are there in their generated responses. Their reasoning does not seem to be plausible. This is discussed later (Section 6.7) when the effects of layering are discussed in detail.

6.0 RESULTS AND DISCUSSIONS

The present study develops a semi-analytical model for the pressure transient analysis of heterogeneous gas reservoirs. Effects of various reservoir situations can be studied with this model. This model has the potential of performing many in-depth studies of composite layered gas reservoirs. In this study, only a few important sensitivity studies have been done. First, different parameters are studied to observe their effect on the pressure transient responses for homogeneous reservoir situations. The parameters, studied, are effects of skin and wellbore storage, velocity coefficient, flow rate, initial pressure, permeability and finite formation damage. Layering effect, closed boundary effect and some composite reservoir responses are studied subsequently.

6.1 Effect of Wellbore Storage and Skin

Initially, the gas produced at the surface comes from the wellbore. For these very early times, the plot of dimensionless pseudopressure and pseudotime has a unit slope. Duration of this wellbore storage dominated period depends on the wellbore storage coefficient, which is a function of the wellbore storage volume and the compressibility of the gas. On the other hand, skin effect is the effect on the pressure transient responses due to the altered permeability region surrounding the wellbore. A high value of skin implies adverse permeability condition in the wellbore vicinity. Thus, the pressure drop will be higher for higher skin values. The effect of skin is accommodated here by the thin skin approach (Craft and Hawkins, 1991).

Agarwal type-curves show the variation of wellbore storage and skin for an infinite-acting homogeneous reservoir with the well located in the center. Similar figure (Figure 6.1) is generated illustrating these effects using the present model. This figure has been generated for a dimensionless flow rate of 0.025, initial pressure of 3000 psia, reservoir permeability of 250 mD and the Geertsma (1974) correlation as the velocity coefficient. Agarwal type-curves are not dependent on these parameters as they depict the liquid solution. On the contrary, the gas responses are affected by these parameters. Figure 6.1 shows the same trend of pseudo-dimensionless pressure with pseudo-dimensionless time as in the Agarwal type-curves of dimensionless pressure with dimensionless time. The figure shows that higher the value of the skin, higher is the pressure drop. The effect of wellbore storage is also shown in the figure. It is evident from the figure that early time pressure drop decreases with the increase in the wellbore storage coefficient. This is because increase in wellbore storage coefficient implies increase in the wellbore storage volume for which the sand face pressure depletion is retarded.

6.2 Effect of Velocity or Turbulence Coefficient (β)

Various investigators have given their views on high velocity effect on the fluid flow through porous media. Geertsma (1974) and Firoozabadi and Katz (1979) were among the first to develop some correlation of the velocity coefficient with the reservoir permeability and porosity. Later, investigators Civan and Evans (1991), Frederick and Graves (1994) and others have found the dependence of this coefficient on the fluid

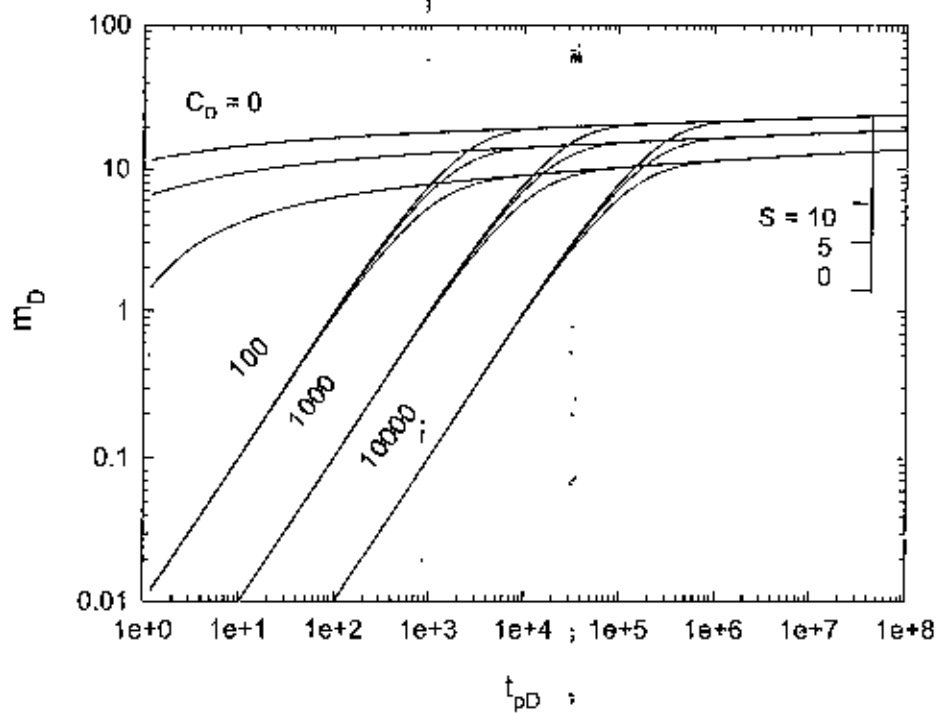


Figure 6.1 : Effects of wellbore storage and skin on pseudo-dimensionless pressure responses for an infinite acting homogeneous reservoir.

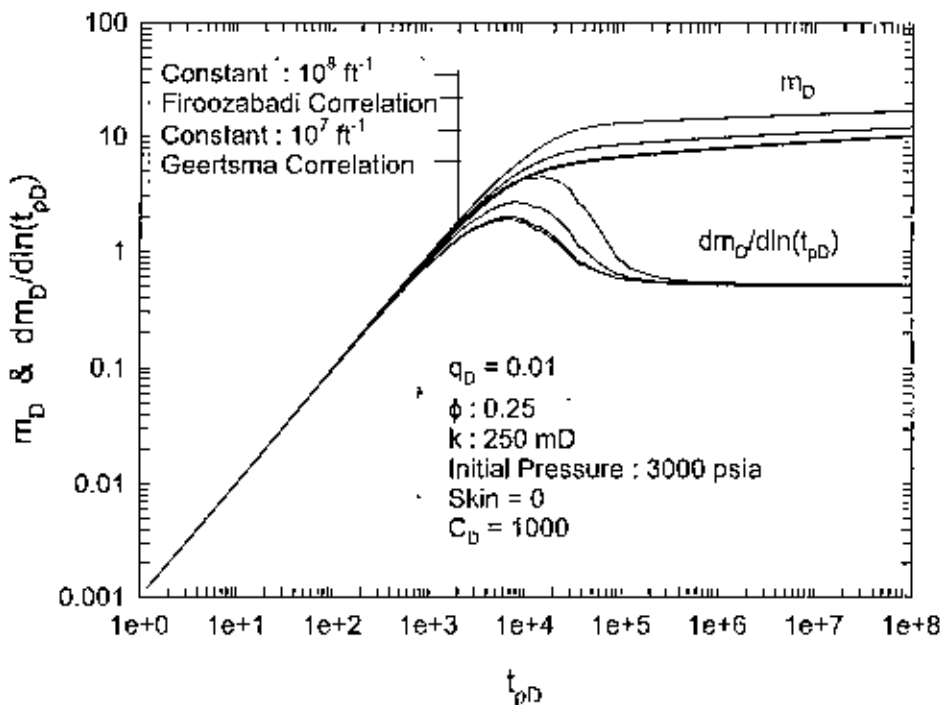


Figure 6.2 : Effect of Velocity Coefficient on Pseudopressure and Derivative Responses (Skin = 0).

saturation too. They have come up with different empirical relations. In many pressure transient analyses, the studies were taken up with arbitrarily fixing the velocity coefficient, β , irrespective to the reservoir permeability, porosity and saturation. In this study since only gas reservoirs are analyzed, the question of fluid saturation is not considered. Hence the Geertsma (1974) and Firoozabadi and Katz (1979) correlation are used. The effect of assuming constant β is also investigated.

Figures 6.2, 6.3 and 6.4 show the effect of the velocity coefficient on dimensionless pseudopressure and derivative responses for a homogeneous, infinite-acting reservoir with skin value of 0, 2 and 5 respectively. These responses have been generated for a constant dimensionless flow rate of 0.01, with reservoir porosity 0.25, permeability 250 mD, initial pressure of 3000 psia and wellbore storage coefficient 1000. From the responses, it is apparent that the Firoozabadi and Katz (1979) correlation gives a higher pressure drop than the Geertsma's (1974) one, for the reservoir situation depicted here. It is also evident from the figures that constant β approach does not reflect the actual reservoir condition. These responses may be quite different from the actual reservoir responses (Geertsma, 1974, or Firoozabadi and Katz, 1979, responses). These figures indicate that a value of 10^7 ft^{-1} for β might be reasonable for the above stated reservoir condition. For these values of permeability, porosity of the reservoir the β coefficient from Geertsma (1974) correlation is about 6283479.1 ft^{-1} whereas from Firoozabadi and Katz (1979) correlation it is about $3.447 \times 10^7 \text{ ft}^{-1}$. From the corresponding semi-log plots of the pressure and the derivatives for skin 0 and 5 (Figures 6.5, 6.6, 6.7 and 6.8), the

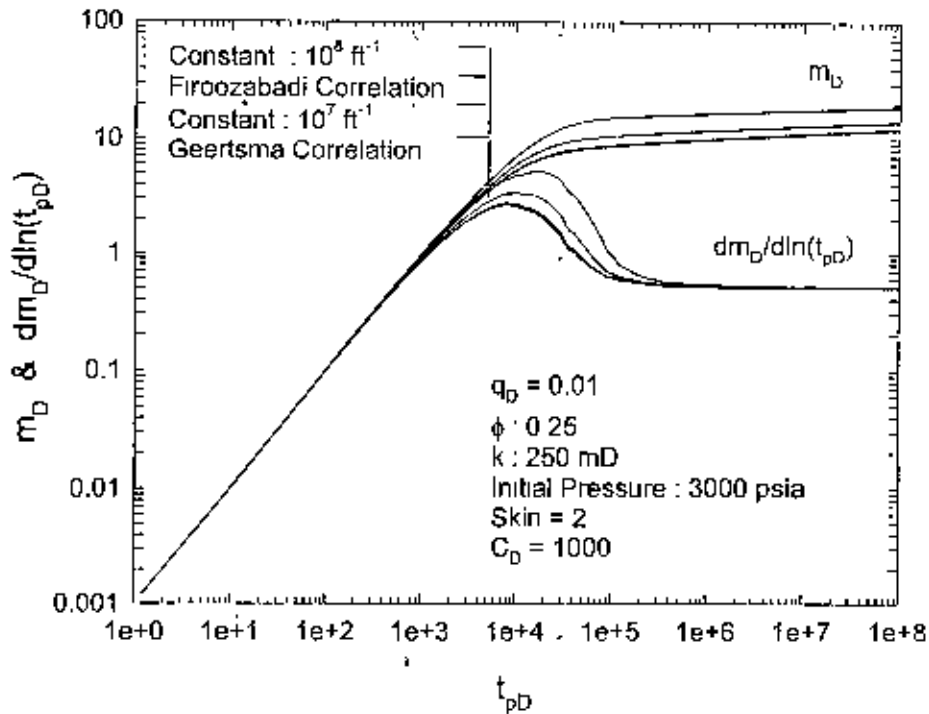


Figure 6.3 : Effect of Velocity Coefficient on Pseudopressure and Derivative Responses (Skin = 2).

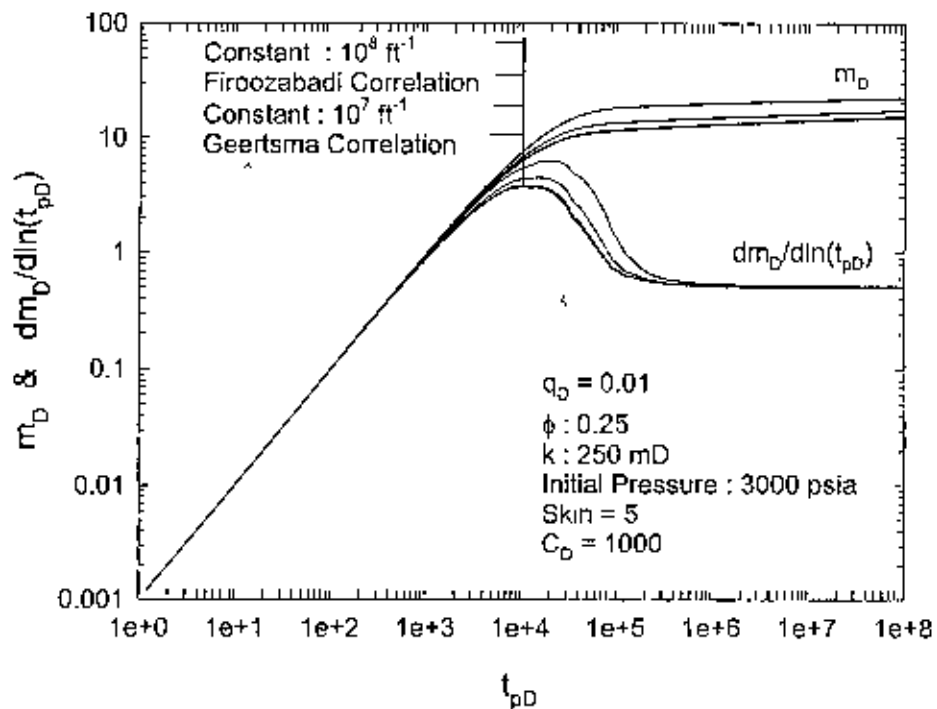


Figure 6.4 : Effect of Velocity Coefficient on Pseudopressure and Derivative Responses (Skin = 5).

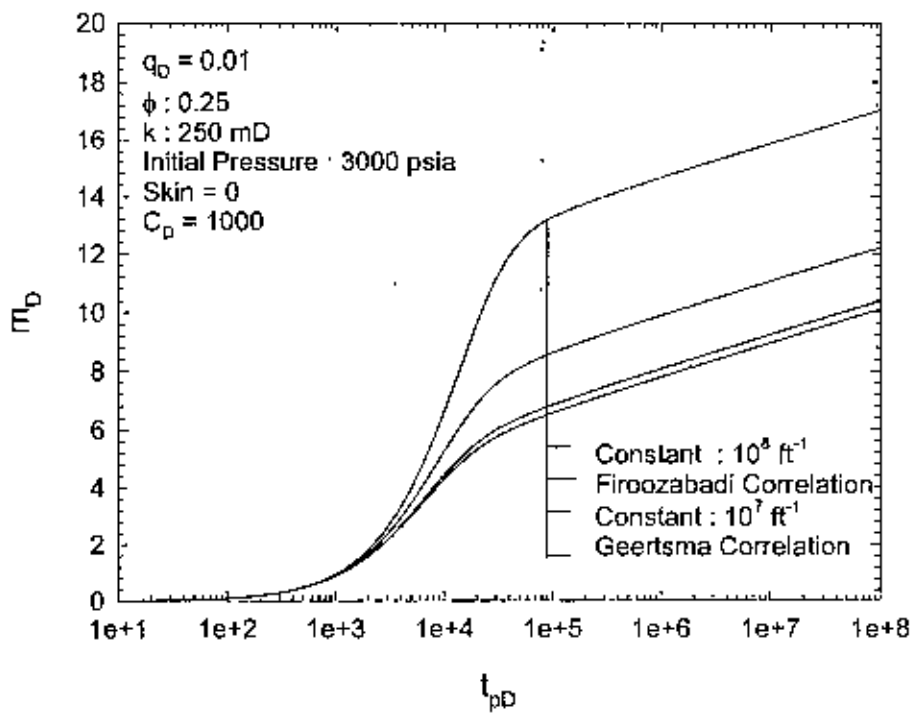


Figure 6.5 : Effect of Velocity Coefficient on Pseudopressure Responses (Skin = 0).

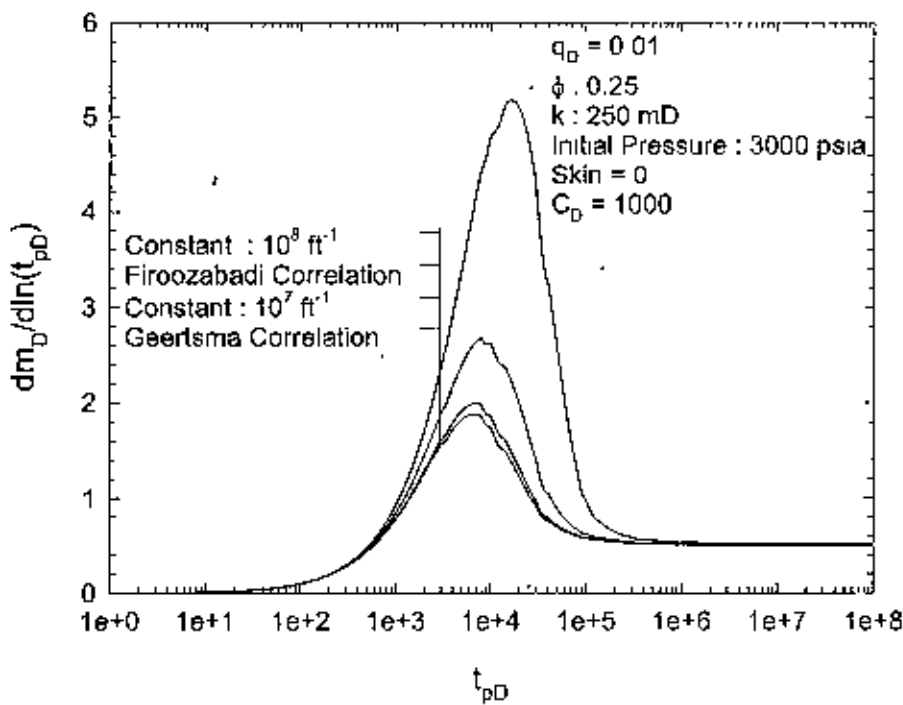


Figure 6.6 : Effect of Velocity Coefficient on Pseudopressure Derivative Responses (Skin = 0).

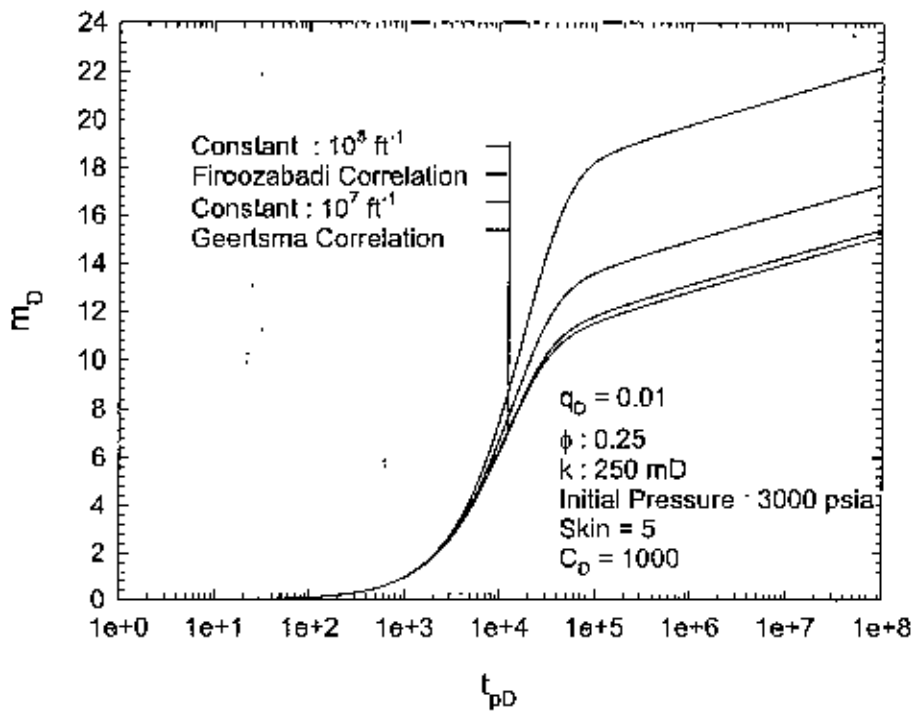


Figure 6.7 : Effect of Velocity Coefficient on Pseudopressure Responses (Skin = 5).

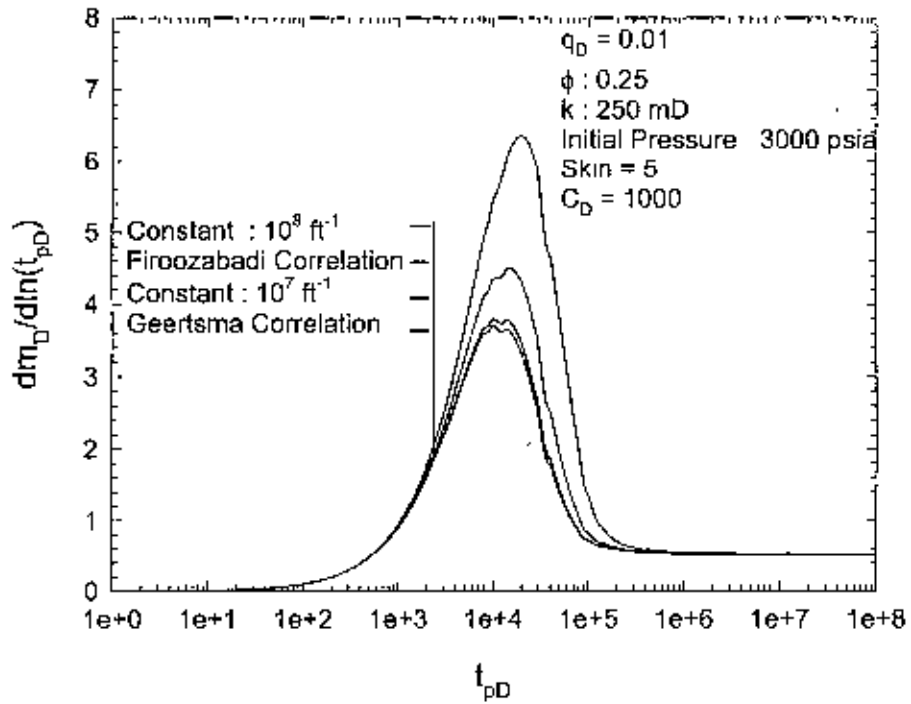


Figure 6.8 : Effect of Velocity Coefficient on Pseudopressure Derivative Responses (Skin = 5).

differences in the responses are amplified. The beginning of the semi-log straight line or the transient state is a function of β . For semi-log straight line to begin, pseudo-dimensionless times are : for Geertsma (1974) correlation - 0.9×10^6 , for constant β value of 10^7 ft^{-1} - 1.6×10^6 , for Firoozabadi and Katz (1979) correlation - 2.0×10^6 , and for constant β value of 10^8 ft^{-1} - 3.5×10^6 . It is also evident from these figures that the separations in the responses are much more prominent in the early time derivative plots (Figures 6.5 and 6.6 for pseudopressure responses and 6.7 and 6.8 for pseudopressure derivative responses). Hence at the early time the derivative responses are more indicative of the reservoir characteristics. Figure 6.9 illustrates the responses with different skin values (0, 2, 5 and 10) for the same reservoir condition with the Geertsma (1974) correlation for β . From the figure, it is observed that for higher skin, the reservoir attains the transient state at a later time.

From these responses it can be concluded that responses with arbitrary values of β are not representative of the actual reservoir condition; hence the constant β options will not be used for further studies. Also it is expected to get higher responses with the Firoozabadi and Katz (1979) correlation than with the Geertsma (1974) correlation for most of the reservoir situations. This is because Firoozabadi and Katz (1979) correlation gives a higher value of β than that given by the latter. Higher the value of β , higher would be the pressure responses.

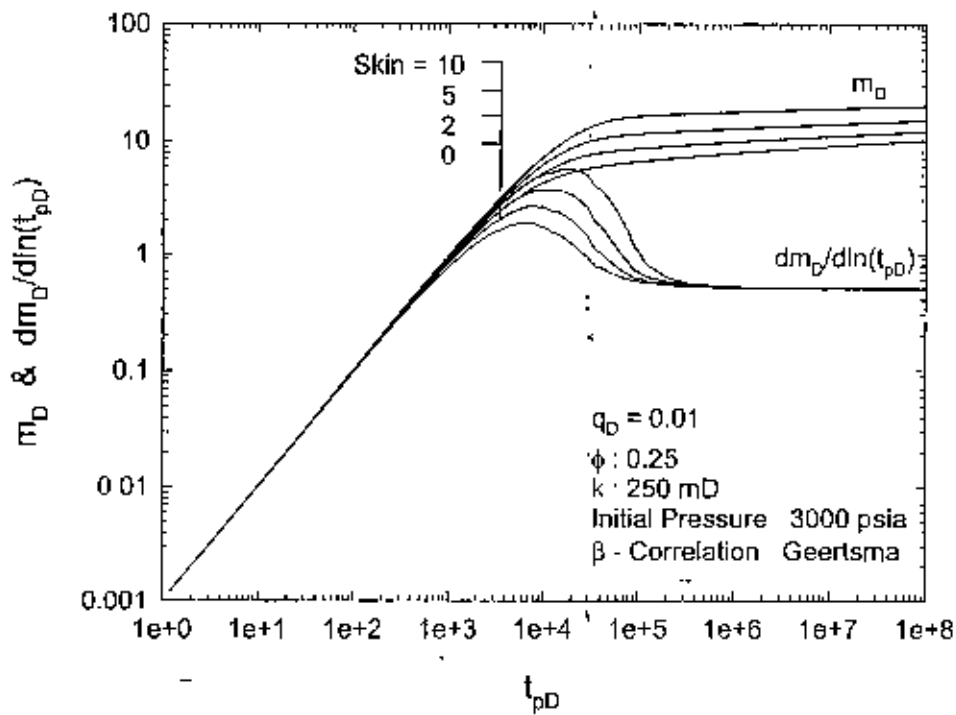


Figure 6.9 : Effect of Skin on Pseudopressure and Derivative Responses with Geertsma Correlation

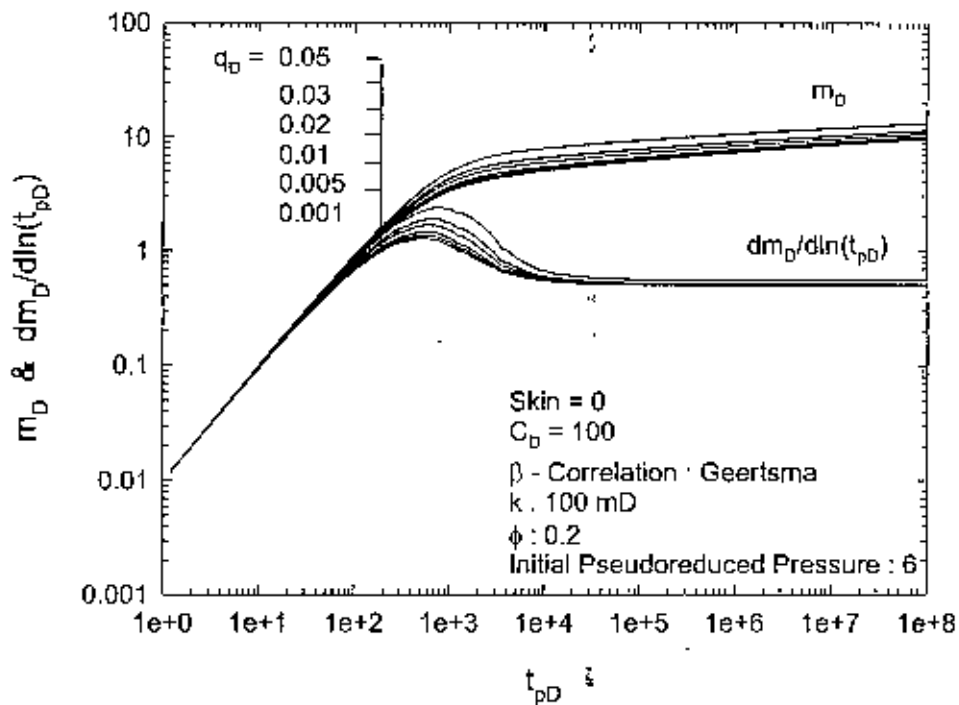


Figure 6.10 : Effect of Flow Rate on Pseudopressure and Derivative Responses (Skin = 0, Geertsma Correlation).

6.3 Effect of Velocity or Flow Rate

For gas reservoir, velocity or the flow rate has a significant effect on the pressure transient responses because of the inertial or the turbulence effect. This effect has been studied by generating a number of responses with different dimensionless flow rates for a homogeneous reservoir. Since the reservoir is homogeneous, the dimensionless flow rate is proportional to the actual flow rate for the same reservoir condition (refer to Equation 4.92). First responses are generated with Geertsma (1974) correlation, then for the same reservoir conditions the corresponding set of figures are generated with Firoozabadi and Katz (1979) correlation.

Figures 6.10, 6.11 show the pseudopressure and derivative responses for skin values of 0 and 5 respectively. Figures 6.12, 6.13, 6.14 and 6.15 show the corresponding semi-log plots for the same skin values. The responses are generated for permeability- 100 mD, porosity- 0.2, wellbore storage coefficient- 100 and initial pseudoreduced pressure- 6 (about 4000 psia). The dimensionless flow rates used are 0.001, 0.005, 0.01, 0.02, 0.03 and 0.05. All these responses are obtained with Geertsma (1974) correlation. Some responses for the same reservoir condition and skin equal to 5 are generated and shown in Figure 6.16 using Firoozabadi and Katz (1979) correlation for β factor. From the responses it is clear that when the flow rate is higher, the pressure drop is higher. For a very high rate ($Q_D > 0.03$, about 118 MMSCFD for this specific reservoir condition) the pressure responses are very high. The semi-log plots of pseudopressures (Figures 6.12 and 6.13) amplify the differences in the dimensionless responses. It is also evident from

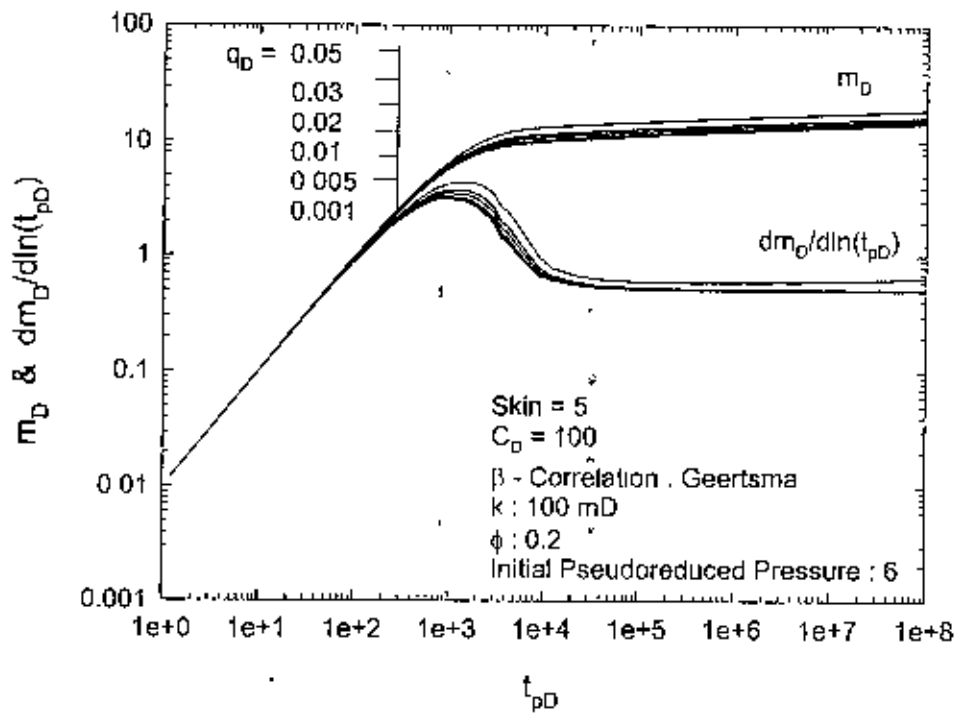


Figure 6.11 : Effect of Flow Rate on Pseudopressure and Derivative Responses (Skin = 5, Geertsma Correlation).

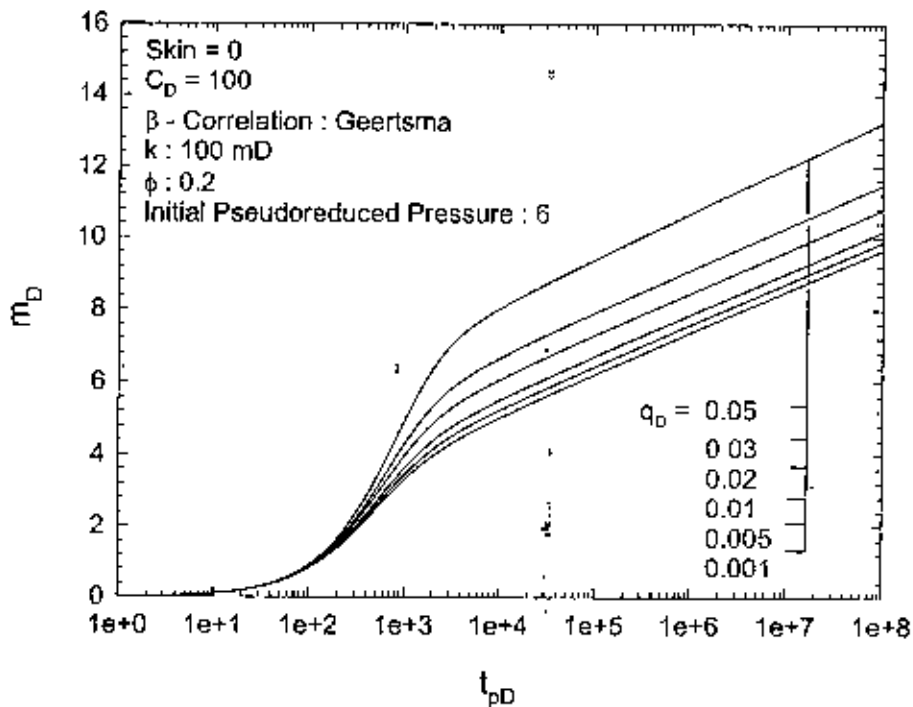


Figure 6.12 : Effect of Flow Rate on Pseudopressure Responses (Skin = 0, Geertsma Correlation).

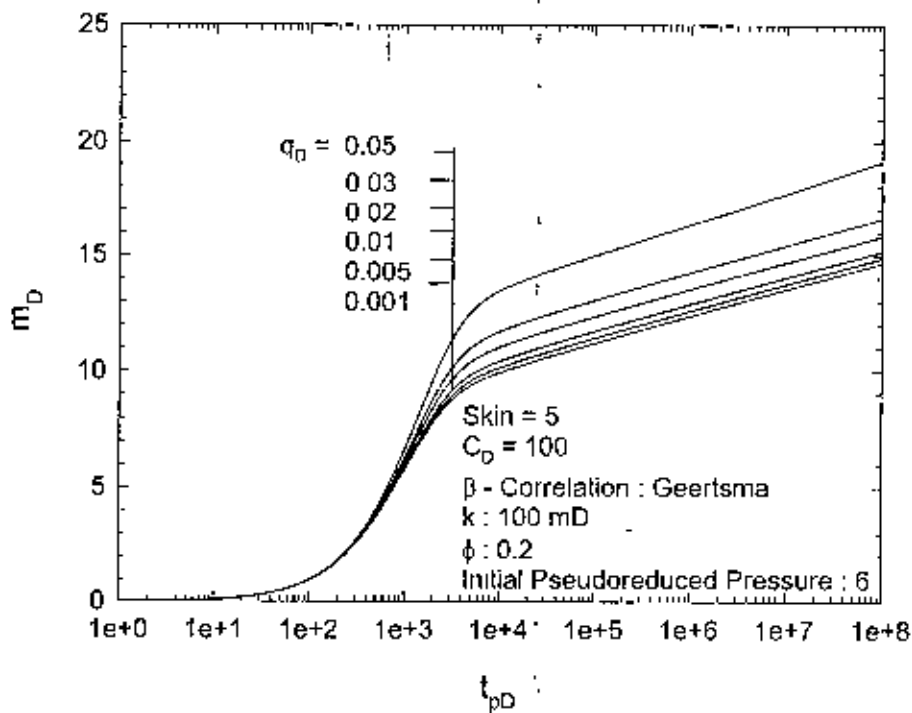


Figure 6.13 : Effect of Flow Rate on Pseudopressure Responses (Skin = 5, Geertsma Correlation).

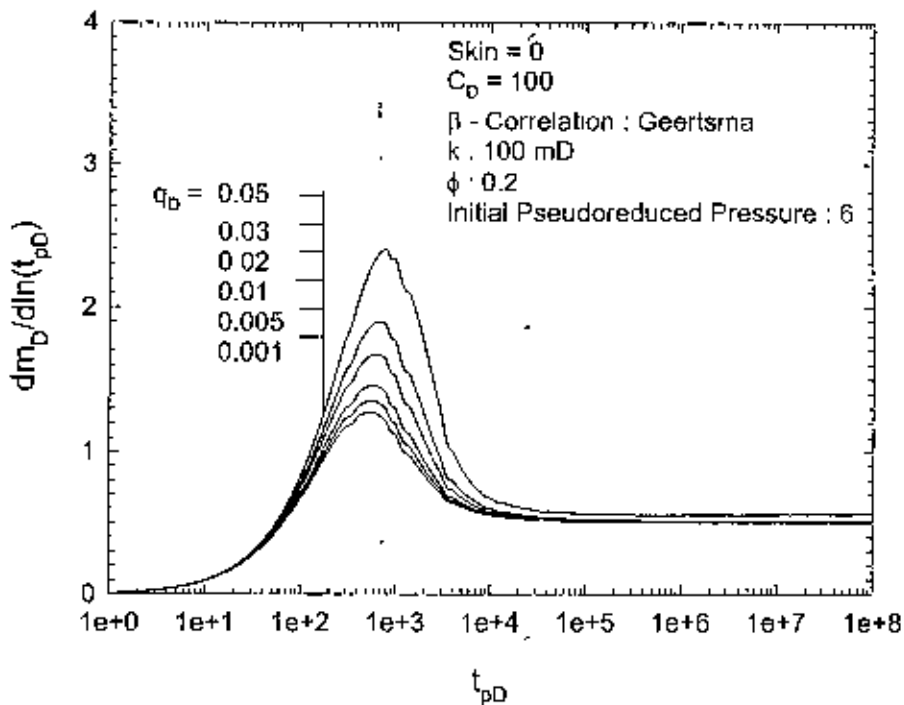


Figure 6.14 : Effect of Flow Rate on Pseudopressure Derivative Responses (Skin = 0, Geertsma Correlation).

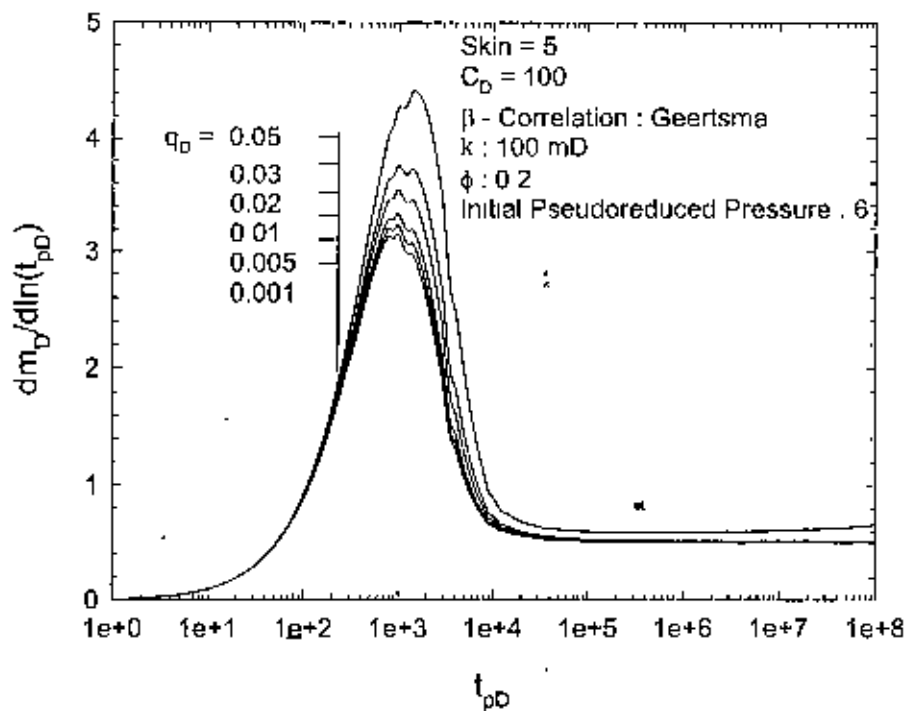


Figure 6.15 : Effect of Flow Rate on Pseudopressure Derivative Responses (Skin = 5, Geertsma Correlation).

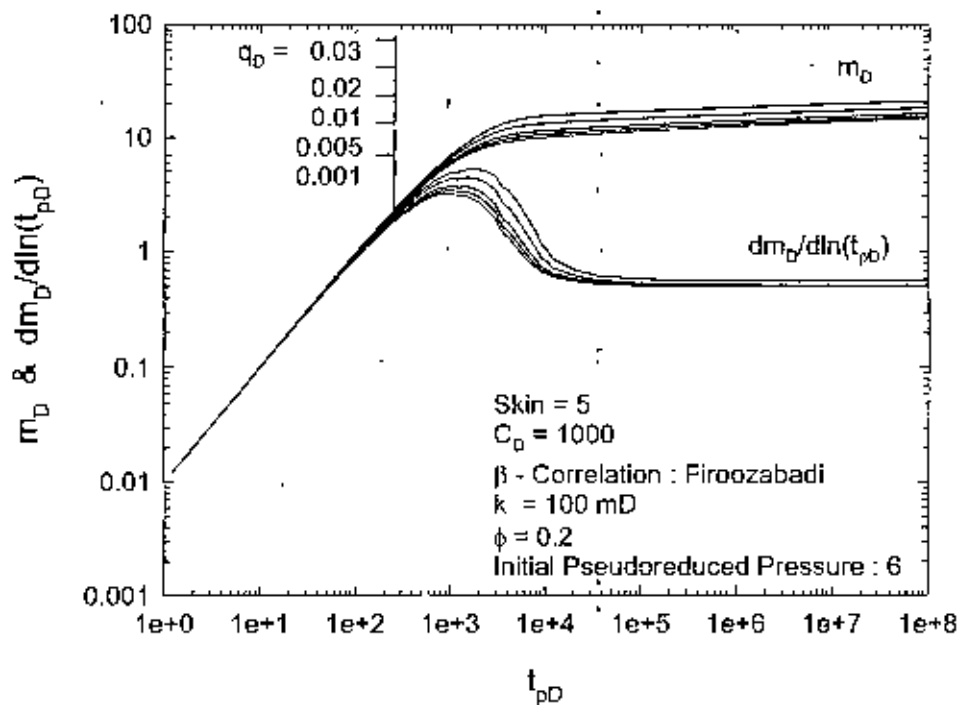


Figure 6.16 : Effect of Flow Rate on Pseudopressure and Derivative Responses (Skin =5, Firoozabadi & Katz Correlation).

the Figures 6.14 and 6.15 that the beginning of transient period is delayed for the higher flow rates. The semi-log slope attains a higher value than 0.5 for $Q_D > 0.03$; for a Q_D of 0.02 the semi-log slope is 0.51, for Q_D of 0.03 it is 0.52 while for Q_D of 0.05 the slope does not attain a constant value. This happens because the pressure declines at a greater rate for higher flow rates. From these two figures it is also apparent that the time between end of wellbore storage dominated state and the transient state increases with the flow rate. Comparing Figure 6.11 with Figure 6.16, both for skin equal to 5, it may be noticed that the pseudopressure drop is even higher in case of Firoozabadi and Katz (1979) correlation than that with Geertsma (1974) correlation because of the higher β value. With Firoozabadi and Katz (1979) correlation, the high velocity effect is more prominent even at a lower flow rate ($Q_D > 0.005$). As a consequence the semi-log straight line also starts later for $Q_D > 0.005$.

6.4 Effect of Initial Pressure

Taking a quick look on the definition of the turbulence intensity, one might suppose that the initial pressure is one of the factors affecting the pressure responses. This is contrary to what has been observed from the responses generated. This is because the high velocity responses depend on the product of turbulence intensity and dimensionless flow rate, i.e. Forchheimer number. This number does not depend on the initial pressure

Figures 6.17 and 6.18 show that the initial pressure is not a factor. These figures are generated for no skin and skin equal to 5 respectively for a reservoir permeability of 10

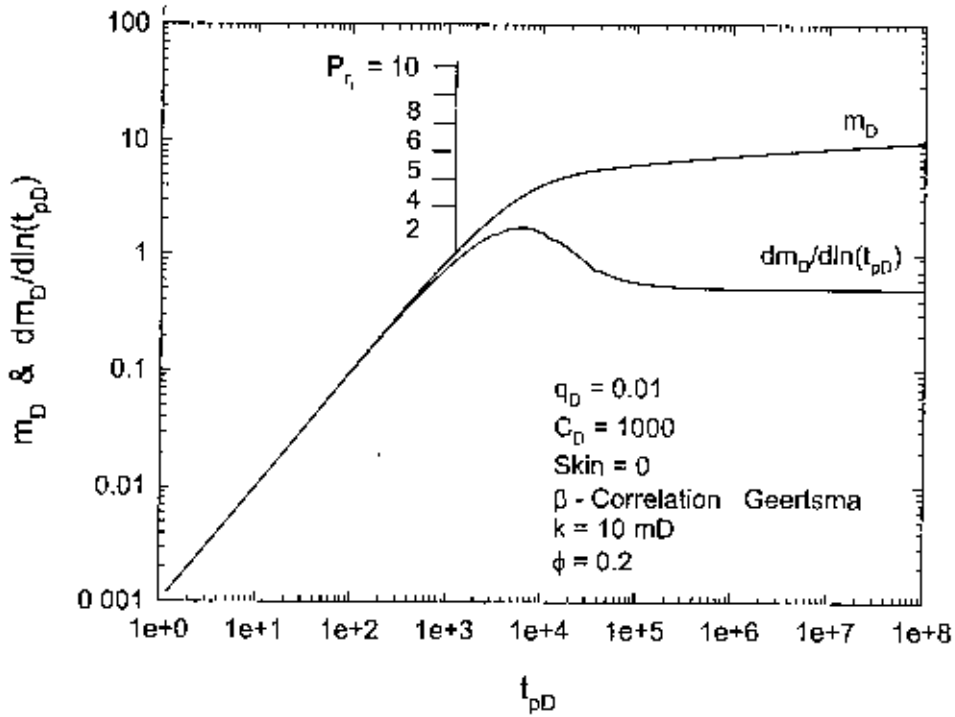


Figure 6.17 : Effect of Initial Pressure on Pseudopressure and Derivative Responses ($Skin = 0$, Constant Q_D basis).

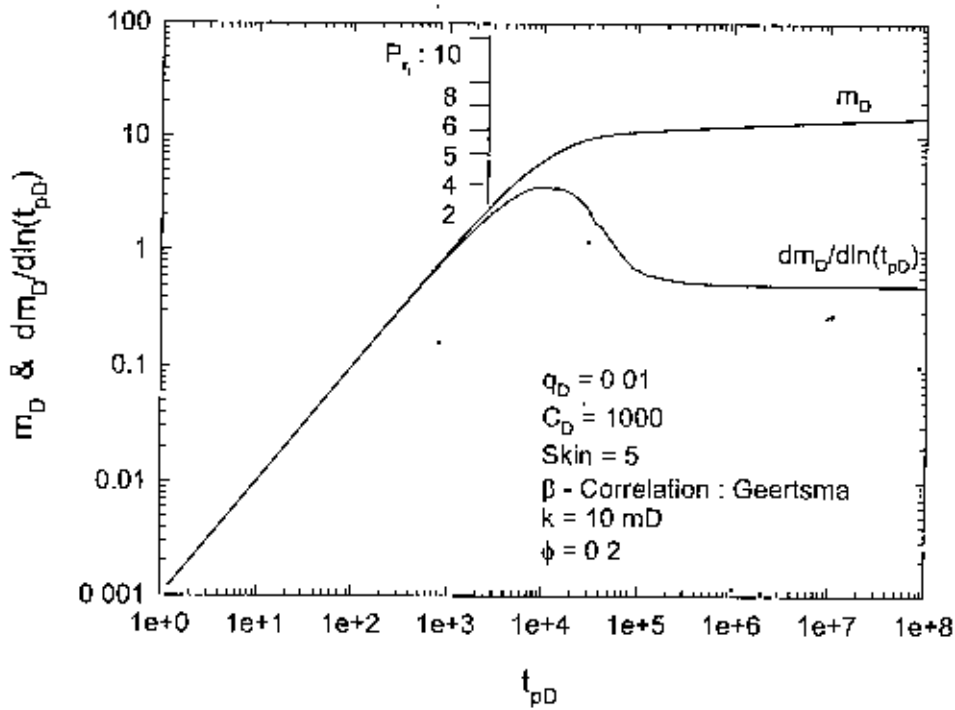


Figure 6.18 : Effect of Initial Pressure on Pseudopressure and Derivative Responses ($Skin = 5$, Constant Q_D basis).

mD, porosity 0.2, wellbore storage coefficient 1000 and $Q_D = 0.01$. The initial pressure is varied from a pseudoreduced pressure of 2 (about 1340 psia) to 10 (around 6700 psia).

6.5 Effect of Permeability

Laminar responses, which are exactly similar to the liquid solutions, do not depend on the permeability of the reservoir. On the contrary, the high velocity effect strongly depends on the permeability. Extensive study has been done to investigate the effect of the reservoir permeability.

Firstly, responses are generated for a constant Q_{sc} , hoping to see variation in the responses with the difference in the permeability. Figures 6.19 and 6.20 illustrate the dimensionless pseudopressure and the derivative responses for a homogeneous, infinite-acting reservoir with $Q_{sc} = 0.05 \text{ m}^3/\text{s}$, porosity 0.2, initial pseudoreduced pressure of 6 and wellbore storage coefficient 1000 with Firoozabadi and Katz (1979) and Geertsma (1974) correlation respectively. The permeability is varied from 0.1 mD to 500 mD. The responses are exactly same for all the permeabilities. The reason for this is actually very simple. The laminar solutions (similar to liquid solutions) are independent of the reservoir permeability, whereas the high velocity effect is greatly dependent on Q_{sc} , and not on the Q_D . So when Q_{sc} remains unchanged the high velocity effect is almost the same. So when the reservoir is homogeneous the responses should not change. Figures 6.19 and 6.20 lead exactly to the same conclusion.

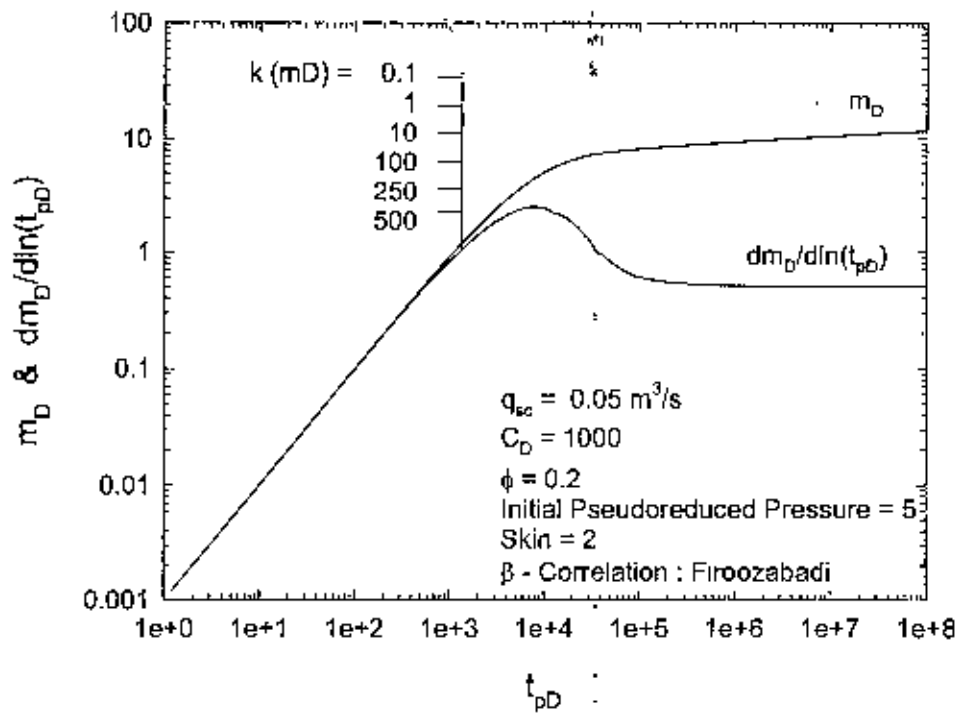


Figure 6.19 : Effect of Permeability on Pseudopressure and Derivative Responses (Firoozabadi & Katz Correlation, Constant Q_{sc} Basis).

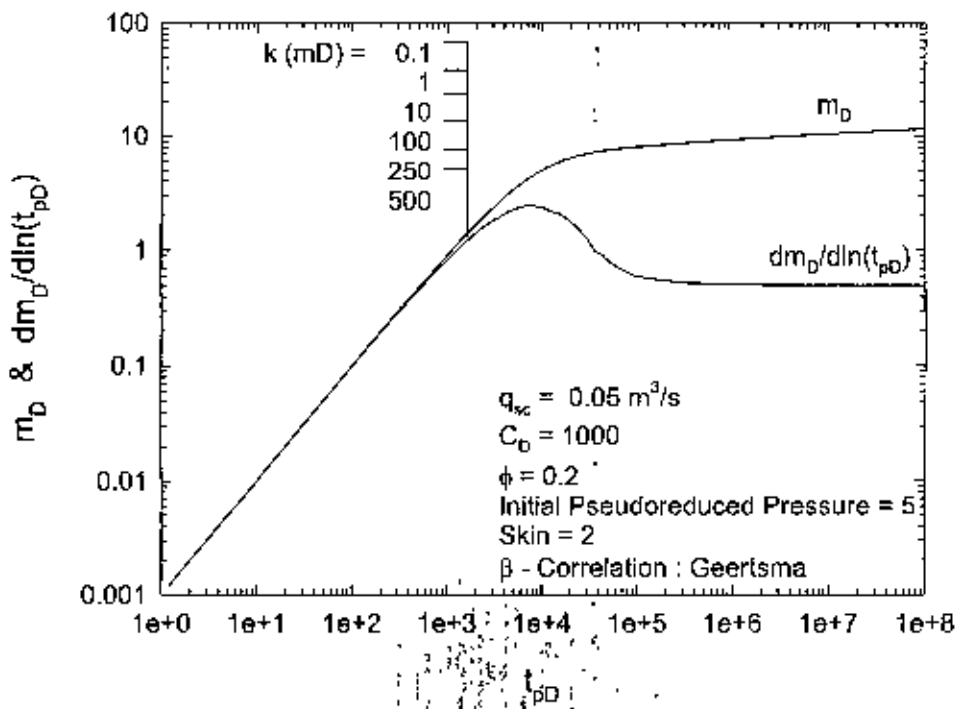


Figure 6.20 : Effect of Permeability on Pseudopressure and Derivative Responses (Geertsma Correlation, Constant Q_{sc} Basis).

Next, responses are generated with the variation of the permeability keeping Q_D constant. This means that Q_{sc} is changing with the permeability, thus the responses also vary. Figures 6.21 and 6.22 are those generated for reservoir porosity of 0.2, wellbore storage coefficient of 1000, initial pseudoreduced pressure 6, and $Q_D = 0.01$ for skin values equal to 5 and 0 respectively. The responses are similar to the anticipated one. Increasing permeability increases the pseudo-dimensionless pressure drop. The reason for this is that increasing the permeability means increasing Q_{sc} for a constant Q_D (refer to Equation 4.92), which leads to increase in the high velocity effect. Thus, the final pressure drop increases. Figures 6.23, 6.24, 6.25 and 6.26 are semi-log responses for both the skins (5 and 0) and pseudopressure and derivative responses. Figures 6.23 and 6.24 show how significant the difference in the pressure responses can be for the both skin cases when permeabilities change. Permeabilities of 0.1 mD to 10 mD responses are almost similar, but the responses increase for $k > 100$ mD. For the case of skin equal to 5 the responses (Figure 6.23) show the similar trend. So skin factor and permeability do not have any combined effect on the pressure transient responses. For the case of skin of 5 at a pseudo-dimensionless time of 10^5 , the values of dimensionless pseudopressure for permeabilities of 10 mD and 500 mD are 11.03 and 16.95 respectively; the difference being 53.67%, while at a later time ($t_{pD} = 10^9$) they are 15.77 and 22.04, respectively; the difference 39.76%. The magnitude of the differences in the responses emphasizes the importance of considering high velocity effect for gas wells. Figures 6.25 and 6.26 show the corresponding derivative responses. These figures reveal that the beginning of the transient state is delayed with the reservoir permeability (for $k > 100$ mD). Also the

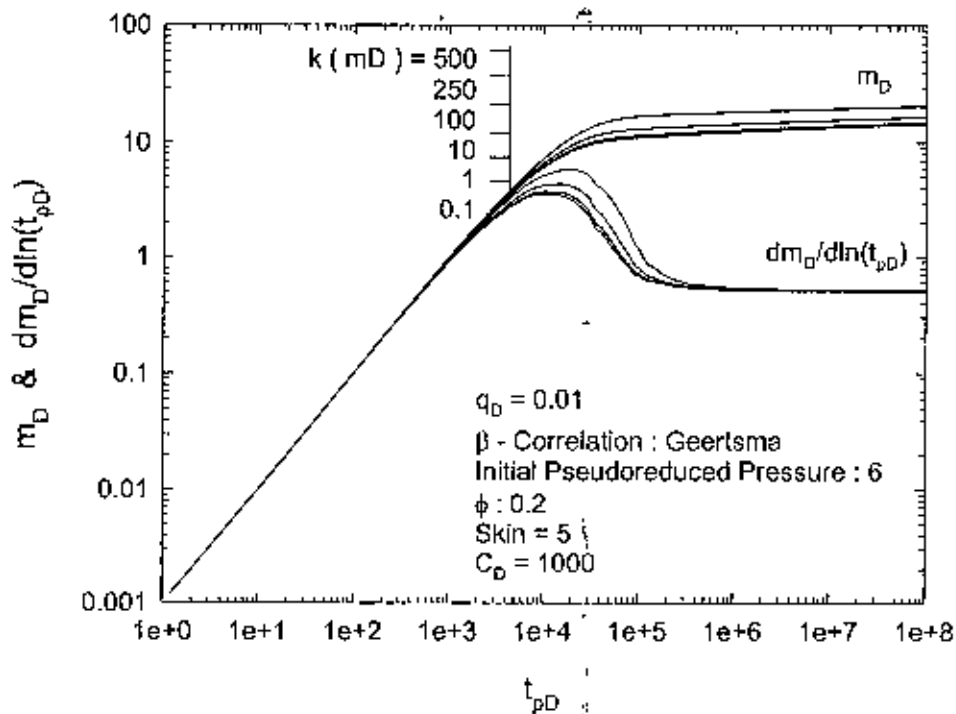


Figure 6.21 : Effect of Permeability on Pseudopressure and Derivative Responses (Skin = 5, Constant Q_D Basis).

91279

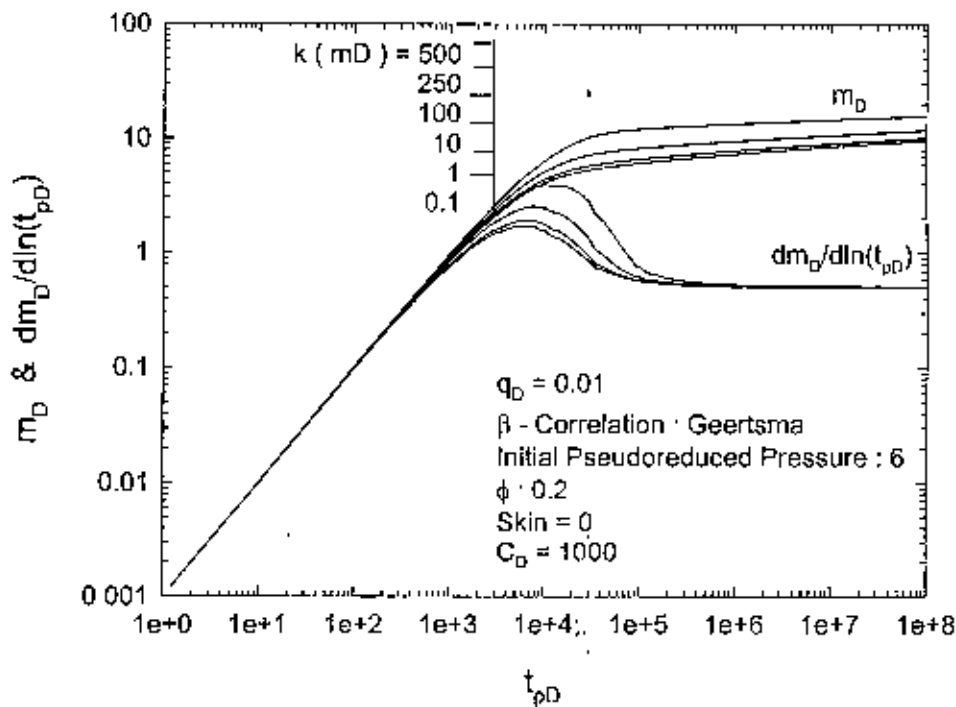


Figure 6.22 : Effect of Permeability on Pseudopressure and Derivative Responses (Skin = 0, Constant Q_D Basis).

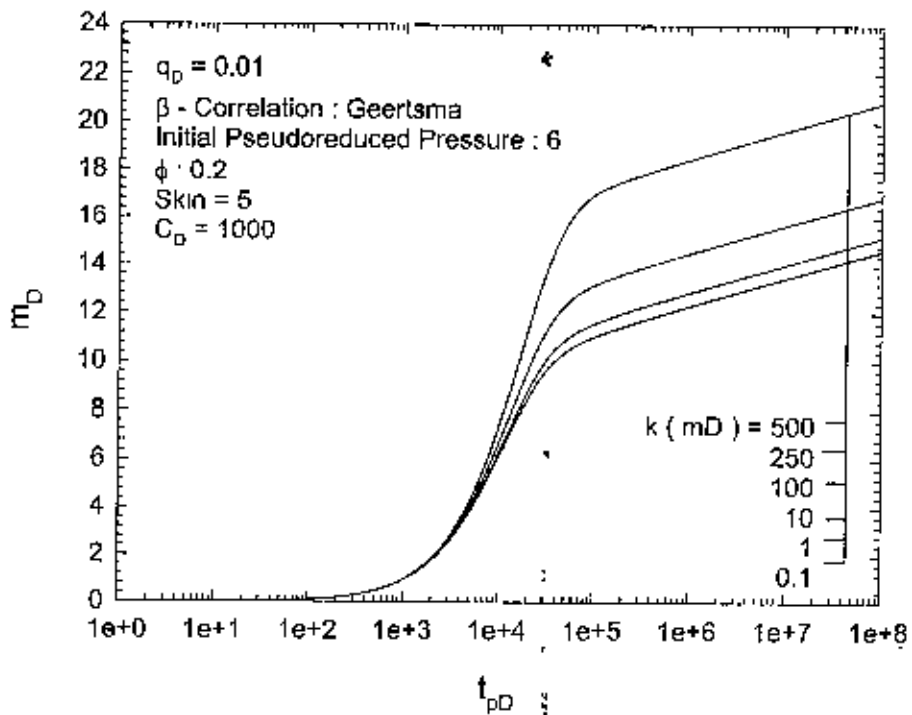


Figure 6.23 : Effect of Permeability on Pseudopressure Responses (Skin = 5, Constant Q_D Basis).

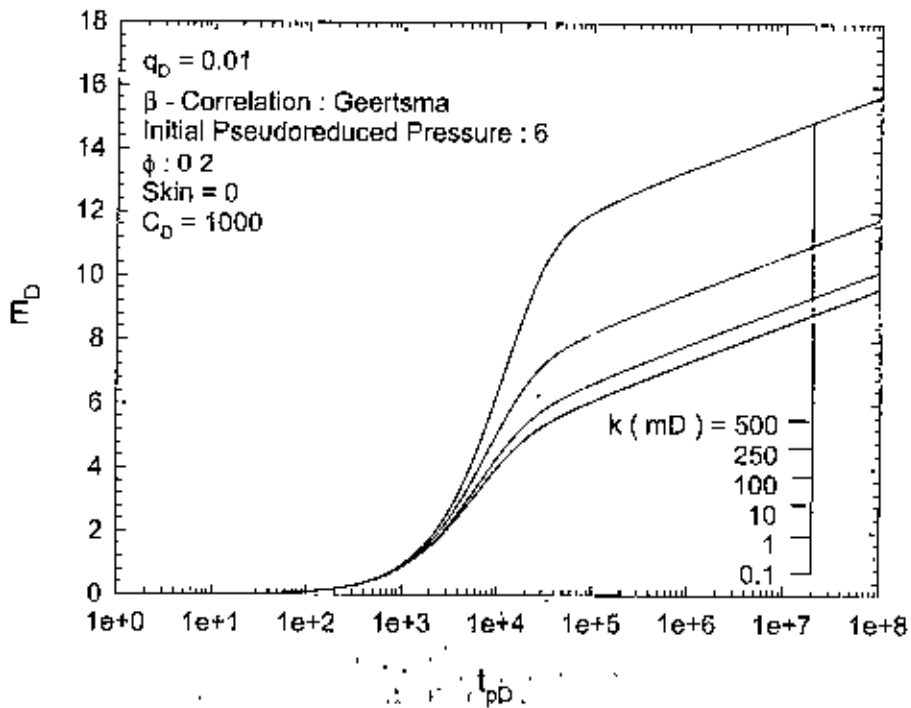


Figure 6.24 : Effect of Permeability on Pseudopressure Responses (Skin = 0, Constant Q_D Basis).

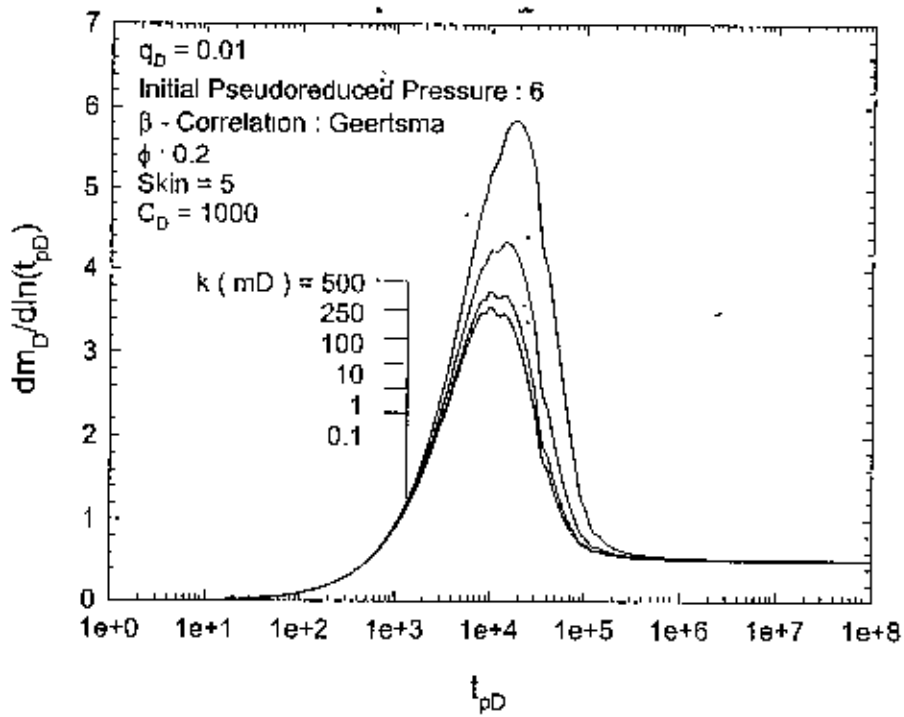


Figure 6.25 : Effect of Permeability on Pseudopressure Derivative Responses (Skin = 5, Constant Q_D Basis).

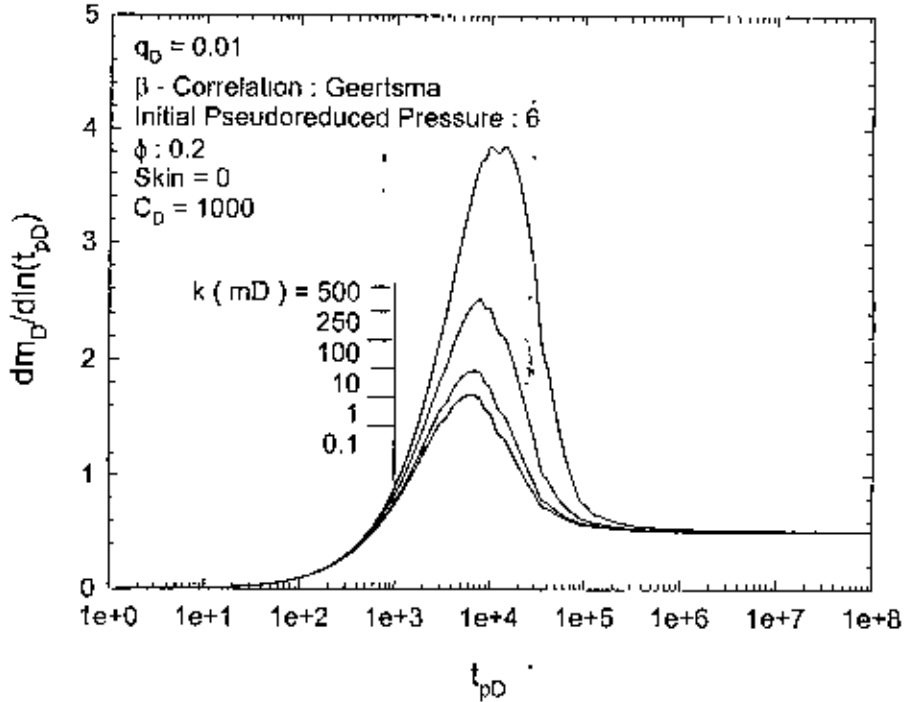


Figure 6.26 : Effect of Permeability on Pseudopressure Derivative Responses (Skin = 0, Constant Q_D Basis).

transition period between the end of wellbore storage dominated state and the transient state increases for higher permeabilities especially for $k > 100$ mD.

Figures 6.27 and 6.28 are the responses for skin 5 and 0, respectively for the same reservoir conditions with Firoozabadi and Katz (1979) correlation. These figures indicate that the responses are even more dispersed for $k > 10$ mD. Otherwise they have the similar trends as those generated with the Geertsma (1974) correlation.

6.6 Effect of Finite Formation Damage

The formation damage near wellbore region has a significant effect on the productivity of the well. Almost every operation in the wellbore is a potential source of formation damage in the vicinity of the wellbore. The effect of this reduced permeability region near the wellbore is usually accounted as thin skin and superimposed on the pressure transient responses with no skin (van Liverdingen and Hurst, 1949). The skin value to be superimposed is determined by the following equation (Craft and Hawkins, 1991),

$$s = \left(\frac{k}{k_s} - 1 \right) \cdot \ln \left(\frac{r_s}{r_w} \right), \quad \dots [6.1]$$

where k_s = permeability of the damage zone,

r_s = radius of the damage zone,

Essentially, in almost all the wellbore operations, the permeability and the porosity of a small finite region around the wellbore are affected. In majority of the cases, the reasons for this damage may be due to fluid invasion, mud particle invasion or drill cuttings, perforation damage, etc. In most of the pressure transient models, this effect is considered

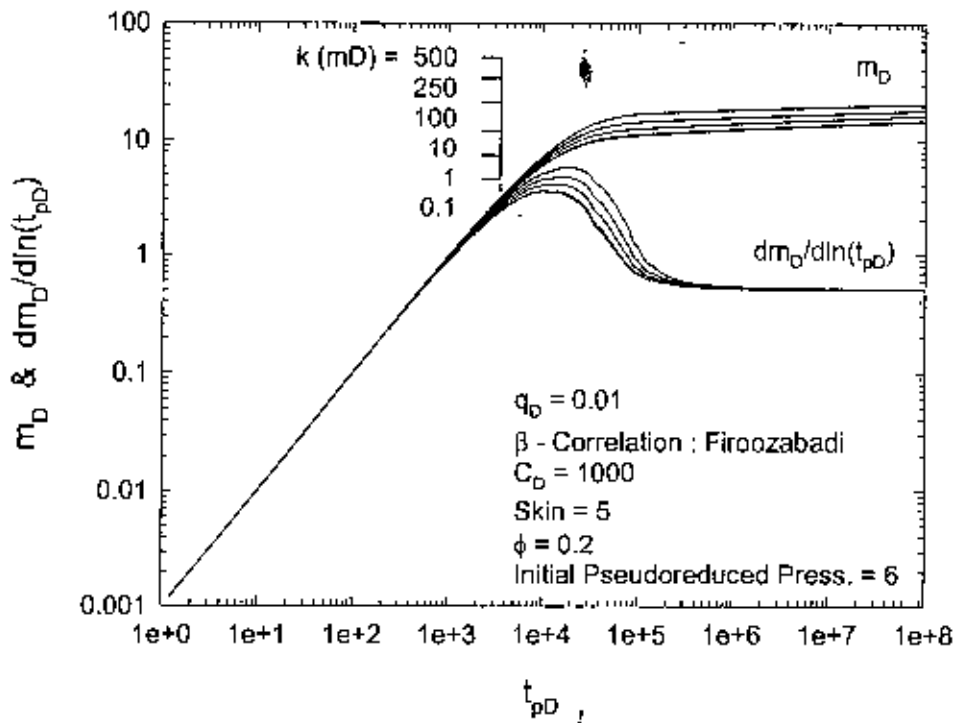


Figure 6.27 : Effect of Permeability on Pseudopressure and Derivative Responses (Skin = 5, Firoozabadi & Katz Correlation, Constant Q_D Basis).

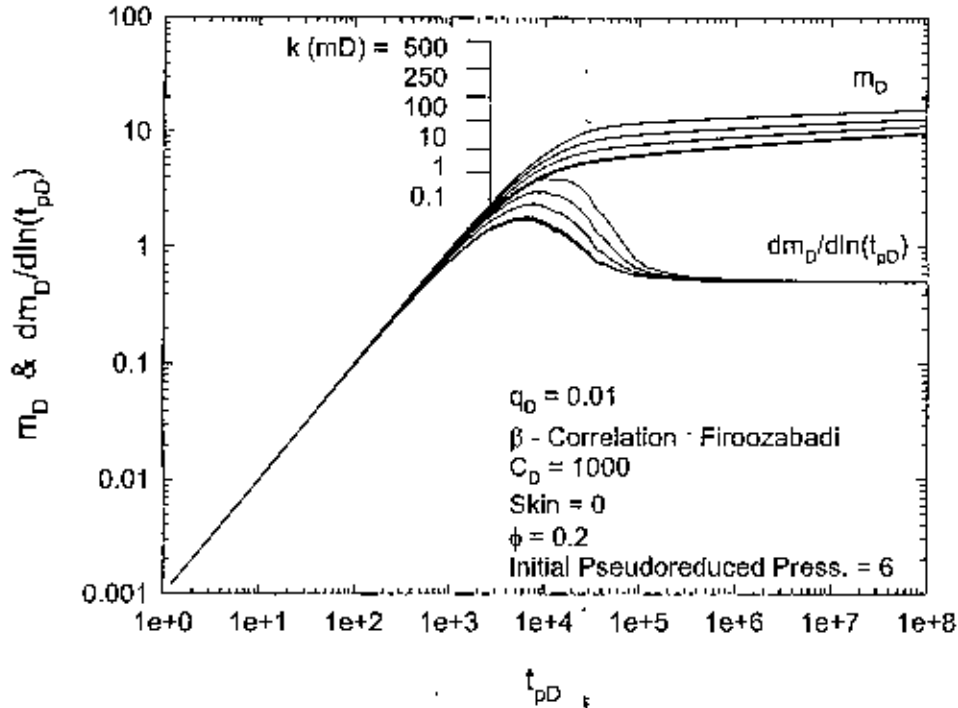


Figure 6.28 : Effect of Permeability on Pseudopressure and Derivative Responses (Skin = 0, Firoozabadi & Katz Correlation, Constant Q_D Basis).

by superimposing the skin value in the homogeneous wellbore solution for mathematical simplicity. This approach of accommodating the effect of formation damage is known as thin skin concept.

The present model has the capability of incorporating finite wellbore damage zone. With this model, the responses of the well for a certain skin are investigated. For a fixed skin, some finite damage zone radii are fixed and the corresponding k_f is measured according to the above equation. Responses are generated for the different situations. Figures 6.29 and 6.30 illustrate the finite skin responses along with the thin skin responses for different finite damage zone radii with Firoozabadi and Katz (1979) and Geertsma (1974) correlation respectively. The responses are generated for a constant Q_{sc} instead of constant Q_D , and skin value of 2. The reason for this is that, for heterogeneous systems, constant Q_D implies different flow rates for different reservoir conditions (refer to Equation 4.92). Comparing the responses for different flow rates would not make sense for studying the effect of formation damage. The undamaged zone properties are assigned permeability of 100 mD, porosity of 0.25, wellbore storage of 1000, initial pseudoreduced pressure of 5 (about 3360 psia), and Q_{sc} value is fixed at 1.0 m³/s. It is apparent from these figures, that finite skin responses are very much different from the thin skin responses. When the finite damage radius decreases, the pressure drops become significantly higher. This is because the smaller the damage zone for some value of skin, the smaller will be the damage zone permeability; this in turn increases turbulence factor, β , and hence the high velocity effect becomes more prominent. Both these correlations

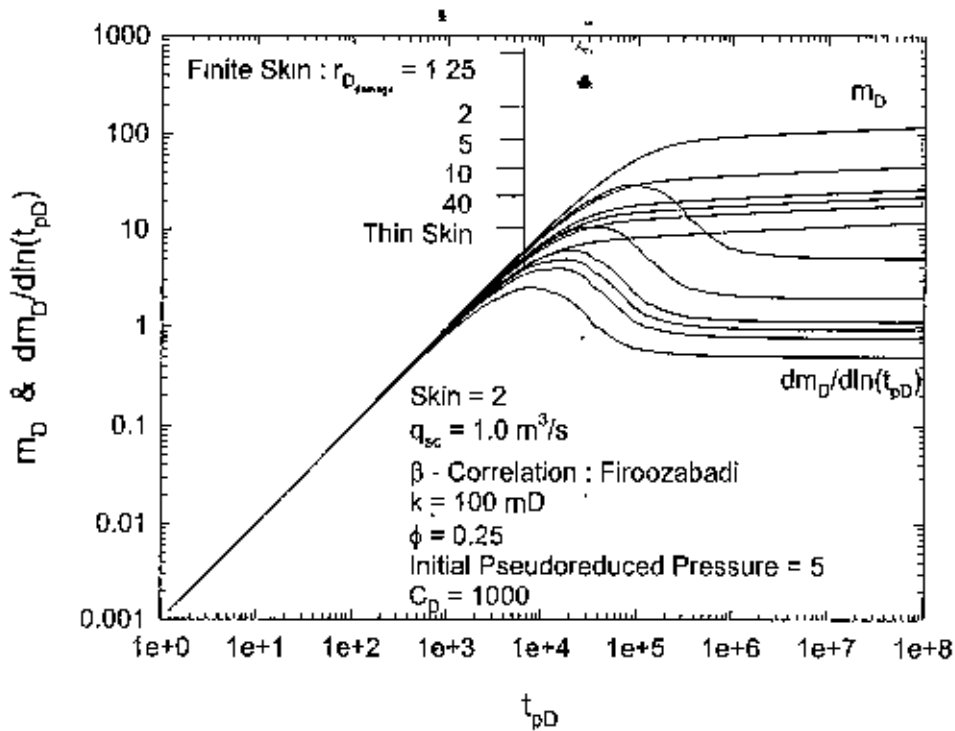


Figure 6.29 : Effect of Finite Formation Damage on Pseudopressure and Derivative Responses (Skin = 2, Firoozabadi & Katz Correlation).

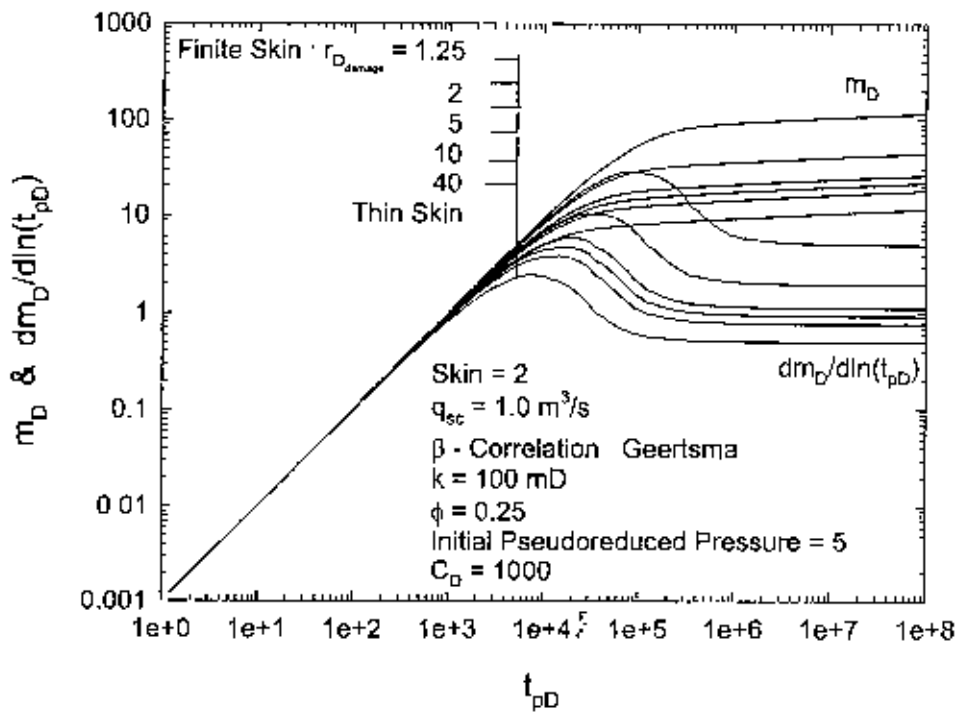


Figure 6.30 : Effect of Finite Formation Damage on Pseudopressure and Derivative Responses (Skin = 2, Geertsma Correlation).

show similar trend. Figures 6.31 and 6.32 are the semi-log plots of pseudo-dimensionless pressure which reveal the extent of the discrepancies in the responses more clearly. At a pseudo-dimensionless time of 10^9 with Firoozabadi and Katz (1979) correlation for dimensionless finite damage radii of 1.25, 40 and thin skin, the dimensionless pseudopressures are 128.77, 19.93 and 12.91 respectively; the differences between the skin responses and these two finite skin cases are 897.4% and 54.4%. While, with Geertsma (1974) correlation, these differences for the corresponding finite skins are 896.1% and 54.1%. Figures 6.33 and 6.34 are the semi-log plots of the pseudo-dimensionless pressure derivatives. It is evident from these figures, that the beginning of the transient state is significantly delayed when the damage zone radius is smaller. Semi-log slope also attains a higher value for smaller finite damage zone radii. This implies that the pressure decline at a greater rate for a smaller damage zone. The duration between the end of wellbore storage dominated state and the transient state is higher for the shorter damage zones. Figure 6.35 illustrates the responses for a skin value of 5 with Geertsma correlation for other reservoir parameters unchanged. Comparing this figure with 6.30 for skin of 2 show that the responses are even more different for finite and thin skins, as the amount of damage increases.

It is apparent, from the preceding sensitivity studies, that for a gas well with high velocity effects, there may be significant discrepancies in the responses if thin skin approach is considered for pressure transient responses of gas reservoirs.

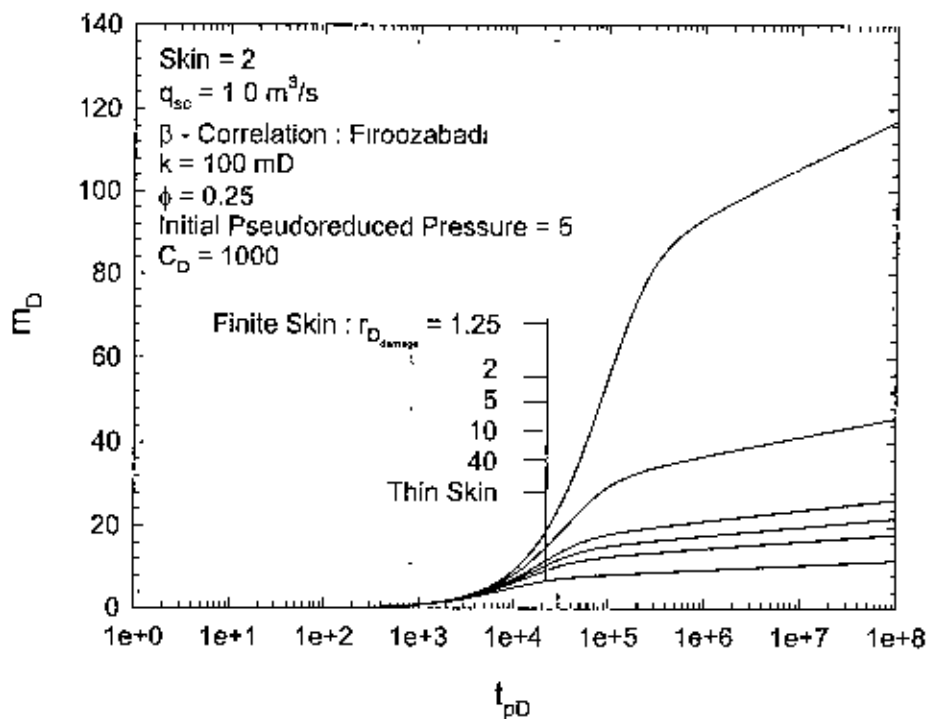


Figure 6.31 : Effect of Finite Formation Damage on Pseudopressure Responses (Skin = 2, Firoozabadi & Katz Correlation).

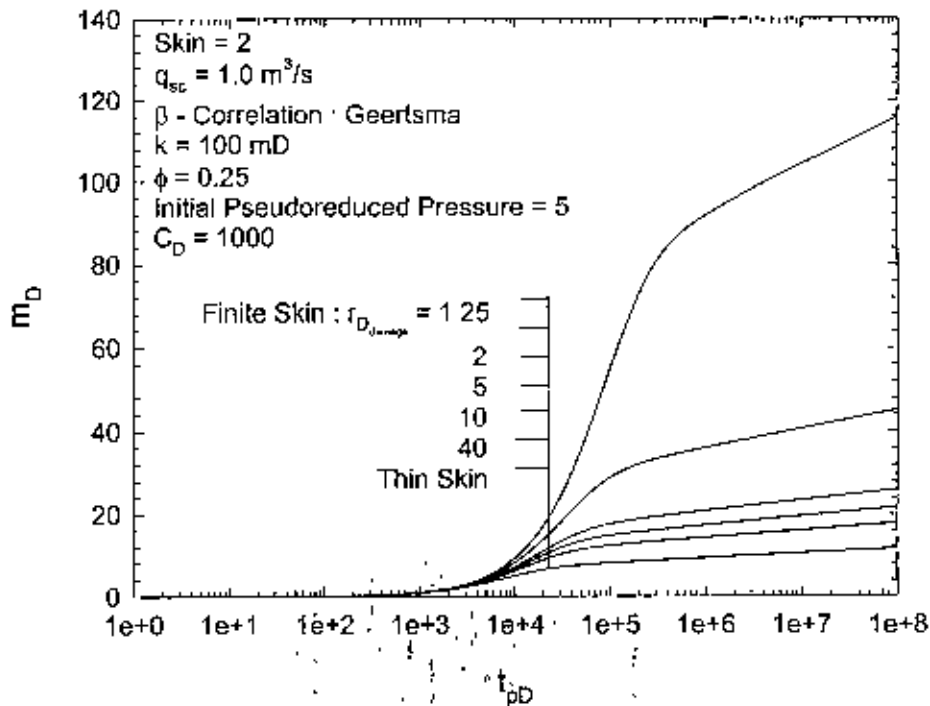


Figure 6.32 : Effect of Finite Formation Damage on Pseudopressure Responses (Skin = 2, Geertsma Correlation).

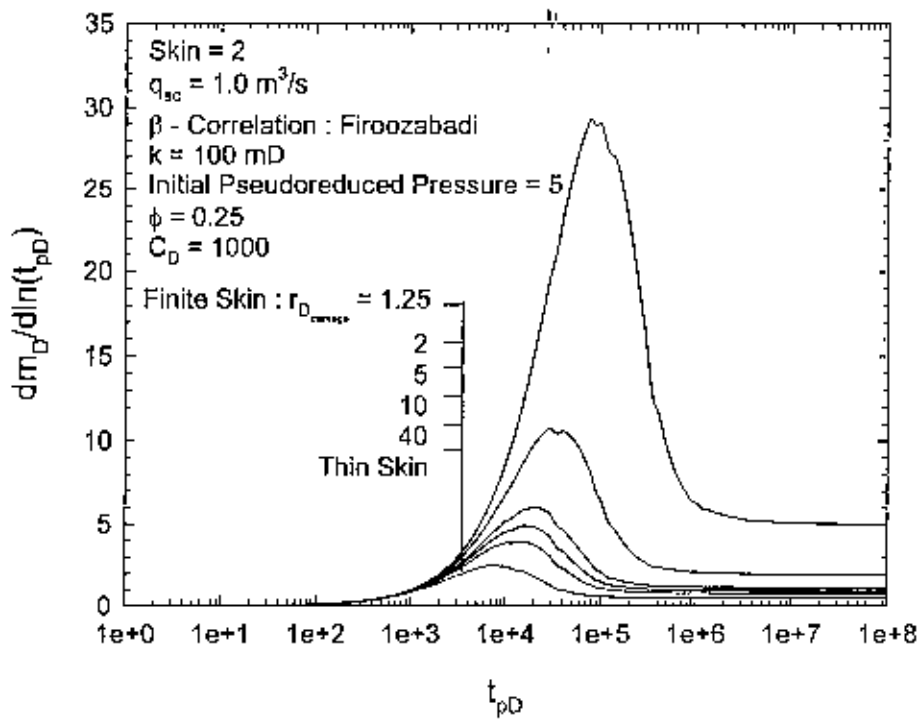


Figure 6.33 : Effect of Finite Formation Damage on Pseudopressure Derivative Responses (Skin = 2, Firoozabadi & Katz Correlation).

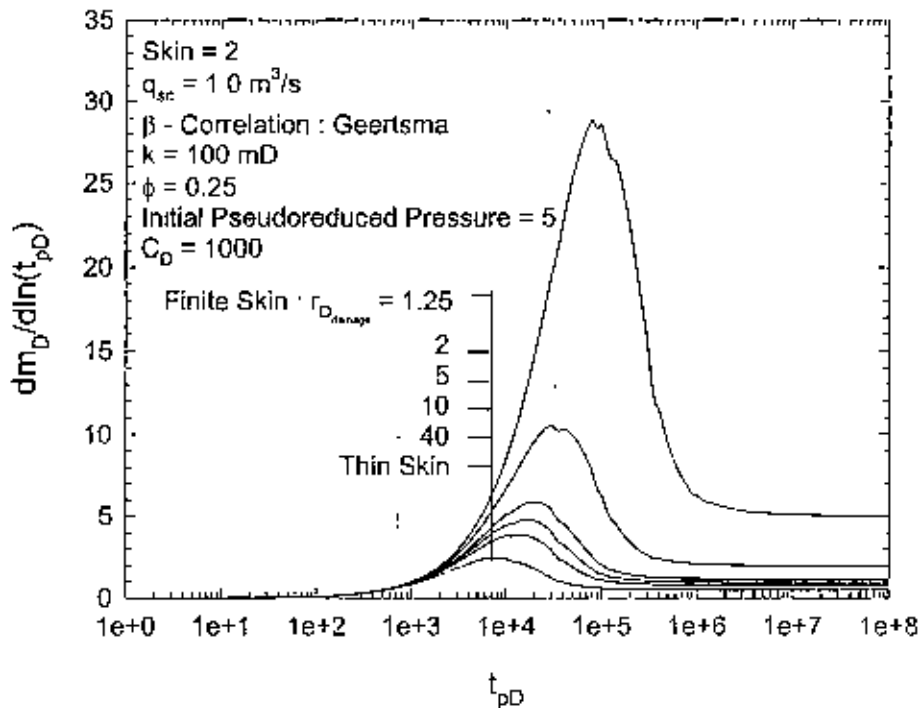


Figure 6.34 : Effect of Finite Formation Damage on Pseudopressure Derivative Responses (Skin = 2, Geertsma Correlation).

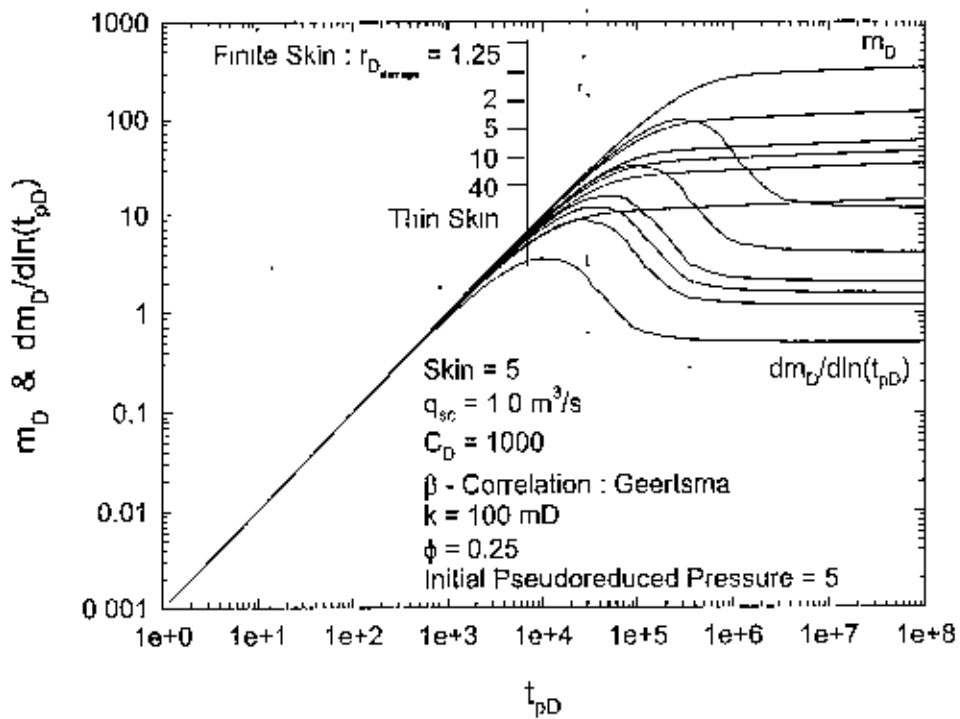


Figure 6.35 · Effect of Finite Formation Damage on Pseudopressure and Derivative Responses (Skin = 5, Geertsma Correlation).

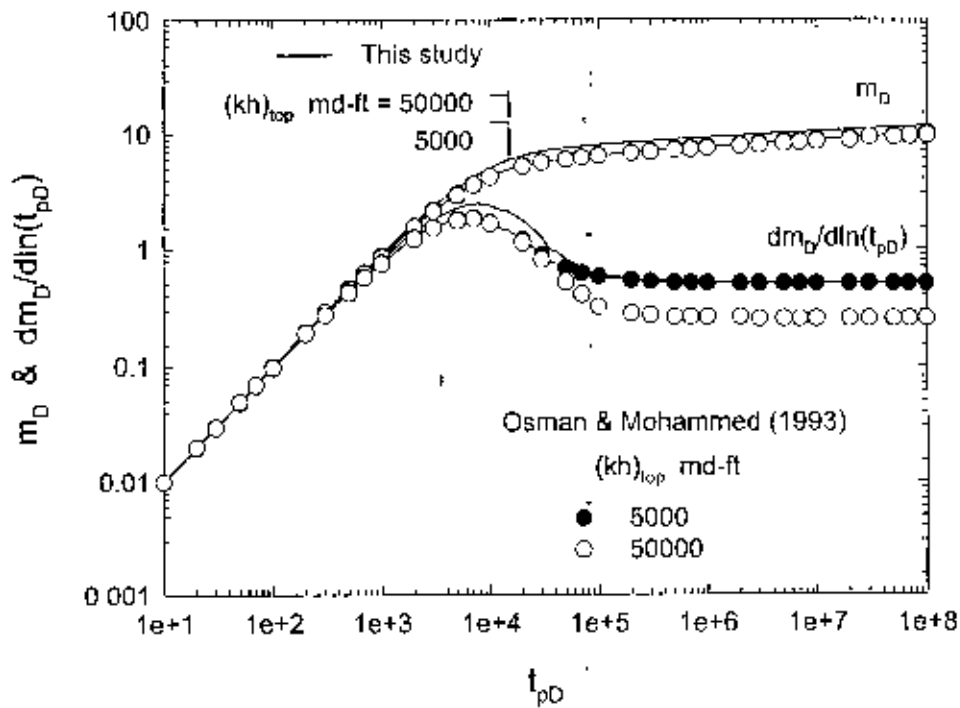


Figure 6.36 : Comparison of this study with Osman and Mohammed (1993) for a 2-layer infinite-acting reservoir system.

6.7 Effect of Layering

The preceding sensitivity studies, conducted, are for single layered reservoirs. In case of multilayered reservoirs, two-layer reservoirs are investigated for the sake of simplicity. However, this model can handle any number of layers. The study of Osman and Mohammed (1993) is considered first in greater detail. They have developed a pressure transient model for a gas well located in an infinite-acting commingled reservoirs. Wellbore storage, skin and turbulence intensity effects are accounted for, in their model. Some of the responses they have found are quite contrasting to what the present model generates. Figure 6.36 shows comparison between these two model responses for a Q_{sc} of 50 MMSCFD. For a two layer reservoir, their responses show separation in the pseudo-dimensionless pressure derivative profiles in the transient state when the flow capacity, (kh) , of the top layer is 10 times that of the bottom layer. Whereas the responses, generated with this model, show that the derivative profiles would be same in the transient state, with separation only in the transition period. The reason, they have given, for this separation is not a justifiable one. They mentioned when flow capacity, (kh) , of a layer increases, the turbulence intensity decreases and thus, decreases also the required pressure drawdown. From the formulating equations, it may be seen that, although with the increase in permeability, velocity coefficient, β (Equation 4.97 or 4.98), decreases, but turbulence intensity, N_T (Equation 4.93), increases and the turbulence factor, $D(\mu)$ (Equation 4.96), may or may not decrease depending on the effect of the product (βk) .

Thus, their rationalization may not be justifiable. Moreover, they have not mentioned any scheme to satisfy the inner boundary conditions.

Some more responses are generated for commingled reservoir, for which there is no crossflow between the layers. Layer characteristics are changed by varying the top layer flow capacity, kh , with respect to that of the bottom layer, by the factors of 1, 10, 100 and 1000. Figure 6.37 reveals the responses for a commingled reservoir for the mentioned conditions with Geertsma (1974) correlation. Flow rate, Q_{sc} , has been kept constant for the comparison, instead of keeping Q_D fixed, because of the layering heterogeneity. This figure has been generated for $(kh)_{bottom} = 200$ mD-ft, no skin, wellbore storage coefficient-1000, $Q_{sc} = 22.88$ MMSCFD ($7.5 \text{ m}^3/\text{s}$), $(\phi h) = 4$ ft. The semi-log plots (Figures 6.38 and 6.39) magnify the differences because of the layering effect. These figures show significant variation in the responses due to changes in the flow capacity, kh , of the layers. At a pseudo-dimensionless time of 10^8 , the pseudo-dimensionless pressures for the top layer having flow capacity 1, 10, 100 and 1000 times that of the bottom layer are : 9.77, 10.39, 12.00 and 16.39 respectively; the corresponding differences being 6.4%, 22.8% and 67.8%. The pseudo-dimensionless pressure responses vary significantly but are parallel in the transient state region. These variations are found to be dependent on the flow rate from the sensitivity studies not included here.

The effect of ordering of the layers is investigated. It is attempted to see whether there is any variation when the bottom layer flow capacity, kh , is changed by the same (as those

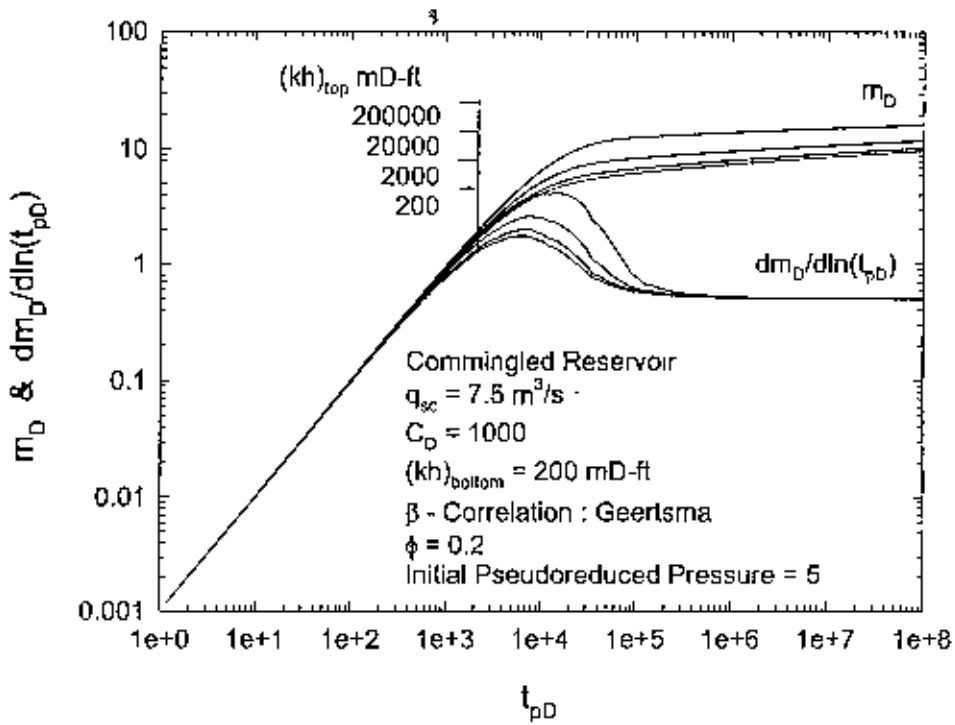


Figure 6.37 : Effect of Layering on Pseudopressure and Derivative Responses of a Commingled Reservoir.

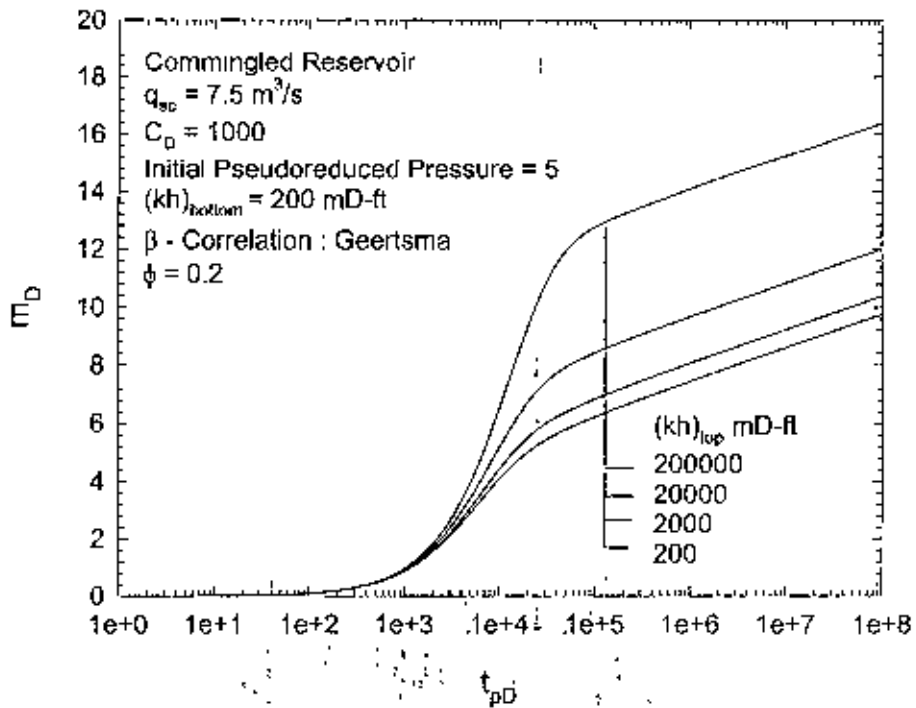


Figure 6.38 : Effect of Layering on Pseudopressure Responses of a Commingled Reservoir.

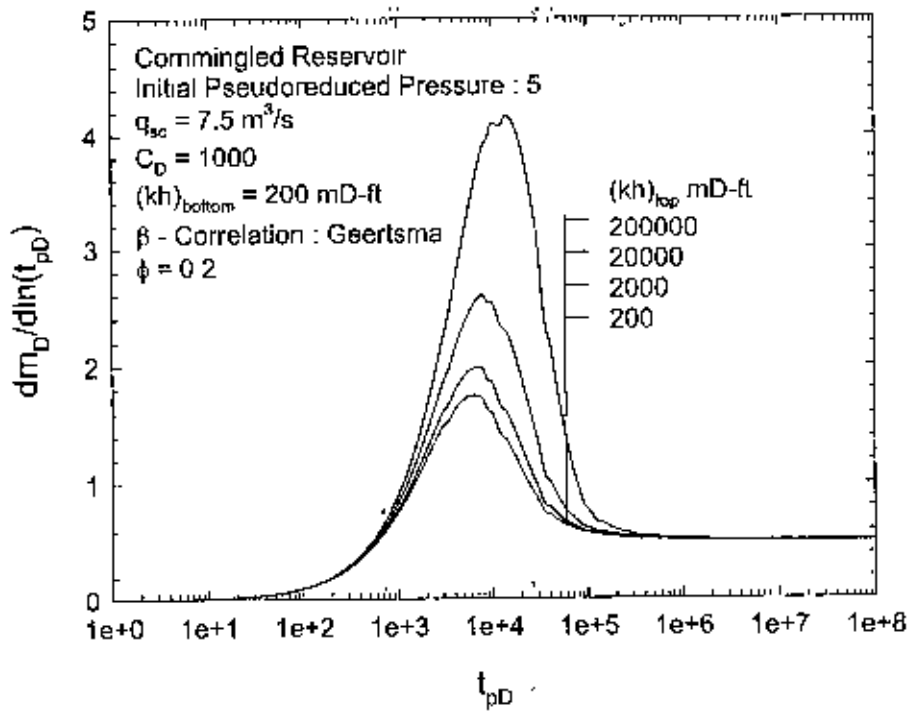


Figure 6.39 : Effect of Layering on Pseudopressure Derivative Responses of a Commingled Reservoir.

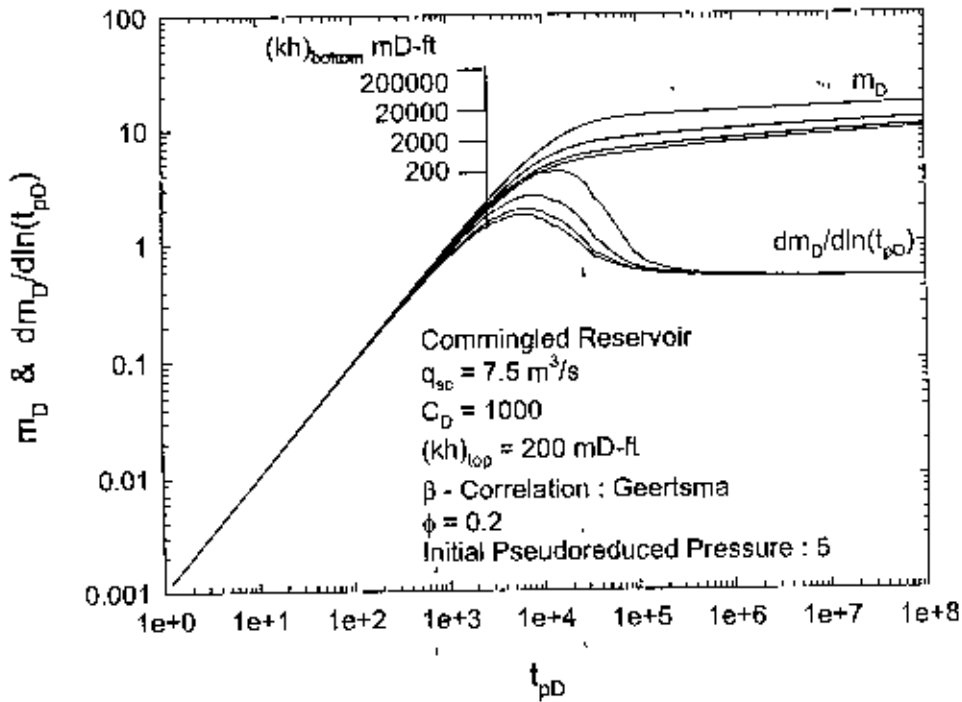


Figure 6.40 : Effect of Layer Ordering on Pseudopressure and Derivative Responses of a Commingled Reservoir.

of the preceding study) multiples of that of the top layer. Figure 6.40 reveals that there is practically no change in the responses when the layer ordering is changed.

Crossflow between the layers have been considered next. This is studied only for the case of $k_v = 0.1k_h$, where k_v is the vertical permeability and k_h is the horizontal permeability. The flow capacity, kh , of the top layer is increased by the same (as in the earlier study) multiples of that of the bottom layer. Figure 6.41 shows the responses for these conditions with Geertsma (1974) correlation. Figure 6.42 and 6.43 are the semi-log plots of the dimensionless pseudo-pressure and the derivative responses respectively. Though it is not so apparent from Figure 6.42, it can be noted that the pseudo-dimensionless pressure profiles converge at a late time with the homogeneous reservoir profile. The time for this convergence is actually a function of the flow rate. Figure 6.44 shows the semi-log plots of pseudo-dimensionless pressure responses for the same conditions but a low flow rate of $0.1\text{m}^3/\text{s}$ (0.3 MMSCFD) in which the convergence is clearly shown. An interesting phenomenon is found to be prevalent in the derivative profiles. The derivative semi-log profiles, in Figure 6.43, show a dip just before attaining the transient state. This implies that just after wellbore storage dominated state, the reservoir productivity is almost solely from the high permeability layer when the crossflow has not set in. But as the crossflow sets in, the reservoir acts like a single layered one.

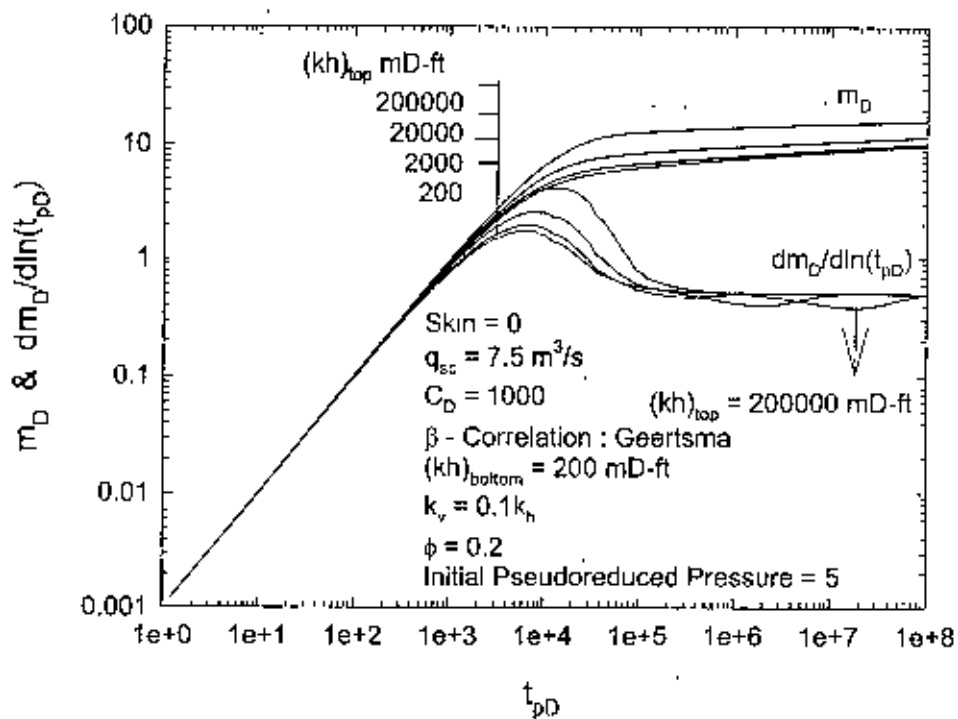


Figure 6.41 : Effect of Layering on Pseudopressure and Derivative Responses of a Reservoir with Interlayer Crossflow.

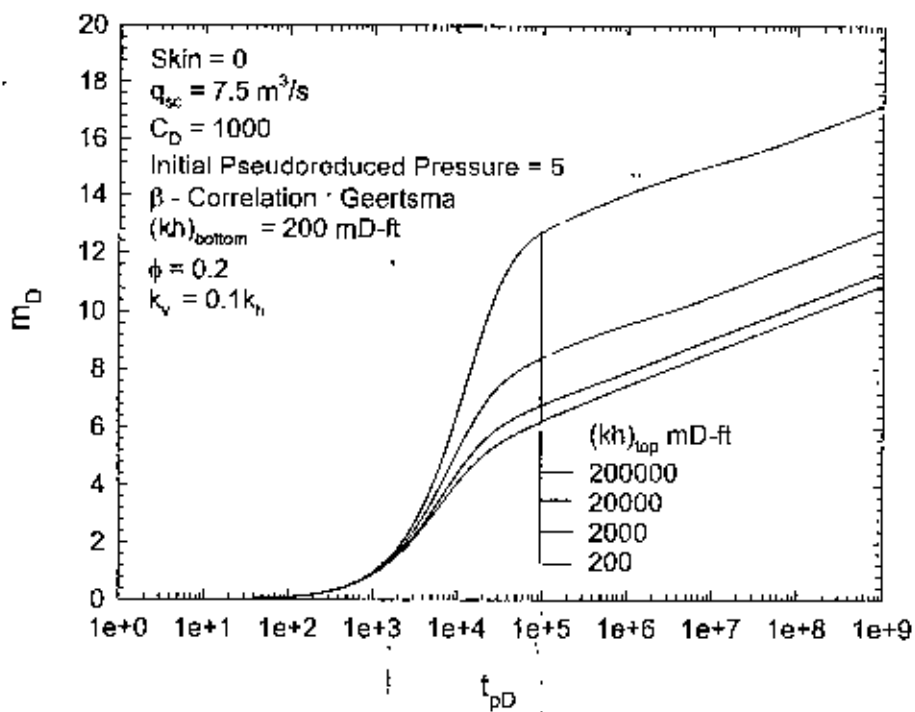


Figure 6.42 : Effect of Layering on Pseudopressure Responses of a Reservoir with Interlayer Crossflow.

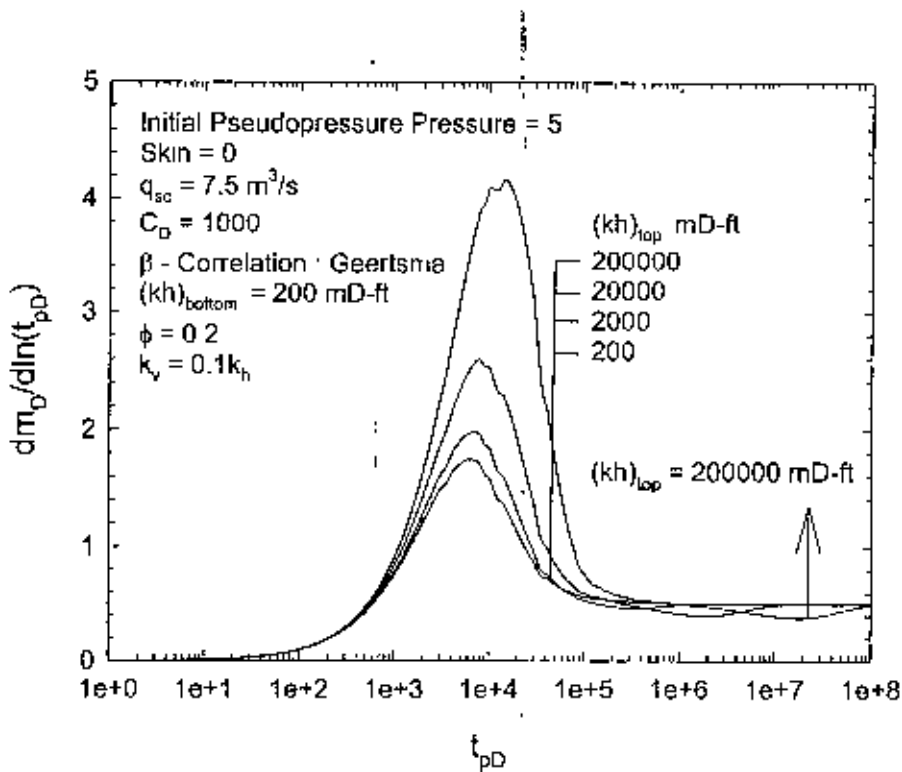


Figure 6.43 : Effect of Layering on Pseudopressure Derivative Responses of a Reservoir with Interlayer Crossflow.

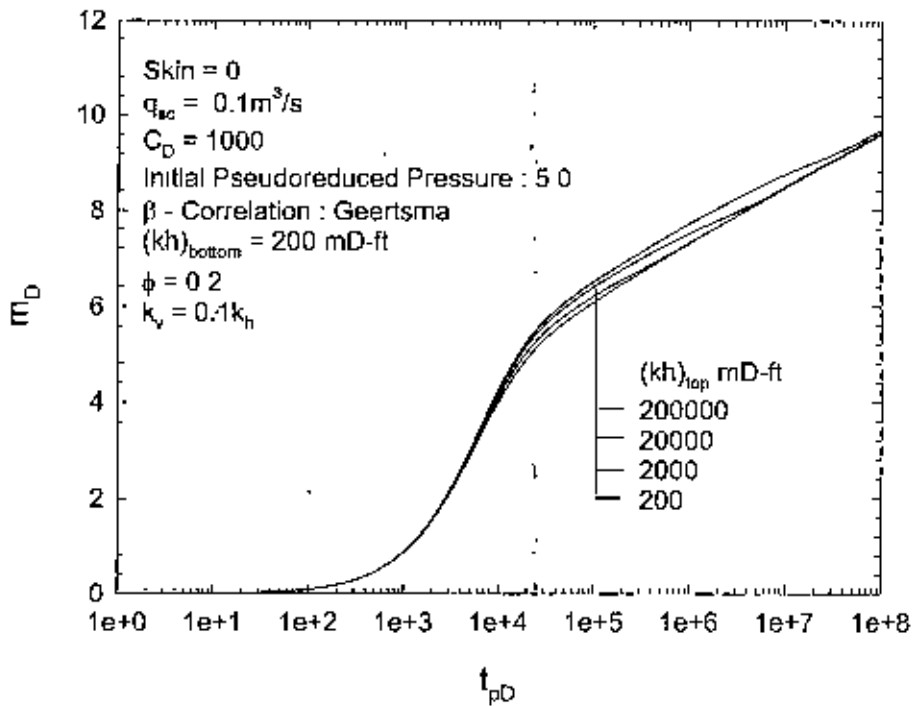


Figure 6.44 : Effect of Layering on Pseudopressure Responses of a Reservoir with Interlayer Crossflow.

6.8 Effect of Closed Outer Boundary

All the previous sensitivity studies are conducted for infinite-acting reservoirs. The present model can handle other outer boundary conditions, like closed and constant outer boundary conditions. A number of responses are generated for a homogeneous reservoir with a closed outer boundary. This condition implies that there is a no flow condition in the external boundary of the reservoir.

Responses are generated for a closed reservoir varying the outer boundary radius. Figure 6.45 shows the pseudo-dimensionless pressure and derivative profiles with Geertsma correlation. The responses are generated for dimensionless outer boundaries of 500, 1000, 2500, 5000 and 7500. The infinite acting response is also shown in the figure. These responses show that the smaller the dimensionless outer boundary radius, the earlier the responses deviate from the infinite acting behavior and attain the pseudosteady states. Further studies need to be done to see whether high velocity effect has any bearing on the closed boundary reservoir responses.

6.9 Effect of Composite Nature of the Reservoir

The present model has the capability to accommodate multilayer composite reservoir as well. Some responses have been generated for composite reservoirs. First case, of the composite reservoirs taken up, is with reservoirs having 2 layers and 3 zones. Zone 1 has a permeability of 20 mD, while the permeability of zone 2 and 3 (both of them having same permeability) are varied to be 10, 20, 50 and 100 mD. The responses are generated for a constant $Q_{sc} = 0.1 \text{ m}^3/\text{s}$, porosity of 0.2, wellbore storage coefficient- 1000, initial

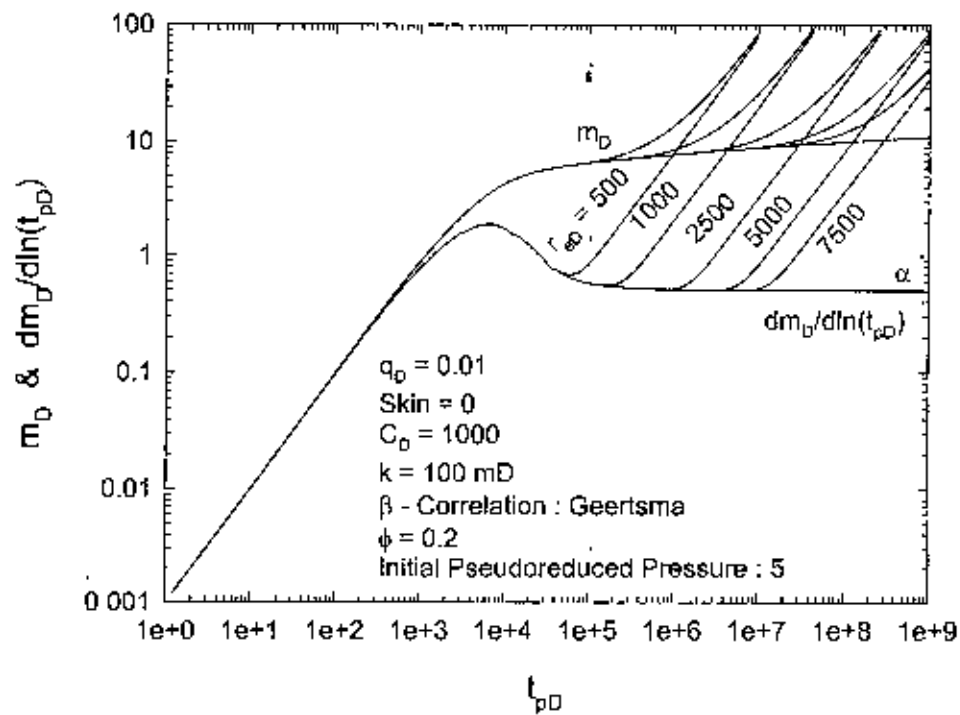


Figure 6.45 : Effect of Outer Boundary Radii on Pseudopressure and Derivative Responses of a Closed Boundary Reservoir.

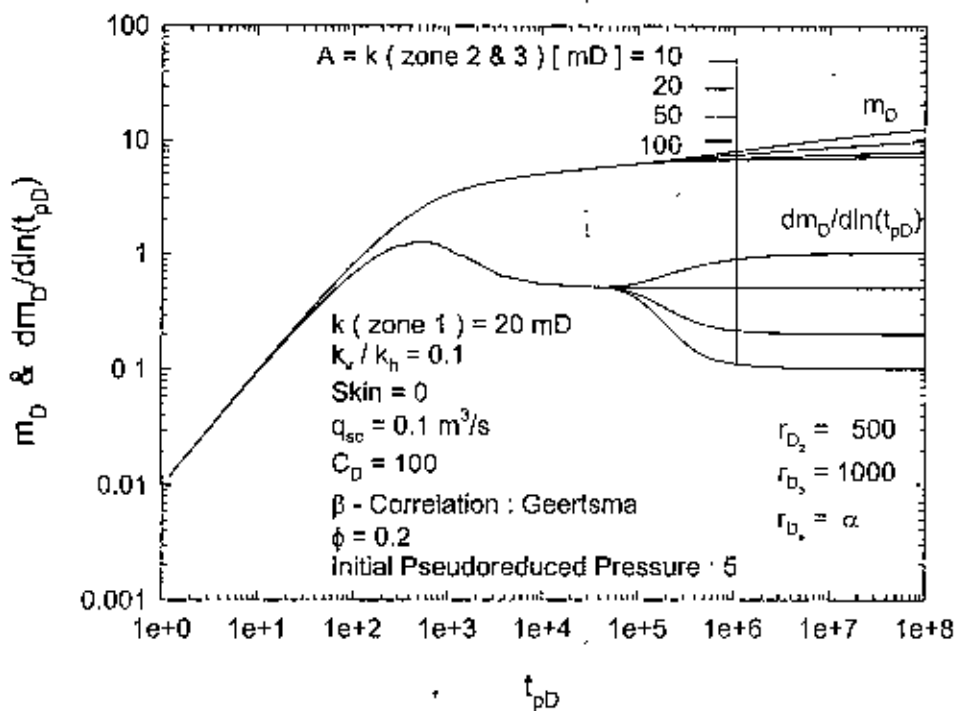


Figure 6.46 : Effect of Outer Zones Permeability on Pseudopressure and Derivative Responses of an Infinite-acting Composite Reservoir.

pseudoreduced pressure- 5, $k_v/k_h=0.1$ and Geertsma (1974) correlation for the β factor. Figure 6.46 illustrates the responses for an infinite-acting reservoir condition. (Figure 6.47 shows the schematic diagram of 2-layer 3-zone composite layer reservoir.) For the first zone boundary, the dimensionless radius is fixed at 500, while that for the second zone boundary is fixed at 1000. Pseudopressure responses, of the four different reservoir situations, become distinguishable at the late time when the pressure transient move across the zones having distinct permeabilities. The derivative profiles are very prominent indicating the reservoir zones with distinct properties. When the pressure transients move through the first zone, transient state is attained for some time before moving into the second zone. The responses, for all the different situations, then have the same transient state derivative values of 0.5. As the pressure transients reach the second zone, responses show a transition period. After this transition period, a second transient state is attained. The derivatives then attain values equal to half the ratios of flow capacity, kh for zone 1, to that of zone 2 and 3. When the first zone has a permeability of 20 mD and the outer zones have 10 mD, the layer thickness being same, this ratio is two. The transient state derivative will then be half of this ratio (=1). From the responses in Figure 6.46, it is apparent that the logarithmic derivative of the pseudo-dimensionless pressure attains the value of 1, for this case.

The same reservoir situations are investigated with a closed outer boundary condition. The outer boundary is fixed at a dimensionless radius of 5000. Figure 6.48 illustrates the pseudo-dimensionless pressure and the derivative profiles together. The pseudopressure

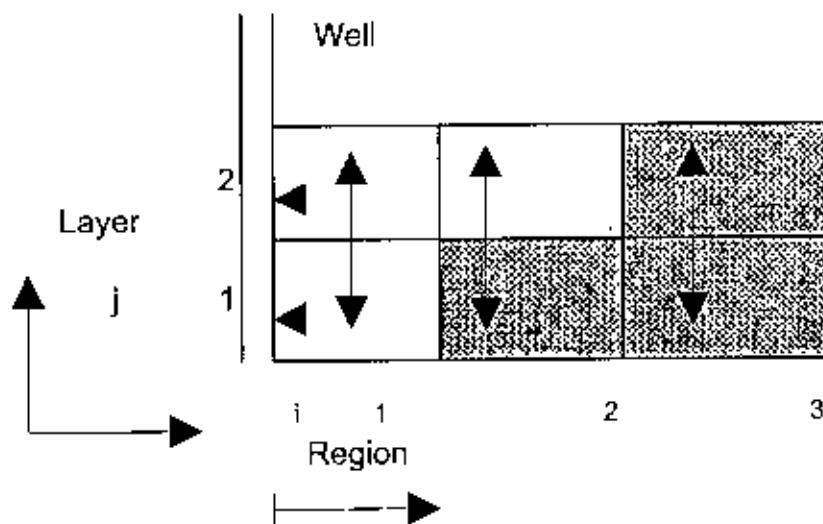


Figure 6.47 : Schematic of a 2-layer 3-zone composite reservoir in a radial geometry with different rock and/or fluid properties in each layer.

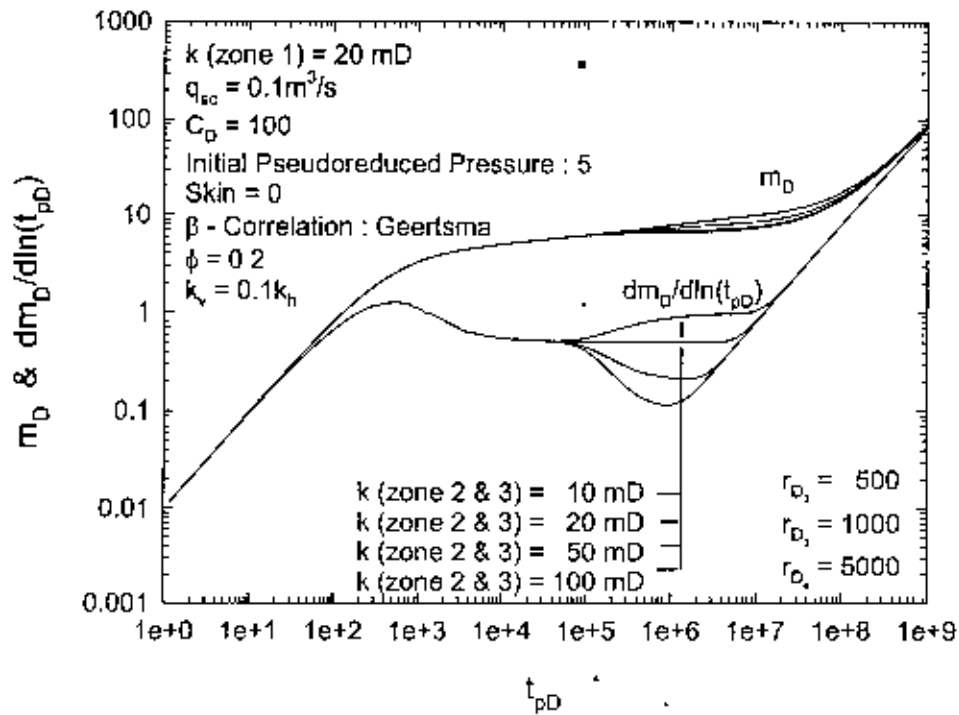


Figure 6.48 : Effect of Outer Zone Permeabilities on Pseudo-pressure and Derivative Responses of a Closed Boundary Reservoir.

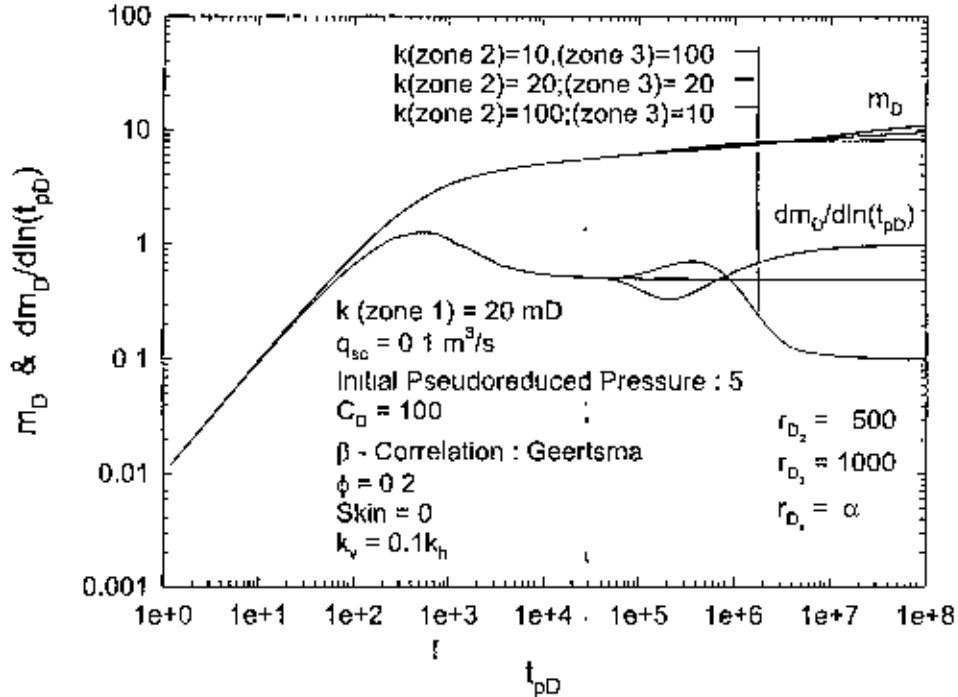


Figure 6.49 : Effect of Ordering of Zone Permeabilities on Pseudo-pressure and Derivative Responses of an Infinite-acting Composite Reservoir.

profiles show the same trend until the pressure transients reach the closed outer boundary. The pseudo-dimensionless pressure profiles are not much informative as it is. The derivative profiles convey the same information as those for the infinite reservoir condition but also indicates the time for the pseudosteady state. When the outer zones have higher permeabilities, the time to attain the pseudosteady state is earlier.

It is attempted to study the variation in the responses when the second and third zones having different permeabilities are interchanged. The first zone has a permeability of 20 mD. In one scenario zone 2 and 3 have permeabilities of 100 and 10 mD respectively and in another scenario zone 2 and 3 permeabilities are swapped. Figure 6.49 illustrates the responses for infinite-acting reservoir condition. The pseudopressure profiles do not carry much information, although there is some separation when the pressure transients move into the second zones. The derivative profiles are quite informative. These responses are same while moving through the first zone. When the pressure transient moves across the second zone, the derivative profiles become distinct indicative of the respective flow capacity, kh , differences of the first and second zone. Then, while moving across the outer zones, the derivatives attain the transient state values equal to the half of the flow capacity, kh , ratios of zone 1 and zone 3.

The same reservoir situations are investigated for the closed boundary reservoir condition. Figure 6.50 shows the responses. The responses are very much expected as the preceding sensitivity studies. The derivative profiles are found to be much more informative of the reservoir conditions.

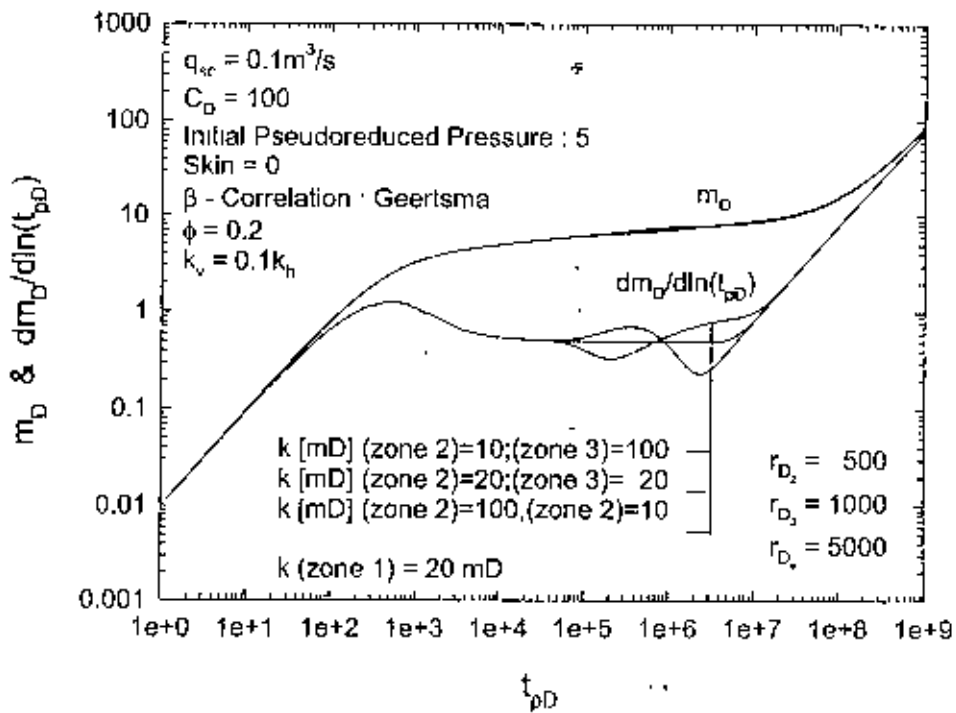


Figure 6.50 : Effect of Ordering of Zone Permeabilities on Pseudo-pressure and Derivative Responses of a Closed Boundary Reservoir.

The present model has the ability of providing more reservoir description than any other model currently available in the literature. Only few of the sensitivity studies are conducted here. Numerous reservoir situations can be investigated with this model.

7.0 CONCLUSIONS

In this study, a composite multilayered reservoir pressure transient model for gas reservoir is developed. This model incorporates wellbore storage, skin, high velocity effects and interlayer crossflow. Due to its structure, the model has the potential of depicting numerous heterogeneity in the reservoir system. Based on the sensitivity studies conducted, some of the conclusions are outlined below.

- Velocity coefficient, β , has a significant effect on the pressure transient responses of gas reservoirs. Analyses, with arbitrarily fixing β , are not representative of the actual reservoir conditions. Geertsma (1974) correlation for β tends to give lower pressure drop compared to the Firoozabadi and Katz (1979) correlation, for most of the reservoir conditions found. For oil reservoirs, no high velocity phenomena exists.
- Flow rate has a strong effect on the pressure transient responses of the gas reservoirs. Higher the flow rate, higher will be the pseudo-dimensionless pressure drop. For a very high flow rate, the logarithmic derivative of the pseudo-dimensionless pressure attains a higher value than 0.5 in the transient state. Whereas, flow rate does not have any bearing on the liquid pressure transient responses.
- Initial pressure does not have any effect on the pressure transient responses.
- The pseudo-dimensionless pressure drop increases with the increase in the reservoir permeability. This is because, as the permeability increases, the flow rate increases for a constant dimensionless flow rate. Thus, the high velocity effect becomes much more

prominent. For a constant flow rate, the permeability does not have much effect on the responses. In the pressure transient responses of oil reservoirs, permeability does not have any effect.

- The thin skin concept may not be a proper approach to accommodate formation damage in the pressure transient analysis of a gas reservoir because of the high velocity effect. This is quite contrary to the liquid pressure transient analysis.
- The pseudo-dimensionless pressure drops are higher when the top layer has higher flow capacity than the bottom layer, for a two layer commingled reservoir. The amount of increase in the pseudo-dimensionless pressure responses depends on the flow rate. The position of the layer does not affect these responses. For multilayer reservoir with crossflow between the layers, the early time responses are almost similar to the commingled system, but at the late time when the crossflow sets in the responses converge to the homogeneous solution.
- Interesting responses have been found to be existing in the pressure transient analyses of the composite reservoirs because of the variation of the reservoir properties. The transient state derivative profiles have been found to be very useful and effective in reservoir characterization.

8.0 RECOMMENDATIONS

In this study, a general semi-analytical model for an n-layer, composite gas reservoir has been developed. Studies described in the preceding chapters show the enormous applicability of the developed model.

There is scope for detailed investigation of each of the areas discussed in the preceding chapters. Reservoir heterogeneity is one aspect that might lead to a number of detailed investigations. This model is adequately devised to handle most of the single gas flow phenomena.

Partial penetration is one of the topics that can be studied in detail with this model. The partial penetration scheme is already included in the program, but sensitivity studies have not been done.

Bottom water drive, edge water drive, water coning, etc. can also be studied with the model making a few modifications.

This model has been designed to study single phase gas reservoirs. Liquid solutions are already a subset of the solution generated with this model. This present model can be extended to develop a model for multi-phase system with all the reservoir heterogeneity. The multi-phase model can be very useful and effective for the pressure transient analysis of any reservoirs.

NOMENCLATURE

- A = Coefficient matrix in Equation [4.112]
- A_i^k = Constant in Equation [4.73]
- B = Formation volume factor, res $m^3/S m^3$
- B_i^k = Constant in Equation [4.74]
- b = Matrix in Equation [4.112]
- C = Wellbore storage coefficient, m^3/Pa
- C_i = Turbulence correlation
- C_D = Dimensionless wellbore storage
- c = Compressibility of gas, Pa^{-1}
- c_j = Elements of the matrix b in Equation [4.114]
- $D(\mu)$ = Turbulence factor
- d_j = Elements of the coefficient matrix A in Equation [4.113]
- E_{ij}^k = Eigenvector for the region i
- F_p = Viscosity ratio
- f = (l,l) th element of the coefficient matrix A in Equation [4.113]
- f_j = Fractional flow rate of layer j
- g = l -th element of the b matrix in Equation [4.114]
- h, h_t = Formation thickness, m
- h_j = Thickness of the layer j
- k = Horizontal permeability, m^2

- k_v = Vertical permeability, m^2
 l = Laplace variable
 M = Molecular weight of the natural gas
 $M_{i,j}$ = (kh) ratio, $\frac{(kh)_{i,j}}{(kh)_{t,j}}$
 m = Number of regions or zones
 m_{ij} = Real gas pseudo-pressure (with subscripts), Pa/s
 m_D = Pseudo-dimensionless pressure
 m_{in} = Initial pseudo-pressure, Pa/s
 m_w = Wellbore pseudo-pressure, Pa/s
 m_{wD} = Pseudo-dimensionless wellbore pressure
 N_{Fo} = Forchheimer number
 N_T = Turbulence intensity
 n = Number of layers
 p = Pressure, Pa
 p_D = Dimensionless pressure
 p_{in} = Initial pressure, Pa
 p_{sc} = Surface Pressure, Pa
 p_{wf} = Wellbore pressure, Pa
 Q = Surface flow rate, $S\ m^3/s$
 Q_D = Dimensionless flow rate

- q = Sandface flow rate, res m³/s
 R = Gas constant
 r = Radial distance, m
 r_a = Radial front distance, m
 r_{aD} = Dimensionless radial front distance
 r_D = Dimensionless radius
 r_{eD} = Dimensionless outer boundary radius
 r_e = Outer boundary distance, m
 r_i = Radius of investigation, m (ft)
 r_w = Wellbore radius, m
 s_j = Wellbore skin of layer j
 T = Temperature, Kelvin
 T_R = Reservoir temperature, Kelvin
 t = Time, sec
 t_u = Pseudo-time
 t_{uD} = Dimensionless pseudo-time
 t_D = Dimensionless time
 X_A = Semi-permeability between layers j and j+1 = $\frac{2}{\left(\frac{h}{k_v}\right)_j + \left(\frac{h}{k_v}\right)_{j+1}}$
 $X_{A(i,j)}$ = Semi-permeability of the zone (i,j) between layers j and j+1
 $X_{B(i,j)}$ = Semi-permeability of the zone (i,j) between layers j and j-1

Greek Symbols

- α_Q = Constant in Equation [4.92]
- α_N = Constant in Equation [4.93]
- α_D = Constant in Equation [4.96]
- α_{p1} = Constant in Equation [4.97]
- α_{p2} = Constant in Equation [4.98]
- β = Turbulence coefficient
- δ_r = Modifier related to turbulence coefficient
- ϕ = Porosity
- γ = Specific gravity
- κ = Transmittivity ratio
- κ_{ij} = Defined by Equation [4.46]
- λ = Crossflow parameter
- $\lambda_{\Delta i0}$ = Defined by Equation [4.48]
- $\lambda_{\Delta i j}$ = Defined by Equation [4.49]
- μ = Viscosity, Pa-s
- μ_i = Initial viscosity, Pa-s
- ρ = Density, Kg/m³
- σ_1, σ_2 = Eigenvalues
- σ_i^k = Eigenvalues for region i
- τ = Variable of integration

- ω = Storativity ratio
- ω_{ij} = Defined by Equation [4.47]
- ∂ = Partial
- ∇ = Differential operator

Subscripts

- A = Crossflow from or to lower layer
- B = Crossflow from or to upper layer
- D = Dimensionless
- D = Turbulence factor in Equation [4.96]
- Fo = Forchheimer
- i = Any region or zone
- j = Any layer
- L = Laminar response
- N = High velocity response
- p = Pseudo-variable
- Q = Flow rate
- sc = Standard condition
- T = Turbulence
- v = Vertical
- w = Wellbore

β_1 = Geertsma's velocity coefficient

β_2 = Firoozabadi and Katz velocity coefficient

REFERENCES

1. Agarwal, R.G., Al-Hussainy, R. and Ramey, H.J., Jr (1970): "An Investigation of Wellbore Storage and Skin Effect in Unsteady Liquid Flow: I. Analytical Treatment," *SPEJ* (September) 279-290.
2. Al-Hussainy, R., Ramey, H.J., Jr and Crawford, P.B. (1966): "The Flow of Real Gases Through Porous Media," *JPT AIME* 237 (May) 624-636.
3. Anbarci, K., Grader, A.S. and Ertekin, T. (1989): "Determination of Front Locations in a Multilayer Composite Reservoir," paper SPE 19799 presented at the Annual Meeting, San Antonio, TX, Oct. 8-11.
4. Carr, N.I., Kobayashi, R. and Burrows, D.B. (1954): "Viscosity of Hydrocarbon Gases Under Pressure," *Trans AIME* 201 (1954) 264-272.
5. Civan, F. and Evans, R.D. (1991): "Non-Darcy Flow Coefficients and Relative Permeabilities for Gas/Brine Systems," paper SPE 21516 presented at SPE Gas Technology Symposium, Houston, TX, Jan. 23-25.
6. Chu, W.C. and Raghavan, R. (1981): "The Effect of Noncommunicating Layers on Interference Test Data," *JPT* (February) 370-382.
7. Churchill, R.V. (1972): *Operational Mathematics*. 3rd Edition, McGraw-Hill, New York.

8. Craft, B.C. and Hawkins, M.F., Jr. (1991): *Applied Petroleum Reservoir Engineering*, 2nd Edition, Prentice Hall PTR, Englewood Cliffs, NJ.
9. Ding, W. (1986): "Well Testing in Gas Reservoirs" M.Sc. Thesis, University of Tulsa, Tulsa, Oklahoma.
10. Dranchuk, P.M. and Abou-Kassem, J.H. (1975): "Calculations of Z Factors for Natural Gases Using Equations of State," *JPT* (July-Sept.) 34-36.
11. Duhamel, J.M.C. (1833): "Memoire sur la methode generale relative au mouvement de la chaleur dans les corps solides prolonges dans les milieux dont la temperature varie avec le temps," *J. de Ec. Polyt.* (Paris) Vol. 14, 20-77.
12. Ehlig-Economides, C.A. and Joseph, J.A (1987): "A New Test for Determination of Individual Layer Properties in a Multilayered Reservoir," *SPEFE* (September) 261-83.
13. Firoozabadi, A. and Katz, D.L. (1979): "An analysis of High-Velocity Gas Flow Through Porous Media," *JPT* (February) 211-216.
14. Forchheimer, P.H. (1901): "Wasserbewegung durch Boden," *Z. Ver. Deutsch. Ing.* 45 1781-1788.
15. Frederick, D.C., Jr and Graves, R.M. (1994): "New Correlations To Predict Non-Darcy Flow Coefficients at Immobile and Mobile Water Saturation," paper SPE 28451 presented at Annual Technical Conference and Exhibition, New Orleans, Sept. 25-28.
16. Gao, C. (1984): "Single-Phase Fluid Flow in a Stratified Porous Medium with Crossflow," *SPEJ* (February) 97-106.

17. Geertsma, J. (1974): "Estimating the Coefficient of Inertial Resistance in Fluid Flow Through Porous Media," *SPEJ* (October) 445-450.
18. Gomes, E. (1994): "Well Test Analysis for Layered Composite Systems." Ph.D. Thesis, University of Alberta, Edmonton, AB.
19. Gomes, E. and Ambastha, A.K. (1992): "An analytical Pressure-Transient Model for Multilayered, Composite Reservoirs With Pseudosteady-State Formation Crossflow," *AOSTRA Journal of Research*, Vol. 8, No. 2 (Spring) 63-77.
20. Hall, K.R. and Yarborough, L. (1973): "A New Equation of State for Z-Factor Calculations," *Oil & Gas J.* (June 18) 82-92.
21. Kirchoff, G. (1894): "Vorlesungen uber de theorie der Warme," Barth, Leipzig.
22. Lee, A.L., Gonzales, M.H. and Eakin, B.F. (1966): "The Viscosity of Natural Gases," *JPT* (August) 997-1000.
23. Lee, R.L., Logan, R.W. and Tek, M.R. (1987): "Effect of Turbulence on Transient Flow of Real Gas Through Porous Media," *SPEFE* (March) 108-120.
24. Mattar, L., Brar, G.S. and Aziz, K. (1975): "Compressibility of Natural Gases," *JCPT* (Oct.-Dec.) 77-80.
25. Onur, M., Reynolds, A.C. and Raghavan, R. (1986) "Interference Testing in Commingled Reservoirs," SPE paper 15121.

26. Oren, P.E., Lee, R.L. and Tek, M.R. (1988): "The Effects of Wellbore Storage, Skin, and Turbulence Intensity on Early-Time Transient Flow of Real Gas Through Porous Media," *SPEFE* (September) 547-554.
27. Osman, M.E. and Mohammed, S.A.A. (1993): "Pressure Analysis of Gas Wells in Multilayered Reservoirs With Skin, Storage, and Non-Darcy Effects," paper SPE 25378 presented at the SPE Asia Pacific Oil & Gas Conference, Singapore, February 8-10.
28. Raghavan, R. (1993): *Well Test Analysis*, P T R Prentice Hall, Englewood Cliffs, NJ, 218-267.
29. Smith, R.V. (1961): "Unsteady-State Gas Flow into Gas Wells," *Trans. AIME* Vol. 222, 1151-1159.
30. Stehfast, H. (1970): "Algorithm 368, Numerical Inversion of Laplace Transforms, D-5," *Comm. Of ACM*, 13, No. 1, (Jan) 49.
31. Swift, G.W. and Keil, O.G. (1962): "The Prediction of Performance Including the Effect of Non-Darcy Flow," *Trans. AIME* 225 791-798.
32. User's Manual (1994), IMSL Math Library, version 2.0, 13-329.
33. van Everdingen, A.F., and Hurst, W. (1949): "The Application of the Laplace Transformation to Flow Problems in Reservoirs," *Trans. AIME* 186, 305-324.
34. Wattenbarger, R.A. and Ramey, H.J., Jr. (1968): "Gas Well Testing Turbulence, Damage, and Wellbore Storage," *JPT* (August) 877-887.

35. Whitson, C.H. and Sognesand, S. (1990): "Application of the van Everdingen-Meyer Method for Analyzing Variable-Rate Well Tests," *SPEFE* (March) 67-75.

APPENDIX A : COMPUTER PROGRAM

- C Program to generate MW and DMW for various reservoir conditions for
- C composite reservoirs

INCLUDE 'MATHD.FI'

IMPLICIT REAL*8 (A-H,M,O-Z)

PARAMETER (L1=2,L2=L1+1,L3=L1+2,IIRING=0,SCTEMP = 288.71D00)
 PARAMETER (SCPRESS = 1 01325D05, P1M = 0 3048D00,DAYS=8 64D04)
 PARAMETER (MDMTS = 9.86923D-16,MMCFTM1C = 2 831685D04)
 PARAMETER (PSIPA=6.894757D03,CPPAS=1 0D-03,PSCPR=(PSIPA**2)/CPPAS)
 PARAMETER (NC = 9,NCPOL=NC*22,NCPOL1=NCPOL+1)
 PARAMETER (IMAXPRESS = 10000,IPRLEN = IMAXPRESS/50 + 1)
 PARAMETER (ICYC=22)

DIMENSION RK(L2,L1),RKV(L2,L1),PHI(L2,L1),H(L1),HW(L1),TD(22)
 DIMENSION T1MR(NCPOL),DMPSPR(NCPOL),DMDPSPR(NCPOL),DMPSTIM(NCPOL)
 DIMENSION PDMAT(NCPOL),TRD1(NCPOL),PSPRESMAT(NCPOL)
 DIMENSION EXTEMP(1000),PRMAT(NCPOL1),DMPSPRF(NCPOL)
 DIMENSION PSPRESMATF(NCPOL),PSTIMMAT(NCPOL1),DMPDTPD(NCPOL)
 DIMENSION DDMDT(NCPOL,NCPOL),DMTIM(L1,NCPOL)
 DIMENSION FINDD(L1),FINCC(L1),FRAXQ(L1,NCPOL)
 DIMENSION WORA(L2,L2),WORB(L2),WORX(L2)
 DIMENSION DMPRMT(L1,NCPOL)

COMMON/GM/CD,INOBC,NL,NZ,NRD,INFP,JWELL,SK(L1),NPL(L1),RD(L3),
 + ST(L2,L1),TS(L2,L1),RM(L1,L1),XA(L2,L1),XB(L2,L1)
 COMMON/CINT2/TEMPR,PRESSINI
 COMMON/CINT1/Z1,Z2,N,LR1,TPC1,TPC2,PPC1,PPC2,WM,SG,YCO2,YH2S,
 + VN2,BASE
 COMMON/CINT4/MINI,QST,TMPR1,PI,TTS,QD,HT
 COMMON/FRAC/X(12)
 COMMON/CINT5/BETA,RW
 COMMON/PRPS/PSEUDOPR(IPRLEN),REALPR(IPRLEN)
 COMMON/CIN6/ PERM(L2,L1),RDR(L3),PHIR(L2,L1)

REAL*8 PSTIMMATA[ALLOCATABLE](:),TPRMAT[ALLOCATABLE](:)

LOGICAL CHECK
 EXTERNAL DQDVAL

CHECK = .TRUE.

OPEN(UNIT=13,FILE='SKN25.IN',STATUS='OLD')
 OPEN(UNIT=23,FILE='PERM2.IN',STATUS='OLD')
 OPEN(UNIT=33,FILE='PERMK2.IN',STATUS='OLD')
 OPEN(UNIT=43,FILE='POR2.IN',STATUS='OLD')
 OPEN(UNIT=53,FILE='H2.IN',STATUS='OLD')
 OPEN(UNIT=63,FILE='RD2.IN',STATUS='OLD')
 OPEN(UNIT=333,FILE='BAK1.DAT',STATUS='OLD')

```

CALL UMACH (-2,3)

OPEN (UNIT=1,FILE='FCDA11.OUT')
OPEN (UNIT=2,FILE='FCDB11.OUT')
OPEN (UNIT=3,FILE='FCDC11.OUT')
OPEN (UNIT=4,FILE='FCDD11.OUT')

Z1 = 0.3D00
Z2 = 1.0D00
BASE = 14.7D00
N = 10000
ERT = 1.0D-07

READ(333,*) (X(I),I=1,12)

WRITE(*,*) 'ENTER THE CODE FOR THE GAS PROPERTIES EVALUATION'
WRITE(*,*) '1 - COMPOSITIONAL ANALYSIS'
WRITE(*,*) '0 - GIVEN SPECIFIC GRAVITY'
READ(*,*) IFLAG

IF(IFLAG EQ 0) THEN
  WRITE(*,*) 'ENTER THE SPECIFIC GRAVITY OF THE GAS'
  READ(*,*) SG
  WRITE(*,*) 'ENTER H2S & CO2 MOLE FRACTIONS'
  READ(*,*) YH2S,YCO2
  WM = 28.964D00*SG
  EPS1 = EPS(YH2S,YCO2)
  TPC1 = TPC(SG,EPS1)
  PPC1 = PPC(SG,TPC1,YH2S,EPS1)
ELSE
  CALL GASGRA(SG,WM,PPC1,TPC1,EPS1)
  PPC2 = PPC1
  TPC2 = TPC1
  YH2S = X(1)
  YCO2 = X(2)
  YN2 = X(3)
ENDIF

NL = 1,1
NZ = NL + 1
NRD = NL + 2

P1 = DACOS(0.0D00)*2.0D00

PRINT*,'ENTER THE LAYER NUMBER,JWELL, FOR WHICH WELLBORE PRESSURE
+WILL BE CALCULATED'
READ(*,*) JWELL

PRINT*,'ENTER RESPONSE FUNCTION CODE'
PRINT*,'1--DRAWDOWN'
PRINT*,'2--BUILDUP'

```

```

READ(*,*) INRES

IF (INRES.EQ.2) THEN
  PRINT*,'ENTER DIMENSIONLESS PRODUCING TIME,TPD,(BASED ON MIN
+FRONT RADIUS)'
  READ(*,*) TPD
END IF

PRINT*,'SELECT CODES FOR GAS CAP AND BOTTOM WATER,INBT'
PRINT*,'1---NO GAS CAP OR BOTTOM WATER'
PRINT*,'2---GAS CAP'
PRINT*,'3---BOTTOM WATER'
PRINT*,'4---BOTH'
READ(*,*) INBT

PRINT*,'SELECT CODES FOR OUTER BOUNDARY CONDITIONS,INODC'
PRINT*,'1---INFINITE'
PRINT*,'2---CLOSED'
PRINT*,'3---CONSTANT PRESSURE'
READ(*,*) INODC

INODC = 2

PRINT*,'ENTER WELLBORE STORAGE COEFFICIENT,CD'
READ(*,*) CD

PRINT*,'ENTER RESERVOIR TEMPERATURE (KELVIN)'
READ(*,*) TEMPR
TEMPR = TEMPR*1.8D00

PRINT*,'ENTER INITIAL RESERVOIR PSEUDOREDUCED PRESSURE'
READ(*,*) PPRI

PRESSINI = PPC1*PPRI
WRITE(3,*) 'PRESSINI (PSI) :',PRESSINI

READ(13,*) (SK(J),J=1,NI.)
CLOSE (13)

PRINT*,'ENTER NUMBER OF TERMS TO BE USED IN STEIFFEST ALGORITHM'
READ(*,*) NT

PRINT*,'ENTER DIMENSIONLESS OUTER RADIUS'
READ(*,*) ROU1D

READ(23,*) RK
CALL DWRRRN('RK [M2]',NZ,NL,RK,L2,I'RING)
CLOSE (23)

READ(33,*) RKV
CLOSE (33)

```

```

READ(43,*) PHI
C  CALL DWRRRN('PHI',NZ,NL,PHI,L2,ITRING)
CLOSE (43)

READ(53,*) II
C  CALL DWRRRN('H',NL,1,H,L1,IIRING)

READ(53,*) HW
CALL DWRRRN('HW [M]',NL,1,HW,L1,ITRING)

READ(53,*) IIT
CLOSE (53)

DO J=1,NZ
  READ(63,*) RD(J)
END DO
RD(NRD) = ROUTD*RD(1)

CALL DWRRRN('RD [M]',NRD,1,RD,L3,ITRING)
CLOSE (63)

C  DO J=1,NL
C    SK(J) = ((RK(NZ,J)/RK(1,J))-1.0D00)*DLOG(RD(2)/RD(1))
C  END DO

CALL DWRRRN('SKIN',NL,1,SK,L1,ITRING)

WRITE(*,*) RD
RW = RD(1)/FTM

RDR(1) = RD(1)/FTM
DO I=1,NZ
  DO J=1,NL
    PERM(I,J) = RK(I,J)/MD/MTS
    PHIR(I,J) = PHI(I,J)
  END DO
  RDR(I+1)=RD(I+1)/FTM
END DO

PRINT*,'ENTER INITIAL DIMENSIONLESS TIME ( MINIMUM FRONT RADIUS )'
READ(*,*) TD1

PRINT*,'ENTER CODES FOR PENETRATION CONDITION'
PRINT*,'0---FULL'
PRINT*,'1---PARTIAL'
READ(*,*) INFP

PRINT*,'ENTER NONDARCY COEFFICIENT BETA CODE'
PRINT*,'1 - GEERTSMA'
PRINT*,'2 - FIROOZABADI'

```

```

READ(*,*) IBETA

PRINT*,'ENTER THE ABONDONMENT PRESSURE (PSI)'
READ(*,*) ABONDP
WRITE(3,*)''
WRITE(3,*) 'ABONDONMENT PRESSURE (PSI) ',ABONDP

PRINT*,'ENTER OPTION FOR DERIVATIVE COMPUTATION'
PRINT*,'0 --- NOT REQUIRED'
PRINT*,'1 --- REQUIRED'
READ(*,*) IDER

HWT = 0.0D00
DO J=1,NL
  IF (HW(J).EQ.0.0D00) THEN
    NPL(J)=0
  ELSE
    NPL(J)=1
    HWT = HWT + HW(J)
  END IF
END DO

BPEN = HWT/HT

WRITE(3,*)''
WRITE(3,*) 'WELL PENETRATION RATIO ',BPEN
*****
C  Nondimensionalizing the radii based on minimum front radius

AR1=RD(1)
AR2=RD(2)
DO I=1,NZ+1
  RD(I)=RD(I)/AR2
END DO
C  CALL DWRRRN('RD',NRD,1,RD,L3,ITRING)

C  Transmissibility and storativity computation

DO J=1,NL
  DO I=1,NZ
    TS(I,J)=RK(I,J)*H(J)
    ST(I,J)=PHI(I,J)*H(J)
  END DO
END DO
C  CALL DWRRRN('TRANSMISSIBILITY',NZ,NL,TS,L2,ITRING)
C  CALL DWRRRN('STORATIVITY',NZ,NL,ST,L2,ITRING)

C  Crossflow parameter, XA(I,J), computation

DO I=1,NZ
  DO J=1,NL

```



```

IF(J.EQ.NL) THEN
  IF((INBT.EQ.2).OR.(INBT.EQ.4)) THEN
    XA(I,J)=2.0D00*RKV(I,I)/H(J)
  ELSE
    XA(I,J)=0.0D00
  END IF
ELSE
  XA(I,J)=2.0D00*RKV(I,J)*RKV(I,J+1)/(H(J)*RKV(I,J+1) +
+   H(J+1)*RKV(I,J))
  END IF
END DO
END DO
C  CALL DWRRRN('XA',NZ,NL,XA,L2,ITRING)

C  Crossflow parameter, XB(I,J), computation

DO I=1,NZ
  DO J=1,NL
    IF (J.EQ.1) THEN
      IF ((INBT.EQ.3).OR.(INBT.EQ.4)) THEN
        XB(I,J)=2.0D00*RKV(I,J)/H(J)
      ELSE
        XB(I,J)=0.0D00
      END IF
    ELSE
      XB(I,J)=2.0D00*RKV(I,J)*RKV(I,J-1)/(H(J)*RKV(I,J-1) +
+   H(J-1)*RKV(I,J))
      END IF
    END DO
  END DO
C  CALL DWRRRN('XB',NZ,NL,XB,L2,ITRING)

C  Mobility ratios, RM(I,J), calculation

DO I=1,NL
  DO J=1,NL
    RM(I,J) = TS(I+1,J)/TS(I,J)
  END DO
END DO
C  CALL DWRRRN('RM',NZ,NL,RM,L2,ITRING)

C  Total transmissibility and storativity calculation
C  WRITE(1,*)
C  WRITE(1,*)'TOTAL TRANSMISSIBILITY   TOTAL STORATIVITY'
TTS=0.0D00
TST=0.0D00

DO J=1,NL
  TTS = TTS + 1S(L2,J)
  TST = TST + ST(1,J)
END DO

```

C WRITE(1,*) TTS ,TST

C Nondimensionalizing the storativities and transmittivities

```
DO I=1,NZ
  DO J=1,NL
    TS(I,J) = TS(I,J)/TTS
    ST(I,J) = ST(I,J)/TST
  END DO
END DO
```

C CALL DWRRRN('DIMLESS TS',NZ,NL,TS,L2,ITRING)
CALL DWRRRN('DIMLESS ST [RW BASIS]',NZ,NL,ST,L2,ITRING)

C Nondimensionalizing the crossflow parameters

```
DO I=1,NZ
  DO J=1,NL
    XA(I,J) = (AR1**2)*XA(I,J)/TTS
    XB(I,J) = (AR1**2)*XB(I,J)/TTS
  END DO
END DO
```

CALL DWRRRN('DIMLESS XA [RW BASIS]',NZ,NL,XA,L2,ITRING)
CALL DWRRRN('DIMLESS XB [RW BASIS]',NZ,NL,XB,L2,ITRING)

C Conversion of crossflow parameters on the basis of minimum front radius

```
DO I=1,NZ
  DO J=1,NL
    XA(I,J) = XA(I,J)/(RD(1)**2)
    XB(I,J) = XB(I,J)/(RD(1)**2)
  END DO
END DO
```

C CALL DWRRRN('XA [MIN. FRONT RADIUS BASIS]',NZ,NL,XA,L2,ITRING)
C CALL DWRRRN('XB [MIN. FRONT RADIUS BASIS]',NZ,NL,XB,L2,ITRING)

```
TPR10 = TEMPR/TPC1  
PPR10 = PRESSINI/PPC1  
CALL ZFAC1(Z1,Z2,N,ERT,TPR10,PPR10,ZNEW0,I)  
VSC0 = VISCOG2(PRESSINI,TEMPR,ZNEW0,WM)  
CALL CR(ZNEW0,TPR10,PPR10,CR10)  
GCT0 = CRT0/PPC1
```

```
REALPR(1) = 14.7D00  
PSEUDOPR(1) = 0.0D00
```

```
DO KC = 2,JPRIEN  
  REALPR(KC) = REALPR(1) + 50.0*REAL(KC - 1)  
  RPRS = REALPR(KC)  
  CALL INTEGPR(RPRS,PSPRS)  
  PSEUDOPR(KC) = PSPRS
```

END DO

CALL INTEG(PRESSINI,MINI)
MINI = MINI*PSCPR

CALL INTEG(ABONDP,ABONDPS)
ABONDPS = ABONDPS*PSCPR

PRINT*,'ENTER WHICH FLOWRATE TO COMPARE WITH'
PRINT*,'0 --- QD'
PRINT*,'1 --- QST'
READ(*,*) INQD

IF(INQD.EQ.1) THEN
PRINT*,'ENTER QST (M3/SFC)'
READ(*,*) QSF
QD = QSF*SCPRESS*TEMPR/(TTS*SCTEMP*MINI*PI*1.8D00)
ELSE
PRINT*,'ENTER DIMENSIONLESS FLOWRATE'
READ(*,*) QD
QST = QD*TTS*SCTEMP*MINI*PI*1.8D00/(SCPRESS*TEMPR)
END IF

WRITE(3,*)''
WRITE(3,*)'QST(M3/SEC)=' ,QST
WRITE(3,*)''
WRITE(3,*)'QD=' ,QD

DO JLAY=1,I.1

C TD vector generation

DO IG=1,10
TD(IG) = (1.0D0 + 0.2D0*REAL(IG))*TD1
TD(IG + 10) = (3.0D0 + 0.5D0*REAL(IG))*TD1
END DO
TD(21) = 9.0D0*TD1
TD(22) = 10.0D0*TD1

C CALL DWRRRN('TD',14,1,TD,14,ITRING)

PRMAT(1) = PRESSINI
PSTIMMAT(1) = 0.0D00

IMAT = 0
IL=8573

IF (INRES.EQ.2) CALL INVERT(JLAY,TPD,NT,IL,MD1,MDM1,QFRA)

DO I=1,NC
DO J=1,22

```

SPC = TD(J)
IF (INRES.EQ.2) TIEN
  SPC1 = SPC + TPD
  CALL INVERT(JLAY,SPC1,N1,IL,MD2,MDM2,QFRA)
END IF

CALL INVERT(JLAY,SPC,NT,IL,MD,MDM,QFRA)

IF (INRES.EQ.1) MDC = MDM

IF(INRES.EQ.2) TIEN
  MD = MD1 + MD - MD2
  MDC = MDM - MDM2
  MDH = (SPC1*SPC/TPD)*MDC
END IF

MDM = SPC*MDC

IF(INRES.EQ.2) SPCH = SPC1/SPC

IMAT = IMAT + 1

TRD1(IMAT) = SPC

SPC = SPC*(AR2**2)/(AR1**2)

DMPSPR(IMAT) = MD
DMDPSPR(IMAT) = MDM
DMPSTIM(IMAT) = SPC
FRAXQ(JLAY,IMAT) = QFRA

TMPRI = TEMPR/1.8D00

CALL MD10MW(MD,MWF)

IF(MWF.LT.ABONDPS) GOTO 2000

PSTIME = SPC*(AR1**2)*TST/TTS

MWF = MWF/PSCPR

PSPRESMAT(IMAT)= MWF
CALL PSEUDRPR(MWF,PWF)

PSTIMMAT(IMAT + 1) = PSTIME
PRMAT(IMAT + 1) = PWF

TD(J) = TD(J)*10.0D0

END DO
END DO

```

```

GOTO 3000

2000 IMATMAX = IMAT - 1
GOTO 4000

3000 IMATMAX = IMAT

4000 DIFE = TST*(GCTO/PSIPA)*(VSC0*CPPAS)/TTS

ITIMMAX = IMATMAX + 1

ALLOCATE (PSTIMMATA(ITIMMAX),TPRMAT(ITIMMAX))

PSTIMMATA(1) = 0.0D00
TPRMAT(1) = PRESSINI

DO JK = 2, ITIMMAX
  PSTIMMATA(JK) = PSTIMMATA(JK-1)
  TPRMAT(JK) = TPRMAT(JK-1)
END DO

ERIDAR = 1.0D-04

DO J=1,IMATMAX
  PSRTIME = PSTIMMATA(J+1)
  WRITE(*,*) 'OK'
  CALL INVPSTIME(J,ITIMMAX,PSTIMMATA,TPRMAT,PSRTIME,RTIME)
  WRITE(*,*) J, RTIME='RTIME'
  TIMR(J) = RTIME
  DMTJM(JLAY,J) = TIMR(J)/(DIFE*AR1**2)

  PDMAT(J) = 2.0D00*PI*TTS*(PRESSINI-TPRMAT(J+1))*PSIPA/(QST*
+ VSC0*CPPAS)
END DO

IF(JLAY.EQ.1) THEN
  WRITE(3,*) ''
  WRITE(3,*) 'TQD =',QD
  WRITE(3,*) ''
  WRITE(3,*) 'K =',TTS/(HT*MDMTS)
END IF

DO J=1,IMATMAX

  EXTEMP(1) = 1.0D-03
  TEMPTD = DMTJM(JLAY,J)
  EXTEMP(2) = DMPSPR(J)
  TPRINV = RADINV(TEMPTD)
  FQ = FRAXQ(JLAY,J)
  K = 2

```

```

DO WHILE(DABS((EXTEMP(K)-EXTEMP(K-1))/EXTEMP(K-1)) GE ERTDAR)

    TEMPMD = EXTEMP(K)
    CALL MDTOMW(TEMPMD,TEMPMW)
    IF(TEMPMW.LT ABONDPS) GOTO 5000
    TEMPMW = TEMPMW/PSCPR
    CALL PSEUDRPR(TEMPMW,TEMPPW)

    IF(TPRINV.GE.RDR(NRD)) THEN
        REINV = RDR(NRD) - 0.1D00
    CALL CORTURB(JLAY,FQ,TEMPPW,REINV,TPR,TPHI,TBETA,TFNO,TRNT,TCEI)
        CALL NDARCYD(JLAY,REINV,TDMU)
    ELSE

CALL CORTURB(JLAY,FQ,TEMPPW,TPRINV,TPR,TPHI,TBETA,TFNO,TRNT,TCEI)
        CALL NDARCYD(JLAY,TPRINV,TDMU)
    END IF

        EXTEMP(K+1) = TCEI*TDMU*FQ*QST*DAYS/MMCFTMTC + DMPSPR(J)

        K = K + 1
    END DO

    DMPSPRF(J) = EXTEMP(K)
    DMPRMT(JLAY,J) = DMPSPRF(J)

C    DMPSPRF(J) = DMPSPRF(J)*FRAXQ(JLAY,J)/TS(1,JWELL)

    WRITE(*,*) J, ' CI=',TCEI, ' TDMU=',TDMU, ' REINV=',TPRINV
    WRITE(3,*) JLAY,J,TPRINV,TRNT,TFNO,TCEI,TDMU

    TMD = DMPSPRF(J)

    CALL MDTOMW(TMD,TMWF)
    IF(TMWF.LT ABONDPS) GOTO 5000
    TMWF = TMWF/PSCPR

    PSPRESMATF(J) = TMWF

    CALL PSEUDRPR(TMWF,TPWF)

    TPRMAT(J + 1) = TPWF
    PRMAT(J + 1) = TPWF
    END DO
    WRITE(*,*) 'OK 999'
    ITIMMAX1 = ITIMMAX
    GOTO 6000

5000 IMATMAX = J - 1
    ITIMMAX1 = IMATMAX + 1

```

```
DEALLOCATE (PSTIMMATA,TPRMAT)
```

```
ALLOCATE (PSTIMMATA(ITIMMAX1),TPRMAT(ITIMMAX1))
```

```
PSTIMMATA(1) = 0.0D00
```

```
TPRMAT(1) = PRESSINI
```

```
DO JK = 2, ITIMMAX1
```

```
  PSTIMMATA(JK) = PSTIMMATA(JK)
```

```
  TPRMAT(JK) = PRMAT(JK)
```

```
END DO
```

```
6000 DO J=1,IMATMAX
```

```
  PSRTIME = PSTIMMAT(J+1)
```

```
  CALL INVPSTIME(J,ITIMMAX1,PSTIMMATA,TPRMAT,PSRTIME,RTIME)
```

```
  WRITE(*,*) 'OK ',J
```

```
  TIMR(J) = RTIME
```

```
  DMTIM(JLAY,J) = TIMR(J)/(DIFE*AR1**2)
```

```
  PDMAT(J) = 2.0D00*PI*ITS*(PRESSINI-TPRMAT(J+1))*PSIPA/(QST*  
+ VSC0*CPPAS)
```

```
END DO
```

```
DEALLOCATE (PSTIMMATA,TPRMAT)
```

```
END DO
```

```
DO J=1,IMATMAX
```

```
  IF(J.EQ.1) THEN
```

```
    TMDN = DMPSTIM(1)
```

```
  ELSE
```

```
    TMDN = DMPSTIM(J) - DMPSTIM(J-1)
```

```
  END IF
```

```
  MDDN = DQDVAL(TMDN,IMATMAX,DMPSFIM,DMPSPR,CHECK)
```

```
  EF = CD/TMDN
```

```
  IF(J.EQ.1) THEN
```

```
    GEE = 0.0D0
```

```
  ELSE
```

```
    GEE = EF*DMPSPRF(J-1)
```

```
  END IF
```

```
DO JLAY=1,L1
```

```
  CTM5 = (DMPRIMT(JLAY,J)-DMPSPR(J))
```

```
  FINDD(JLAY) = - (MDDN + CTM5)/TS(1,ILAY)
```

```
  IF(J.EQ.1) THEN
```

```

      CTM2 = 0.0D0
    ELSE
      CTM2 = - FRAXQ(JLAY,J-1)*MDDN
    END IF

    IF(J.EQ.1) THEN
      CTM1 = 0.0D0
    ELSE
      CTM1 = FRAXQ(JLAY,1)*DMPSPR(J)
    END IF

    SUMC = 0.0D0

    DO JIK=1,J-2
      CTM4 = FRAXQ(JLAY,JIK+1) - FRAXQ(JLAY,JIK)
      TMDK = DMPSTIM(J) - DMPSTIM(JIK)
      MDDK = DQDVAL(TMDK,IMA1MAX,DMPSTIM,DMPSPR,CHECK)
      CTM4 = CTM4*MDDK
      SUMC = SUMC + CTM4
    END DO

    CTM = (CTM1 + CTM2 + SUMC)/TS(1,JLAY)

    FINCC(JLAY) = CTM

  END DO

  DO IR=1,L1
    DO IC=1,L1
      WORA(IR,IC) = 0.0D0
    END DO
    WORA(IR,L2) = 1.0D0

    WORA(IR,IR) = FINDI(IR)
  END DO

  DO IC=1,L1
    WORA(L2,IC) = 1.0D0
    WORD(IC) = FINCC(IC)
  END DO

  WORA(L2,L2) = EF
  WORD(L2) = 1.0D0 + GEE

  CALL DLSASF(L2, WORA, L2, WORD, WORX)
  DMPSPR(J) = WORX(L2)
  FRAXQ(1,J) = WORX(1)
  FRAXQ(2,J) = WORX(2)

END DO

```


IF (IDER.EQ.1) THEN

TOL = 0.000001D0
BGSTEP = 0.05D0

DDMD1(1,1) = 0.0D0
X = DMPSTIM(1) + BGSTEP
Y = DQDVAL(X,IMATMAX,DMPSTIM,DMPSPRF,CHECK)
DDMDT(1,2) = (Y - DMPSPRF(1))/BGSTEP

K=2

DO WHILE(DABS(DDMDT(1,K)-DDMDT(1,K-1)).GT.TOL)
 BSTEP = BGSTEP/REAL(K)
 X = DMPSTIM(1) + BSTEP
 Y = DQDVAL(X,IMATMAX,DMPSTIM,DMPSPRF,CHECK)
 DDMDT(1,K+1) = (Y - DMPSPRF(1))/BSTEP
 K = K+1
END DO

DMPDIPD(1) = DDMDT(1,K)*DMPSTIM(1)

DDMDT(IMATMAX,1) = 0.0D0
X = DMPSTIM(IMATMAX) - 2.0D0*BGSTEP
Y = DQDVAL(X,IMATMAX,DMPSTIM,DMPSPRF,CHECK)
DDMDT(IMATMAX,2) = (DMPSPRF(IMATMAX)-Y)/(2.0D0*BGSTEP)

K=2

DO WHILE(DABS(DDMDT(IMATMAX,K)-DDMDT(IMATMAX,K-1)).GT.TOL)
 BSTEP = BGSTEP/REAL(K)
 X = DMPSTIM(IMATMAX) - 2.0D0*BSTEP
 Y = DQDVAL(X,IMATMAX,DMPSTIM,DMPSPRF,CHECK)
 DDMDT(IMATMAX,K+1) = (DMPSPRF(IMATMAX)-Y)/(2.0D0*BSTEP)
 K = K+1
END DO

DMPDIPD(IMATMAX) = DDMDT(IMATMAX,K)*DMPSTIM(IMATMAX)

DO I=2,IMATMAX-1

 BGSTEP = 0.05D0

 KKC = 1
425 ICYC = KKC*ICYC
 IF(I.GT.ICYC) THEN
 KKC=KKC+1
 GOTO 425
 END IF

 STEP = 10.0**(KKC-1)

```
BGSTEP = DGSTEP*STEP
```

```
DDMDT(I,1) = 0.0D0
```

```
X1 = DMPSTIM(I) - 2.0D0*BGSTEP
```

```
X2 = DMPSTIM(I) + 2.0D0*BGSTEP
```

```
Y1 = DQDVAL(X1,IMATMAX,DMPSTIM,DMPSPRF,CHECK)
```

```
Y2 = DQDVAL(X2,IMATMAX,DMPSTIM,DMPSPRF,CHECK)
```

```
DDMDT(I,2) = (Y2 - Y1)/(4.0D0*BGSTEP)
```

```
K = 2
```

```
DO WHILE(DABS(DDMDT(I,K)-DDMDT(I,K-1)).GT.TOL)
```

```
  BSTEP = BGSTEP/REAL(K)
```

```
  X1 = DMPSTIM(I) - 2.0D0*BSTEP
```

```
  X2 = DMPSTIM(I) + 2.0D0*BSTEP
```

```
  Y1 = DQDVAL(X1,IMATMAX,DMPSTIM,DMPSPRF,CHECK)
```

```
  Y2 = DQDVAL(X2,IMATMAX,DMPSTIM,DMPSPRF,CHECK)
```

```
  DDMDT(I,K+1) = (Y2 - Y1)/(4.0D0*BSTEP)
```

```
  K = K + 1
```

```
END DO
```

```
DMPDTPD(I) = DDMDT(I,K)*DMPSTIM(I)
```

```
WRITE(*,*) I, 'OK'
```

```
END DO
```

```
END IF
```

```
DO I=1,IMATMAX
```

```
  WRITE(1,*) DMPSTIM(I),DMPSPRF(I),DMPSPR(I)
```

```
  WRITE(2,*) DMPSTIM(I),DMPDTPD(I),DMDPSPR(I)
```

```
  WRITE(4,*) DMPSTIM(I),FRAXQ(1,I),FRAXQ(2,I)
```

```
END DO
```

```
8  FORMAT(2X,F20.6,2X,F20.8)
```

```
STOP
```

```
END
```

```
C *****
```

```
C Subroutine for eigenvalue, eigenvector, and Bessel function calculation  
C from IMSL /MATH /LIBRARY. It calculates all coefficients and solves the  
C system of simultaneous equations. Wellbore pressure, its derivative and  
C fractional flow rate are also calculated
```

```
SUBROUTINE LAP(S,JL,MWDL,MDMI,QFR)
```

```
IMPLICIT REAL*8 (A-H,M,O-Z)
```

```
PARAMETER (LL1=2,LL2=LL1+1,LL3=LL1+2,LL4=2*LL1+1,IRING=0)
```

```
PARAMETER (IPATH=1,NCODA=1,LLDA=LL1,LDB=LL1,N=LL1,UDFVEC=1.1.1)
```

```
PARAMETER (NEQ=LL4,LDA2=NEQ)
```

```

DIMENSION A(LL1,LL1),EVAL(LL1),EVEC(L,I,1,LL1),AEI(L,I,2,LL1,I,I,1),
+ AA(LL4,LL4),B(LL4),X(LL4),SGMA(LL2,LL1),BB(LL1,LL1)

COMMON/GM/CD,INOBC,NL,NZ,NRD,INFP,JWELL,SK(LL1),NPL(LL1),RD(LL3),
+ ST(LL2,LL1),TS(L,I,2,I,I,1),RM(L,I,1,I,I,1),XA(I,I,2,I,I,1),XB(I,I,2,LL1)

C CALL DWRRRN('TS IN LAP',NZ,NL,TS,LL2,I,TRING)
C CALL DWRRRN('ST IN LAP',NZ,NL,ST,LL2,I,TRING)

ICOUNT = 0

DO I=1,NZ

  DO J=1,NI,
    DO J1=1,NL
      BB(J,J1) = 0.0D00
      A(J,J1) = 0.0D00
    END DO
  END DO

  DO J=1,NL
    IF (J.EQ.1) THEN
      A(J,J+1) = -XA(I,J)
    ELSE IF (J.EQ.NL) THEN
      A(J,J-1) = -XB(I,J)
    ELSE
      A(J,J+1) = -XA(I,J)
      A(J,J-1) = -XB(I,J)
    END IF
    A(J,J) = ST(I,J)*S + XA(I,J) + XB(I,J)
    BB(J,J) = TS(I,J)
  END DO

C CALL DWRRRN('A',NI,NL,A,J,I,1,TRING)
C CALL DWRRRN('BB',NI,NL,BB,J,I,1,TRING)

C Eigenvalues (EVAL(J)) & eigenvectors (EVEC(L,I)) calculation

CALL DGVCSP(N,A,LDA,BB,LDB,EVAL,EVEC,L,DEVEC)

C Storing eigenvalues & eigenvectors

DO J=1,NL
  DO J1=1,NL
    AEI(I,J,J1) = EVEC(J,J1)
  END DO
END DO

C CALL DWRRRN('EVEC',NI,NL,EVEC,J,I,1,TRING)

DO J=1,NI
  T = EVAL(J)

```

```

        SGMA(I,J) = DSQRT(T)
    END DO
C     CALL DWRRRN('SGMA SQUARE',NL,1,EVAL,LL1,ITRING)

    END DO

C     Initializing the augmented matrix

    DO I1=1,LL4
        DO I2=1,LL4
            AA(I1,I2) = 0.0D00
            B(I1) = 0.0D00
        END DO
    END DO

C     Setting up the matrices AA(I,J) & B(J) from the boundary conditions

C     Wellbore condition
C     For full penetration

    IF(INFP.EQ.0) THEN
        I=1
        DO J=1,N-1
            DO K=1,N
                ARG6=SGMA(I,K)*RD(I)
                AA(J,K)=AEI(I,J,K)*DBSK0E(ARG6)
+                + SK(J)*AEI(I,J,K)*ARG6*DBSK1E(ARG6)
-                - AEI(I,J+1,K)*DBSK0E(ARG6)
+                + SK(J+1)*AEI(I,J+1,K)*ARG6*DBSK1E(ARG6)

                N2 = N**2 + N + K

                AA(J,N2)=AEI(I,J,K)*DBSI0E(ARG6)
+                + SK(J)*AEI(I,J,K)*ARG6*DBSI1E(ARG6)
-                - AEI(I,J+1,K)*DBSI0E(ARG6)
+                + SK(J+1)*AEI(I,J+1,K)*ARG6*DBSI1E(ARG6)
            END DO
        END DO

        DO K=1,N
            SUM1 = 0.0D00
            SUM2 = 0.0D00
            DO J=1,N
                ARG6=SGMA(I,K)*RD(I)
                S1=TS(I,J)*AEI(I,J,K)*ARG6*DBSK1E(ARG6)
                SUM1 = SUM1 + S1
                S2=-TS(I,J)*AEI(I,J,K)*ARG6*DBSI1E(ARG6)
                SUM2 = SUM2 + S2
            END DO

            AA(N,K) = SUM1

```

```

      N3 = N**2 + N + K
      AA(N,N3) = SUM2
    END DO

```

```

    B(N) = 1.0D00/S

```

C For partial penetration

```

ELSE

```

```

  I = 1

```

```

  DO J=1,NL

```

```

    DO K=1,N

```

```

      IF (NPL(J) EQ 0) THEN

```

```

        ARG6=SGMA(I,K)*RD(I)

```

```

        AA(J,K)=-AEI(I,J,K)*DBSK1E(ARG6)*ARG6

```

```

        N2 = N**2 + N + K

```

```

        AA(J,N2)=AEI(I,J,K)*DBSK1E(ARG6)*ARG6

```

```

      END IF

```

```

    END DO

```

```

  END DO

```

```

DO J=1,N-1

```

```

  DO K=1,N

```

```

    IF (NPL(J).EQ.1.AND.NPL(J+1).EQ.1) THEN

```

```

      ARG6=SGMA(I,K)*RD(I)

```

```

      AA(I,K)=AEI(I,J,K)*DBSK0E(ARG6)

```

```

+       + SK(J)*AEI(I,J,K)*ARG6*DBSK1E(ARG6)

```

```

+       - AEI(I,I+1,K)*DBSK0E(ARG6)

```

```

+       - SK(J+1)*AEI(I,J+1,K)*ARG6*DBSK1E(ARG6)

```

```

      N2 = N**2 + N + K

```

```

      AA(J,N2)=AEI(J,J,K)*DBSK0E(ARG6)

```

```

+       - SK(J)*AEI(I,J,K)*ARG6*DBSK1E(ARG6)

```

```

+       - AEI(I,J+1,K)*DBSK0E(ARG6)

```

```

+       + SK(J+1)*AEI(I,J+1,K)*ARG6*DBSK1E(ARG6)

```

```

    END IF

```

```

  END DO

```

```

END DO

```

```

DO K=1,N

```

```

  SUM1 = 0.0D00

```

```

  SUM2 = 0.0D00

```

```

  DO J=1,N

```

```

    IF(NPL(J).EQ.1) THEN

```

```

      ICOUNT = ICOUNT + 1

```

```

      ARG6=SGMA(I,K)*RD(I)

```

```

      S1=TS(I,J)*AEI(I,J,K)*ARG6*DBSK1E(ARG6)

```

```

      SUM1 = SUM1 + S1

```

```

S2=TS(I,J)*AEI(I,J,K)*ARG6*DBS11E(ARG6)
SUM2 = SUM2 + S2
END IF
END DO

```

```

AA(N,K) = SUM1
N3 = N**2 + N + K
AA(N,N3) = SUM2
END DO

```

```

B(N) = 1.0D00/S
END IF

```

C Setting up equations from interface boundary conditions

```

DO I=1,N
DO J=1,N
DO K=1,N
ARG1 = SGMA(I,K)*RD(I+1)
ARG2 = SGMA(I+1,K)*RD(I+1)
FACTOR1 = SGMA(I,K)*(RD(I)-RD(I+1))
IF(FACTOR1 LT.-174 0D00) FACTOR1 = -170.0D00

```

C Equations from pressure continuity condition

```

N3 = I*N + J
N4 = N*(I-1) + K

AA(N3,N4)=AEI(I,J,K)*DBSK0E(ARG1)*DEXP(FACTOR1)
N5 = N + N*(I-1) + K
AA(N3,N5)=-AEI(I+1,J,K)*DBSK0E(ARG2)
N6 = N**2 + N + N*(I-1) + K
AA(N3,N6)=AEI(I,J,K)*DBS10E(ARG1)*DEXP(-FACTOR1)
N7 = N + N6
AA(N3,N7)=-AEI(I+1,J,K)*DBS10E(ARG2)

```

C Equations from flow continuity condition

```

N8 = N**2 + N*I + J
AA(N8,N4)=AEI(I,J,K)*SGMA(I,K)*DBSK1E(ARG1)*
+ DEXP(FACTOR1)
AA(N8,N5)=-AEI(I+1,J,K)*SGMA(I+1,K)*
+ DBSK1E(ARG2)*RM(I,J)
AA(N8,N6)=-AEI(I,J,K)*SGMA(I,K)*DBS11E(ARG1)*
+ DEXP(-FACTOR1)
AA(N8,N7)=-AEI(I+1,J,K)*SGMA(I+1,K)*
+ DBS11E(ARG2)*RM(I,J)

END DO
END DO
END DO

```

C Outer Boundary Conditions

C For infinite acting reservoir

IF (INOBC EQ.1) THEN

C For closed outer boundary

ELSE IF (INOBC EQ.2) THEN

DO J=1,N

DO K=1,N

N9 = 2*(N**2) + N + J

N10 = N**2 + K

ARG3 = SGMA(NZ,K)*RD(NRD)

FACTOR2 = SGMA(NZ,K)*(RD(NZ)-RD(NRD))

IF(FACTOR2.LT.-174.0D00) FACTOR2 = -170.0D00

AA(N9,N10)=AEI(NZ,J,K)*SGMA(NZ,K)*DBS11E(ARG3)*
+ DEXP(FACTOR2)

N11 = 2*(N**2) + N + K

AA(N9,N11)=-AEI(NZ,J,K)*SGMA(NZ,K)*DBS11E(ARG3)*
+ DEXP(-FACTOR2)

END DO

END DO

C For constant pressure outer boundary

ELSE IF (INOBC EQ.3) THEN

DO J=1,N

DO K=1,N

N9 = 2*(N**2) + N + J

N10 = N**2 + K

ARG3 = SGMA(NZ,K)*RD(NRD)

FACTOR2 = SGMA(NZ,K)*(RD(NZ)-RD(NRD))

AA(N9,N10)=AEI(NZ,J,K)*DBS10E(ARG3)*DEXP(FACTOR2)

AA(N9,N11)=AEI(NZ,J,K)*DBS10E(ARG3)*DEXP(-FACTOR2)

END DO

END DO

END IF

C Solution of the system of equations

C CALL DWRRRN('AA',NEQ,NEQ,AA,LI4,ITRING)

C CALL DWRRRN('B',NEQ,1,B,LL4,ITRING)

CALL DLSARG(NEQ,AA,IDA2,B,IPATH,X)

C CALL DWRRRN('X',NEQ,1,X,LI4,ITRING)

C Calculation of the wellbore pressure

```

FACT1 = 0.0D00
SUM = 0.0D00
SUM1 = 0.0D00
J=JL
I=1
DO K=I,N
  N12 = N**2 + N + K
  ARG4=SGMA(I,K)*RD(I)
  MW=AEI(I,J,K)*DBSK0(ARG4)*X(K)*DEXP(ARG4) +
+ AEI(I,J,K)*DBS0(ARG4)*X(N12)*DEXP(-ARG4) +
+ SK(J)*AEI(I,J,K)*ARG4*DBSK1(ARG4)*X(K)*DEXP(ARG4) -
+ SK(J)*AEI(I,J,K)*ARG4*DBS11(ARG4)*X(N12)*DEXP(-ARG4)
  SUM = SUM + MW
  QF=AEI(I,J,K)*ARG4*DBSK1(ARG4)*X(K)*DEXP(ARG4) -
+ AEI(I,J,K)*ARG4*DBS11(ARG4)*X(N12)*DEXP(-ARG4)
  SUM1 = SUM1 + QF
END DO

MWDL = SUM
C MWDL = MWDL/(1.0D00 + CD*((S*RD(1))**2)*MWDL)
MDML = S*MWDL

QFR = SUM1*TS(I,JL)

RETURN
END
*****
SUBROUTINE INVERT(JL,TD,N,IL,MD,MDM,QFR)

```

C Inversion from Laplace space to real space

```

IMPLICIT REAL*8 (A-H,M,O-Z)

DIMENSION V(50)

IF(N.EQ.IL) GOTO 85
IL = N
DLOGTW = 0.69314718055999D00
N2 = N/2

DO IN=1,N
  KL = (IN + 1)/2
  KU = MIN0(IN,N2)
  V(IN) = 0.0D00
  DO K=KL,KU
    T1 = FACT(2*K)
    T2 = FACT(N2 - K)
    T3 = FACT(K)
    T4 = FACT(K - 1)
    T5 = FACT(IN - K)
    T6 = FACT(2*K - IN)

```



```

      TT = (K**N2)* T1/(T2*T3*T4*T5*T6)

      V(IN) = V(IN) + TT
    END DO
    V(IN) = V(IN)*((-1)**(N2 + 1N))
  END DO

```

```

85 MD = 0.0D00
   MDM = 0.0D00
   QFR = 0.0D00
   AT=DLOGTW/TD

```

```

DO IN=1,N
  ARG = REAL(IN)*AT

  CALL LAP(ARG,JI,MWDL,MDML,QFRL)

  MD = MD + V(IN)*MWDL
  MDM = MDM + V(IN)*MDML
  QFR = QFR + V(IN)*QFRL
END DO

```

```

MD = MD*AT
MDM = MDM*AT
QFR = QFR*AT

```

```

RETURN
END

```

C FUNCTION for FACTORIAL COMPUTATION

```

FUNCTION FACT(NF)
  IMPLICIT REAL *8 (A-H,O-Z)

```

```

  IF(NF GE 0) THEN
    FCT = 1.00D00
    DO I=2,NF
      FCT = FCT*REAL(I)
    END DO
    FACT = FCT
  ELSE
    FACT = 0.00D00
  END IF

```

```

RETURN
END

```

C FUNCTION EPS(YI2S,YCO2)

```

  IMPLICIT REAL *8 (A-H,M,O-Z)

```

```
A = YH2S + YCO2
D = YH2S
```

```
EPS = 120.0D00*((A**0.9) - (A**1.6)) + 15.0D00*((D**0.5) -
+ (B**4.0))
```

```
END
```

```
C=====
FUNCTION TPC(SG,EP)
```

```
IMPLICIT REAL*8 (A-H,M,O-Z)
```

```
TPC = 169.2D00 + 349.5D00*SG - 74.0D00*(SG**2)
TPC = TPC - EP
```

```
END
```

```
C=====
FUNCTION PPC(SG,TPC,YH2S,EP)
```

```
IMPLICIT REAL*8 (A-H,M,O-Z)
```

```
PPC = 756.8D00 - 131.0D00*SG - 3.6D00*(SG**2)
PPC = PPC*TPC/((TPC + EP) + YH2S*(1.0D00 - YH2S)*EP)
```

```
END
```

```
C=====
SUBROUTINE ZFAC1(Z1,Z2,N,ERR,TPR,PPR,ZNEW,I)
```

```
IMPLICIT REAL*8 (A-H,M,O-Z)
```

```
DO 10 I=1,N
```

```
F1 = F(Z1,TPR,PPR)
F2 = F(Z2,TPR,PPR)
```

```
ZNEW = Z2 - F2*((Z2 - Z1)/(F2 - F1))
```

```
FZ = F(ZNEW,TPR,PPR)
```

```
IF(DABS(FZ) LE ERR) THEN
```

```
    RETURN
```

```
ENDIF
```

```
TZ = Z1
```

```
Z1 = Z2
```

```
Z2 = ZNEW
```

```
10 CONTINUE
```

```
RETURN
```

```
END
```

```
C=====
FUNCTION F(Z,TPR,PPR)
```

```
IMPLICIT REAL*8 (A-H,M,O-Z)
```

```
COMMON /GMM/ A1,A2,A3,A4,A5,A6,A7,A8,A9,A10,A11,R1,C,C1,C2,C3
```

```
A1 = 0.3265D00
```

```
A2 = -1.07D00
```

```
A3 = -0.5339D00
```

```
A4 = 0.01569D00
```

```
A5 = -0.05165D00
```

```
A6 = 0.5475D00
```

```
A7 = -0.7361D00
```

```
A8 = 0.1844D00
```

```
A9 = 0.1056D00
```

```
A10 = 0.6134D00
```

```
A11 = 0.721D00
```

```
R1 = RHO(Z,TPR,PPR)
```

```
C = A11*(R1**2)
```

```
C1 = A1 + (A2/TPR) + (A3/(TPR**3)) + (A4/(TPR**4)) + (A5/(TPR**5))
```

```
C2 = A6 + (A7/TPR) + (A8/(TPR**2))
```

```
C3 = A9*((A7/TPR) + (A8/(TPR**2)))
```

```
C4 = A10*(1.0D00 + C)*((R1**2)/(TPR**3))*EXP(-C)
```

```
F = Z - (1.0D00 + C1*R1 + C2*(R1**2) - C3*(R1**5) + C4)
```

```
END
```

```
C
```

```
=====
```

```
FUNCTION RHO(Z,TPR,PPR)
```

```
IMPLICIT REAL*8 (A-H,M,O-Z)
```

```
RHO = 0.27D00*PPR/(Z*TPR)
```

```
END
```

```
C
```

```
=====
```

```
FUNCTION DF(Z,TPR)
```

```
IMPLICIT REAL*8 (A-H,M,O-Z)
```

```
COMMON /GMM/ A1,A2,A3,A4,A5,A6,A7,A8,A9,A10,A11,R1,C,C1,C2,C3
```

```
C6 = (2.0D00*A10*(R1**2)/((TPR**3)**7))
```

```
C7 = C6*(1.0D00 + C - (C**2))*EXP(-C)
```

```
DF = 1.0D00 + C1*R1/Z + 2.0D00*C2*(R1**2)/Z - 5.0D00*C3*(R1**5)/Z  
+ C7
```

```
DF = DF/TPR
```

```
END
```

```
C
```

```
=====
```

```
SUBROUTINE DZDRHO(TPR,DZDR)
```

```

IMPLICIT REAL*8 (A-H,M,O-Z)
COMMON /GMM/ A1,A2,A3,A4,A5,A6,A7,A8,A9,A10,A11,R1,C,C1,C2,C3

```

```

C5 = (2.0D00*A10*R1/TPR**3)*(1.0D00 + C - C**2)*DEXP(-C)

```

```

DZDR = C1 + 2.0D00*C2*R1 - 5.0D00*C3*(R1**4) + C5

```

```

RETURN
END

```

```

C-----
SUBROUTINE CR(Z,TPR,PPR,RC)

```

```

IMPLICIT REAL*8 (A-H,M,O-Z)

```

```

CALL DZDRHO(TPR,DZ1)
R1 = RHO(Z,TPR,PPR)

```

```

RC = 1.0D00/PPR - (0.27D00/((Z**2)*TPR))*(DZ1/(1.0D00 + R1*DZ1/Z))

```

```

RETURN
END

```

```

C-----
FUNCTION VISCOG(P,T,Z,WM)

```

```

IMPLICIT REAL*8 (A-H,M,O-Z)

```

```

RR = 1.4935D-03*P*WM/(Z**1)
D = (9.4D00 + 0.02D00*WM)*(T**1.5)
E = 209.0D00 + 19.0D00*WM + T
RK = D/E
X = 3.5D00 + 986.0D00/T + 0.01D00*WM
Y = 2.4D00 - 0.2D00*X

```

```

VISCOG = RK*(EXP(X*(RR**Y)))/(10.0D00**4)

```

```

END

```

```

C-----
FUNCTION VISCOG2(P,T,Z,WM)

```

```

IMPLICIT REAL*8 (A-H,M,O-Z)

```

```

RR = 1.4935D-03*P*WM/(Z*T)
D = (9.379D00 + 0.01607D00*WM)*(T**1.5)
E = 209.2D00 + 19.26D00*WM + 1
RK = D/E
X = 3.448D00 + 986.4D00/T + 0.01009D00*WM
Y = 2.447D00 - 0.2224D00*X

```

```

VISCOG2 = RK*(EXP(X*(RR**Y)))*1.0D-04

```

```

END

```

```

C-----
FUNCTION PSEUPC(SG,YH2S,YCO2,YN2)

IMPLICIT REAL*8 (A-H,M,O-Z)

PSEUPC = 678.0D00 - 50.0D00*(SG-0.5) - 206.7D00*YN2 + 440.0D00*YCO2
+      + 606.7D00*YH2S

END
C-----
FUNCTION PSEUTC(SG,YH2S,YCO2,YN2)

IMPLICIT REAL*8 (A-H,M,O-Z)

PSEUTC = 326.0D00 + 315.7D00*(SG-0.5D00) - 240.0D00*YN2 -
+      83.3D00*YCO2 + 133.3D00*YH2S

END
C-----
SUBROUTINE ZFAC2(ERT,N,P,T, PSEUPC,PSEUTC,Z,1YH)

IMPLICIT REAL*8 (A-H,M,O-Z)

PR = P/PSEUPC
RTR = PSEUTC/T

A = 6.125D-02 * RTR * DEXP(-1.2D00*((1.0D00 - RTR)**2))
B = RTR * ( 14.76D00 - 9.76D00 * RTR + 4.58D00 * (RTR**2) )
C = RTR * ( 90.7D00 - 242.2D00 * RTR + 42.4D00 * (RTR**2) )
D = 2.18D00 + 2.82D00 * RTR
Y = 1.0D-03

DO 100 IYH=1,N

F = -A*PR + (Y + Y*Y + Y**3 - Y**4)/((1.0D00 - Y)**3) - B*Y*Y + C*(Y**D)

IF(DABS(F) .LE. ERT) THEN
  Z = A*PR/Y
  RETURN
ELSE
  DFDY = (1.0D00 + 4.0D00*Y*(1.0D00 + Y - Y*Y) + Y**4)/((1.0D00 - Y)**4)
+      - 2.0D00*B*Y + D*C*(Y**(D - 1.0D00))
  Y = Y - F/DFDY
ENDIF

100 CONTINUE

Z = A*PR/Y

RETURN
END

```

C-----

FUNCTION VISC(SG,T,TR,PR,YC,YH,YN)

IMPLICIT REAL*8 (A-JI,M,O-Z)

AA1 = -2.4621182D-00
AA2 = 2.97054714D-00
AA3 = -2.86264054D-01
AA4 = 8.05420522D-03
AA5 = 2.80860949D-00
AA6 = -3.49803305D-00
AA7 = 3.6037302D-01
AA8 = -1.04432413D-02
AA9 = -7.93385684D-01
AA10 = 1.39643306D-00
AA11 = -1.49144925D-01
AA12 = 4.41015512D-03
AA13 = 8.39387178D-02
AA14 = -1.86408848D-01
AA15 = 2.03367881D-02
AA16 = -6.09579263D-04

U = (1.709D-05 - 2.062D-06*SG)*(T - 460.0D00)

V = (8.188D-03 - 6.15D-03*DLOG10(SG))

UV = U + V

CN = YN*(8.48D-03*DLOG10(SG) + 9.59D-03)

CCO = YC*(9.08D-03*DLOG10(SG) + 6.24D-03)

CH = YH*(8.49D-03*DLOG10(SG) + 3.73D-03)

UM = UV + CN + CCO + CH

X1 = AA1 + AA2*PR + AA3*(PR**2) + AA4*(PR**3)

X2 = TR*(AA5 + AA6*PR + AA7*(PR**2) + AA8*(PR**3))

X3 = (TR**2)*(AA9 + AA10*PR + AA11*(PR**2) + AA12*(PR**3))

X4 = (TR**3)*(AA13 + AA14*PR + AA15*(PR**2) + AA16*(PR**3))

X = X1 + X2 + X3 + X4

VISC = DEXP(X)*UM/1R

END

C-----

SUBROUTINE INTEG(PRES,PSEUDOP)

IMPLICIT REAL*8 (A-H,M,O-Z)

COMMON/CINT1/Z1,Z2,N,ERT,1,PC1,TPC2,PPC1,PPC2,WM,SG,YCO2,YH2S,
+ YN2,BASF

DIMENSION T(100,100)

A = BASE

B = PRES

T(1,1) = (B - A)*(FNCP(A) + FNCP(B))/2.0D00
T(1,2) = T(1,1)/2.0D00 + (B - A)*FNCP((A + B)/2.0D00)/2.0D00
T(2,1) = (4.0D00*T(1,2) - T(1,1))/3.0D00

J=2

DO WHILE (DABS((T(J,1) - T(J-1,1))/T(J,1)).GE.ERT)

J = J + 1

DELX = (B - A)/(2.0D00**(J-1))
X = A - DELX
NJ = 2**(J-2)
SUM = 0.0D00

DO I=1,NJ
X = X + 2.0D00*DELX
SUM = SUM + FNCP(X)
END DO

T(1,J) = T(1,J-1)/2.0D00 + DELX*SUM

DO L = 2,J
K = J + 1 - L
T(L,K) = (T(L-1,K+1)*4.0D00**(L-1) - T(L-1,K))/(4.0D00**(L-1)
+ -1.0D00)
END DO

END DO

PSFUDOP = T(J,1)

RETURN
END

C=====

FUNCTION FNCP(X)

IMPLICIT REAL*8 (A-H,M,O-Z)

COMMON/CINT1/Z1,Z2,N,ERT,TPC1,TPC2,PPC1,PPC2,WM,SG,YCO2,YH2S,
+ YN2,BASE
COMMON/CINT2/TEMPR,PRESSINI

TPR1 = TEMPR/TPC1
PPR1 = X/PPC1
CALL ZFAC1(Z1,Z2,N,ERT,TPR1,PPR1,ZNEW1,I)
VISG1 = VISCOG2(X,TEMPR,ZNEW1,WM)

FNCP = 2.0D00*X/(ZNEW1*VISG1)

END

C SUBROUTINE GASGRA(G,WM,PSEUPC,PSEUTC,B)

IMPLICIT REAL*8 (A-H,M,O-Z)

COMMON /FRAC/ X(12)

DIMENSION RMW(12),PC(12),TC(12)

DATA RMW /34.08D00,44.011D00,28.014D00,16.043D00,30.07D00,44.1D00,
+ 58.124D00,58.124D00,72.151D00,72.151D00,86.178D00,128.0205D00 /

DATA PC / 1306.0D00,1070.6D00,493.1D00,667.8D00,707.8D00,616.3D00,
+ 529.1D00,550.7D00,490.4D00,488.6D00,445.7D00,410.0D00 /

DATA TC / 672.5D00,547.6D00,227.3D00,343.1D00,549.8D00,665.7D00,
+ 734.7D00,765.3D00,828.8D00,845.5D00,888.5D00,958.3D00 /

G = 0.0D00
TCMA = 0.0D00
PCMA = 0.0D00
PSMW = 0.0D00

DO I=1,12

WM = WM + RMW(I)*X(I)

G = G + RMW(I)*X(I)/28.966D00

TCMA = TCMA + TC(I)*X(I)

PCMA = PCMA + PC(I)*X(I)

END DO

A = X(1) + X(2)

B = 120.0D00*(A**0.9 - A**1.6) + 15.0D00*(X(1)**0.5 - X(1)**4.0)

PSEUTC = TCMA - B

PSEUPC = PCMA*PSEUTC/(TCMA + X(1)*(1.0D00 - X(1))*B)

RETURN

END

C SUBROUTINE INVPSPRES(PSEUDO,PRES)

IMPLICIT REAL*8 (A-H,M,O-Z)

PARAMETER (N=1, NPARAM=50)

C SPECIFICATIONS FOR LOCAL VARIABLES

DIMENSION A(1,1), PARAM(NPARAM), Y(N)

C SPECIFICATIONS FOR SUBROUTINES

EXTERNAL DIVPAG, SSET

C SPECIFICATIONS FOR FUNCTIONS

EXTERNAL FCN, FCNJ

C Initialize


```

CALL SSET (NPARAM, 0 0, PARAM, 1)
C
IDO = 1
T = 0.0D00
Y(1) = 14 7D00
TOL = 1.0D-06
TEND = PSEUDO
C          Integrate ODE
C          The array a(*,*) is not used.
CALL DIVPAG (IDO, N, FCN, FCNJ, A, T, TEND, TOL, PARAM, Y)
PRES = Y(1)
IDO = 3
CALL DIVPAG (IDO, N, FCN, FCNJ, A, T, TEND, TOL, PARAM, Y)

RETURN
END

```

```

-----
C
SUBROUTINE FCN (N, X, Y, YPRIME)
C          SPECIFICATIONS FOR ARGUMENTS
IMPLICIT REAL*8 (A-H,M,O-Z)
DIMENSION Y(N), YPRIME(N)

P = Y(1)
CALL CALPRES(P,Z,VS)
YPRIME(1) = Z*VS/(2.0D00*P)

RETURN
END

```

```

-----
C
SUBROUTINE FCNJ (N, X, Y, DYPDY)
C          SPECIFICATIONS FOR ARGUMENTS
IMPLICIT REAL*8 (A-H,M,O-Z)
DIMENSION Y(N), DYPDY(N,*)
C          This subroutine is never called
RETURN
END

```

```

-----
C
SUBROUTINE CALPRES(PR,ZNEW,VSC)

IMPLICIT REAL*8 (A-H,M,O-Z)

COMMON/CINT1/Z1,Z2,N,ERT,TPC1,TPC2,PPC1,PPC2,WM,SG,YCO2,YH2S,
+   YN2,BASE
COMMON/CINT2/TEMPR,PRESSINI

IPR1 = TEMPR/TPC1
PPR1 = PR/PPC1
CALL ZFAC1(Z1,Z2,N,ERT,IPR1,PPR1,ZNEW,I)
VSC = VISCOG2(PR,TEMPR,ZNEW,WM)

RETURN

```

END

```
C-----  
SUBROUTINE MDTOMW(MD,MW)  
  
IMPLICIT REAL*8 (A-H,M,O-Z)  
  
PARAMETER (SCTEMP = 288.71D00,SCPRESS = 1.01325D05)  
  
COMMON/CINT4/MINI,QST,TMPRI,PI,TTS,QD,HT  
  
MW = MINI - MD*QST*TMPRI*SCPRESS/(PI*TTS*SCTEMP)  
  
RETURN  
END  
C-----  
SUBROUTINE INVPSTIME(KCY,IMAX,PSTIMA,PRTEMP,PTIME,TIM)  
  
IMPLICIT REAL*8 (A-H,M,O-Z)  
  
COMMON/CIN1/Z1,Z2,N,ERT,TPC1,TPC2,PPC1,PPC2,WM,SG,YCO2,YH2S,  
+ YN2,BASE  
  
PARAMETER (ICYCLE=22)  
  
DIMENSION PSTIMA(IMAX),PRTEMP(IMAX),T(100)  
  
KKC = 1  
225 ICYCLE = KKC*ICYCLE  
IF(KCY.GT.ICYCLE) THEN  
  KKC=KKC+1  
  GOTO 225  
END IF  
  
J=1  
ERD = 1.0D-05  
  
C IF(KKC EQ 3) THEN  
  N=100  
C ELSE  
C   N = 50*KKC  
C   ENDF  
  
250 A = 0.0D00  
  B = PTIME  
  
  CALL FAND(A,IMAX,PSTIMA,PRTEMP,FANA)  
  CALL FAND(B,IMAX,PSTIMA,PRTEMP,FANB)  
  
  DELX = (B-A)/(2.0D00*N)  
  
  SUM = FANA + FANB
```

```

SUM1 = 0.0D00

N1 = 2*N - 1

DO I=1,N1,2

    X = A + I*DELX
    CALL FAND(X,IMAX,PSTIMA,PRTEMP,FANX)
    SUM1 = SUM1 + FANX

END DO

N2 = 2*N - 2

SUM2 = 0.0D00

DO I=2,N2,2

    X = A + I*DELX
    CALL FAND(X,IMAX,PSTIMA,PRTEMP,FANX)
    SUM2 = SUM2 + FANX

END DO

T(J) = DELX*(SUM + 4.0D00*SUM1 + 2.0D00*SUM2)/3.0D00

IF(J.EQ.1) THEN
    J=J+1
    N = N + 50
    GOTO 250
ELSE IF(DABS((T(J)-T(J-1))/J(J-1)) GT ERD) THEN
    J=J+1
    N=N+ 50
    GOTO 250
END IF

TIM = T(J)

RETURN
END

```

```

SUBROUTINE FAND(X,IMAX,PSTIMA,PRTEMP,FANX)

```

```

IMPLICIT REAL*8 (A-H,M,O-Z)

```

```

PARAMETER (PSIPA=6.894757D03, CPPAS=1.0D-03)

```

```

DIMENSION PSTIMA(IMAX),PRTEMP(IMAX)

```

```

CALL CALTIM(X,IMAX,PSTIMA,PRTEMP,GCT,VSC)

```

FANS = (GCT/PSIPA)*(VSC*CPPAS)

END

C-----
SUBROUTINE CALTIM(X,IMAX,PSTIMA,PRTEMP,GCT,VSC)

IMPLICIT REAL*8 (A-H,M,O-Z)

PARAMETER (PSIPA=6.894757D03, CPPAS=1.0D-03, PSCPR=(PSIPA**2)/CPPAS)

DIMENSION PSTIMA(IMAX), PRTEMP(IMAX)

COMMON/CINT1/Z1,Z2,N,ERT,TPC1,TPC2,PPC1,PPC2,WM,SG,YCO2,YH2S,
+ YN2,BASE
COMMON/CINT2/TEMPR,PRESSINI

TPR1 = TEMPR/TPC1

CALL INTRPOL(X,IMAX,PSTIMA,PRTEMP,PW)

PPR1 = PW/PPC1

CALL ZFAC1(Z1,Z2,N,ERT,TPR1,PPR1,/NEW,I)

VSC = VISCOG2(PW,TEMPR,ZNEW,WM)

CALL CR(ZNEW,TPR1,PPR1,CRT)

GCT = CRT/PPC1

RETURN

END

C-----
SUBROUTINE TURBINT(JL,RINV,PERME,PHIT,BETA,RN1)

IMPLICIT REAL*8 (A-H,M,O-Z)

PARAMETER (PSIPA=6.894757D03, CPPAS=1.0D-03, PSCPR=(PSIPA**2)/CPPAS)

PARAMETER (MDMTS=9.86923D-16, CONN1=1.564D-18)

PARAMETER (CONBETA1=4.8511D04, CONBETA2=2.6D10)

PARAMETER(LF=2,LF1=LF+1,LF2=LF+2)

COMMON/CINT1/Z1,Z2,N,ERT,TPC1,TPC2,PPC1,PPC2,WM,SG,YCO2,YH2S,
+ YN2,BASE

COMMON/CINT2/TEMPR,PRESSINI

COMMON/CINT4/MINI,QST,IMPR1,PI,TTS,QD,IIT

COMMON/CINT5/IBETA,RW

COMMON/CINT6/ PERM(LF1,LF),RDR(LF2),PHIR(LF1,LF)

TPR = TEMPR/TPC1

PPR = PRESSINI/PPC1

CALL ZFAC1(Z1,Z2,N,ERT,TPR,PPR,ZNEW,I)

VSC = VISCOG2(PRESSINI,TEMPR,ZNEW,WM)

I=1

```

1973 IF(RINV.GE.RDR(I) AND.RINV.LT.RDR(I+1)) THEN
  IM = I
  SUMMA = 0.0D0
  SUMMA1 = 0.0D0
  DO J=1,IM
    IF(J.NE.IM) THEN
      SUMMA = SUMMA + (DLOG(RDR(J+1)/RDR(J)))/PERM(J,JL)
      SUMMA1 = SUMMA1 + PHIR(J,JL)*(RDR(J+1) - RDR(J))
    ELSE
      SUMMA = SUMMA + (DLOG(RINV/RDR(J)))/PERM(J,JL)
      SUMMA1 = SUMMA1 + PHIR(J,JL)*(RINV - RDR(J))
    END IF
  END DO
ELSE
  I = I + 1
  GO TO 1973
END IF

PERME = DLOG(RINV/RDR(1))/SUMMA
PHIT = SUMMA1/(RINV - RDR(1))

VA = PERME**2
VB = TEMPR*VSC*RW

IF(IBETA.FQ.1) THEN
  BETA = CONBETA1/(DSQR1(PERME)*(PHIT**5.5))
ELSE
  BETA = CONBETA2/(PERME**1.2)
END IF

RNT = CONNT*VA*BETA*SG*MINI/(VB*PSCPR)

RETURN
END

```

```

C
SUBROUTINE FORCHN(JL,QF,RINV,PERME,PHIT,BETA,RNT,FNO)

IMPLICIT REAL*8 (A-H,M,O-Z)

COMMON/CINT4/MINI,QST,TPR1,PI,TTS,QD,IIT

CALL TURBINT(JL,RINV,PERME,PHIT,BETA,RNT)

FNO = QD*RNT*QF

RETURN
END

```

```

C
SUBROUTINE CORTURD(JL,QF,PRESS,RINV,PERME,PHIT,BETA,FNO,RNT,CEE1)

IMPLICIT REAL*8 (A-H,M,O-Z)

```

```

COMMON/CINT5/IBETA,RW
CALL FORCHN(JL,QF,RINV,PERME,PHIT,BETA,RNT,FNO)
IF(FNO.GT.0.0D00 AND.FNO.LT.0.1D00) THEN
    CEF1 = 1.0D00
ELSE IF(FNO.GE.0.1D00.AND.FNO.LE 1.0D00) THEN
    CALL VSCRATIO(PRESS,FMU)
    CBE1 = (1.0D00 - RW/RINV)*FMU
ELSE IF(FNO.GT.1.0D00) THEN
    CALL VSCRATIO(PRESS,FMU)
    CBE1 = (1.0D00 - RW/RINV)*FMU/(FNO**0.028D00)
END IF
RETURN
END

```

```

SUBROUTINE VSCRATIO(PRESS,FMU)
IMPLICIT REAL*8 (A-H,M,O-Z)
COMMON/CINT1/Z1,Z2,N,ERT,TPC1,TPC2,PPC1,PPC2,WM,SG,YCO2,YH2S,
+ YN2,BASE
COMMON/CIN12/TEMPR,PRESSINI
TPR = TEMPR/TPC1
PPR0 = PRESSINI/PPC1
PPR1 = PRESS/PPC1
CALL ZFAC1(Z1,Z2,N,ERT,TPR,PPR0,ZNEW0,I)
CALL ZFAC1(Z1,Z2,N,ERT,TPR,PPR1,ZNEW1,I)
VSC0 = VISCOG2(PRESSINI,TEMPR,ZNEW0,WM)
VSC1 = VISCOG2(PRESS,TEMPR,ZNEW1,WM)
FMU = VSC0/VSC1
RETURN
END

```

```

FUNCTION RADINV(TD)
IMPLICIT REAL*8 (A-H,M,O-Z)
COMMON/CINT5/IBETA,RW

```

RADINV = 1.5D00*RW*DSQRT(TD)

FND

=====

SUBROUTINE NDARCYD(JL,RINV,DMU)

IMPLICIT REAL*8 (A-H,M,O-Z)

PARAMETER (PSIPA=6.894757D03, CPPAS=1.0D-03, PSCPR=(PSIPA**2)/CPPAS)

PARAMETER (CONDMU = 2.224D-12, MDMTS = 9.86923D-16)

PARAMETER (FTM = 0.3048D00, ICYCLE=22, CONBETA1=4.8511D04)

PARAMETER(LF=2, LF1=LF+1, LF2=LF+2, CONBETA2=2.6D10)

COMMON/CINT5/IBETA,RW

COMMON/CINT1/Z1,Z2,N,ERT,TPC1,TPC2,PPC1,PPC2,WM,SG,YCO2,YH2S,

+ YN2,BASE

COMMON/CINT2/TEMPR,PRESSINI

COMMON/CINT4/MINI,QST,TMPR1,PI,TTS,QD,HT

COMMON/CING/ PERM(LF1,LF),RDR(LF2),PHIR(LF1,LF)

PPR1 = PRESSINI/PPC1

TPR1 = TEMPR/TPC1

CALL ZFAC1(Z1,Z2,N,ERT,TPR1,PPR1,ZNEW1,I)

VSC1 = VISCOG2(PRESSINI,TEMPR,ZNEW1,WM)

I=1

1997 IF(RINV.GE.RDR(I).AND.RINV.LE.RDR(I+1)) THEN

IM = I

SUMMA = 0.0D00

SUMMA1 = 0.0D00

SUMMA2 = 0.0D00

DO J=1,JM

IF(J.NE.IM) THEN

IF(IBETA.EQ.1) THEN

VPR = DSQRT(PERM(J,JL))*CONBETA1/(PHIR(J,JL)**5.5)

ELSE

VPR = CONBETA2/(PERM(J,JL)**0.2)

END IF

SUMMA = SUMMA + VPR*(1.0D00/RDR(J) - 1.0D00/RDR(J+1))

ELSE

IF(IBETA.EQ.1) THEN

VPR = DSQRT(PERM(J,JL))*CONBETA1/(PHIR(J,JL)**5.5)

ELSE

VPR = CONBETA2/(PERM(J,JL)**0.2)

```

END IF

SUMMA = SUMMA + VPR*(1.0D00/RDR(J) - 1.0D00/RINV)

END IF
END DO
ELSE
I = I + 1
GOTO 1997
END IF

VB = CONDMU*SG/(HT/FIM)

DMU = SUMMA*VB/VSCI

RETURN
END

```

```

C SUBROUTINE PSEUDRPR(X,QT)

IMPLICIT REAL*8 (A-H,M,O-Z)
C
PARAMETER (IMAXPRESS = 10000,IPRLEN = IMAXPRESS/50 + 1)

COMMON/PRPS/PSEUDOPR(IPRLEN),REALPR(IPRLEN)

LOGICAL CHECK
EXTERNAL DQDVAL

CHECK = .TRUE.

QT = DQDVAL(X,IPRLEN,PSEUDOPR,REALPR,CHECK)

RETURN
END

```

```

C SUBROUTINE INTRPOL(X,IMAX,PSTIMA,PRTEMP,QT)

IMPLICIT REAL*8 (A-H,M,O-Z)
C
DIMENSION PSTIMA(IMAX),PRTEMP(IMAX)

LOGICAL CHECK
EXTERNAL DQDVAL

CHECK = .TRUE.

QT = DQDVAL(X,IMAX,PSTIMA,PRTEMP,CHECK)

RETURN
END

```

